Axions in Stockholm 2025

HAYSTAC & ALPHA Status and Plans

Karl van Bibber
University of California Berkeley

July 4, 2025

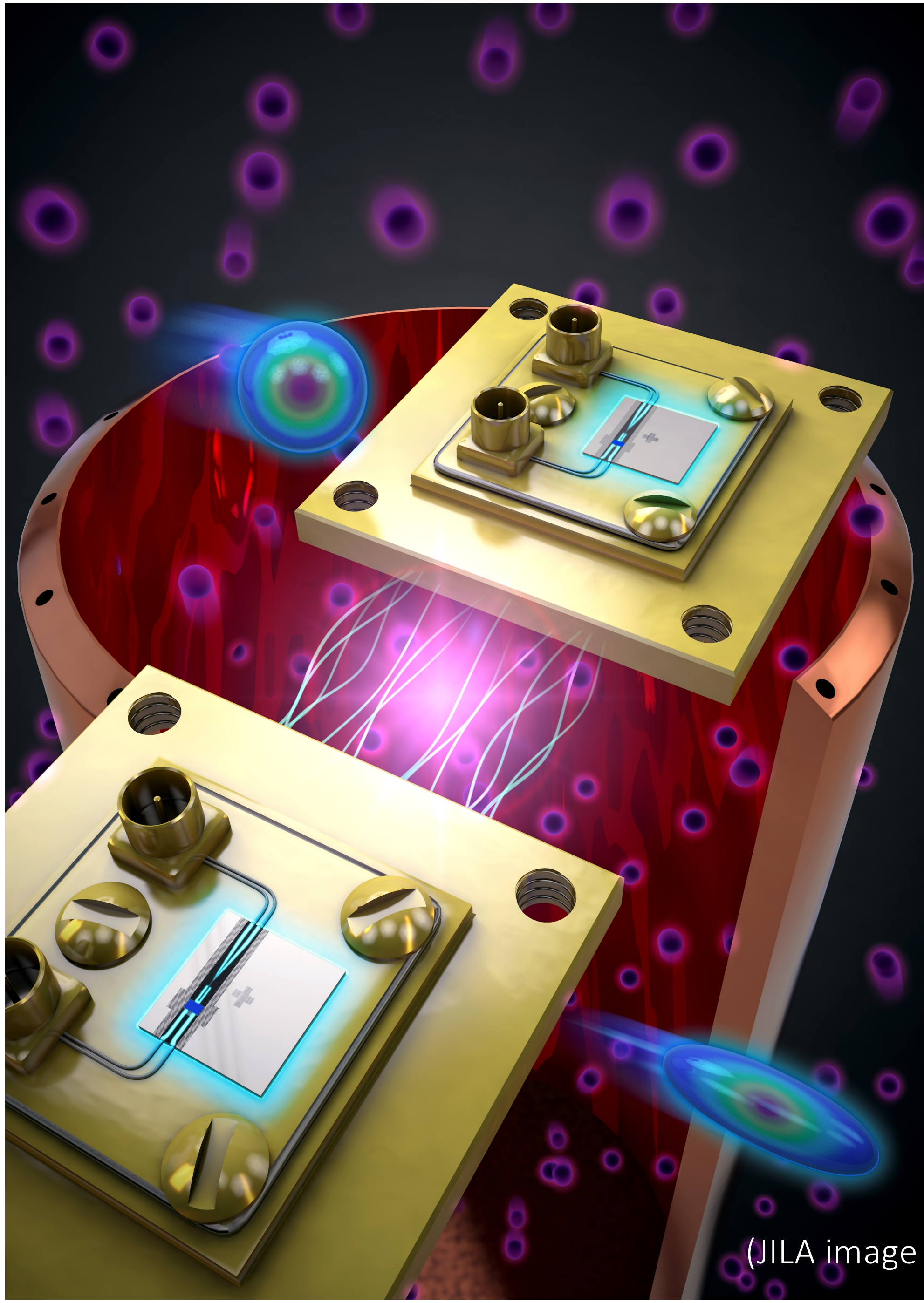

(JILA image courtesy Lehnert Group and Steven Burrows)

HAYSTAC & ALPHA in a nutshell

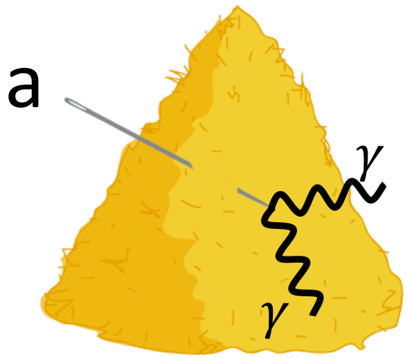

- *Three institutions, 2010 – , @ Yale*
- *Pathfinder & technology test-bed*
- *Innovation: quantum enhancement*
- *Fringe of post-inflation axion, < 40 μeV*

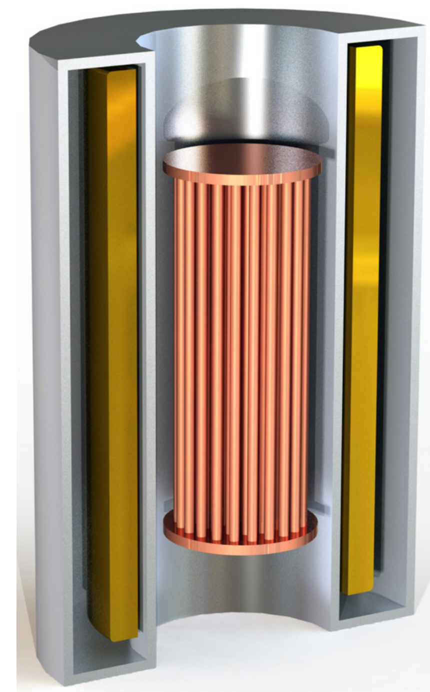

- *International, 2023 – , @ Yale*
- *Pathfinder & technology test-bed*
- *Innovation: photonics & metamaterials*
- *Deep post-inflation axion, 40 - 200 μeV*

HAYSTAC & ALPHA in a nutshell

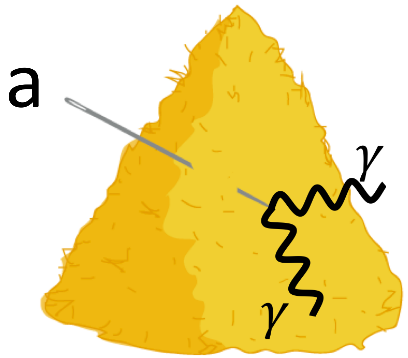

- *Three institutions, 2010 – , @ Yale*
- *Pathfinder & technology test-bed*
- *Innovation: quantum enhancement*
- *Fringe of post-inflation axion, < 40 μeV*

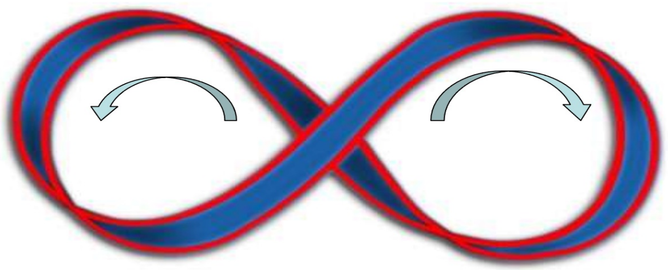

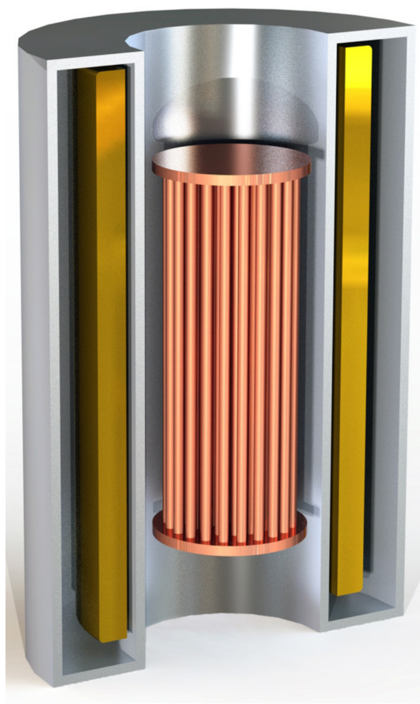

- *International, 2023 – , @ Yale*
- *Pathfinder & technology test-bed*
- *Innovation: photonics & metamaterials*
- *Deep post-inflation axion, 40 - 200 μeV*

The pre- and post-inflation axion

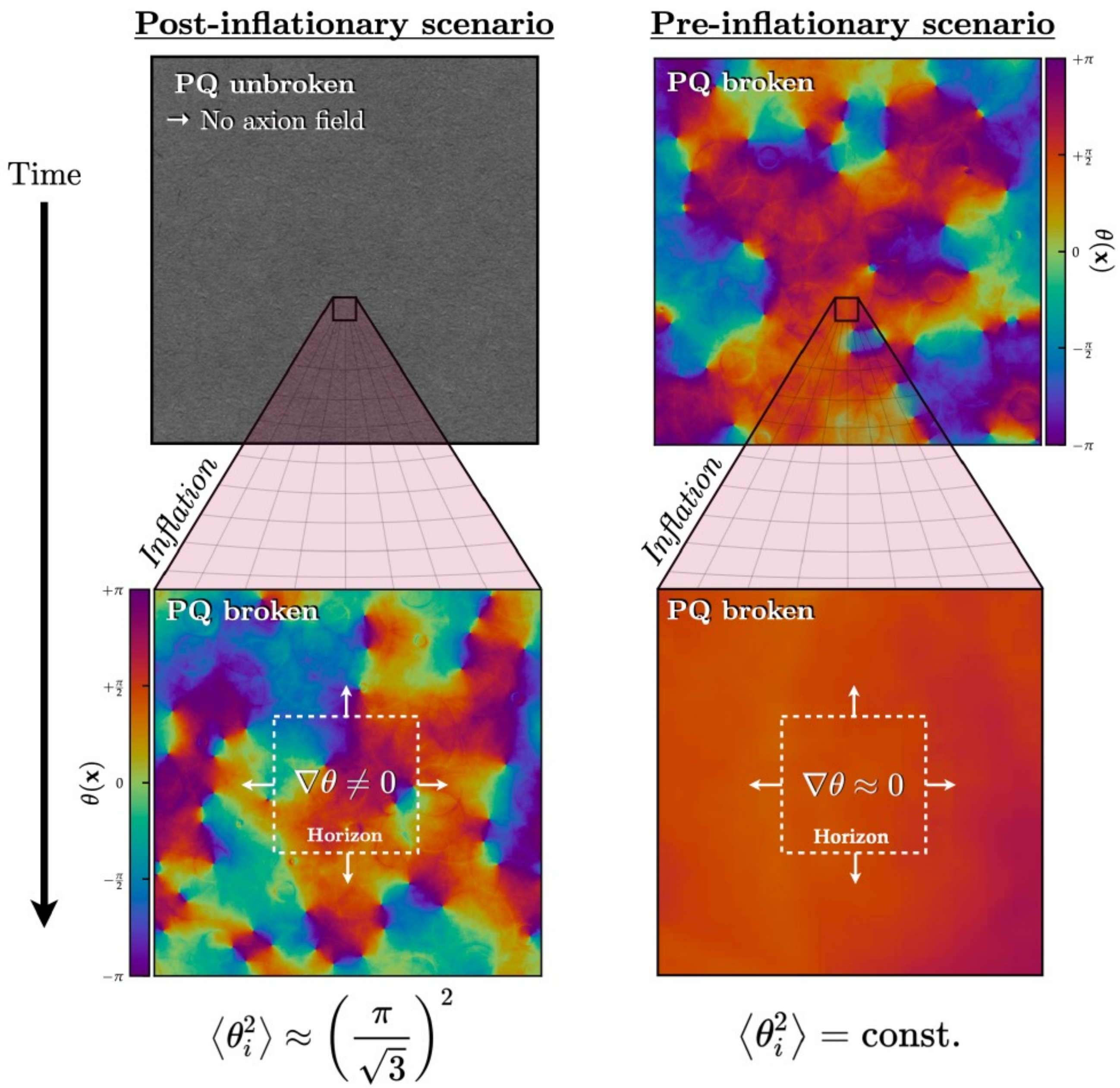

If this were the case, the Post-Inflation axion mass would be exactly and trivially prescribed.

But there is a complication: radiation from topological strings (cosmic strings).

In principle, this also could be exactly calculated, but this is a much harder problem.

(C.A.J. O'Hare)

Adaptive Mesh Refinement (AMR) simulation of post-inflation axion production

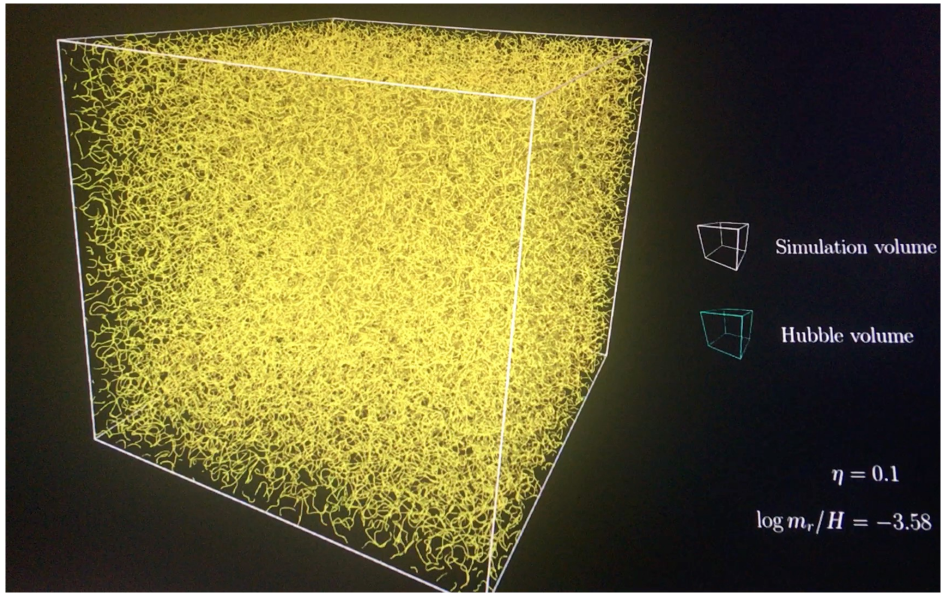

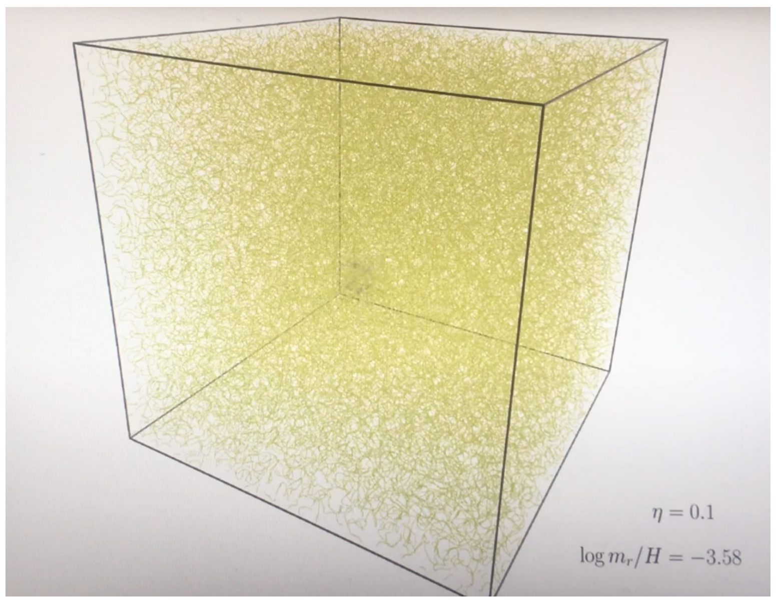

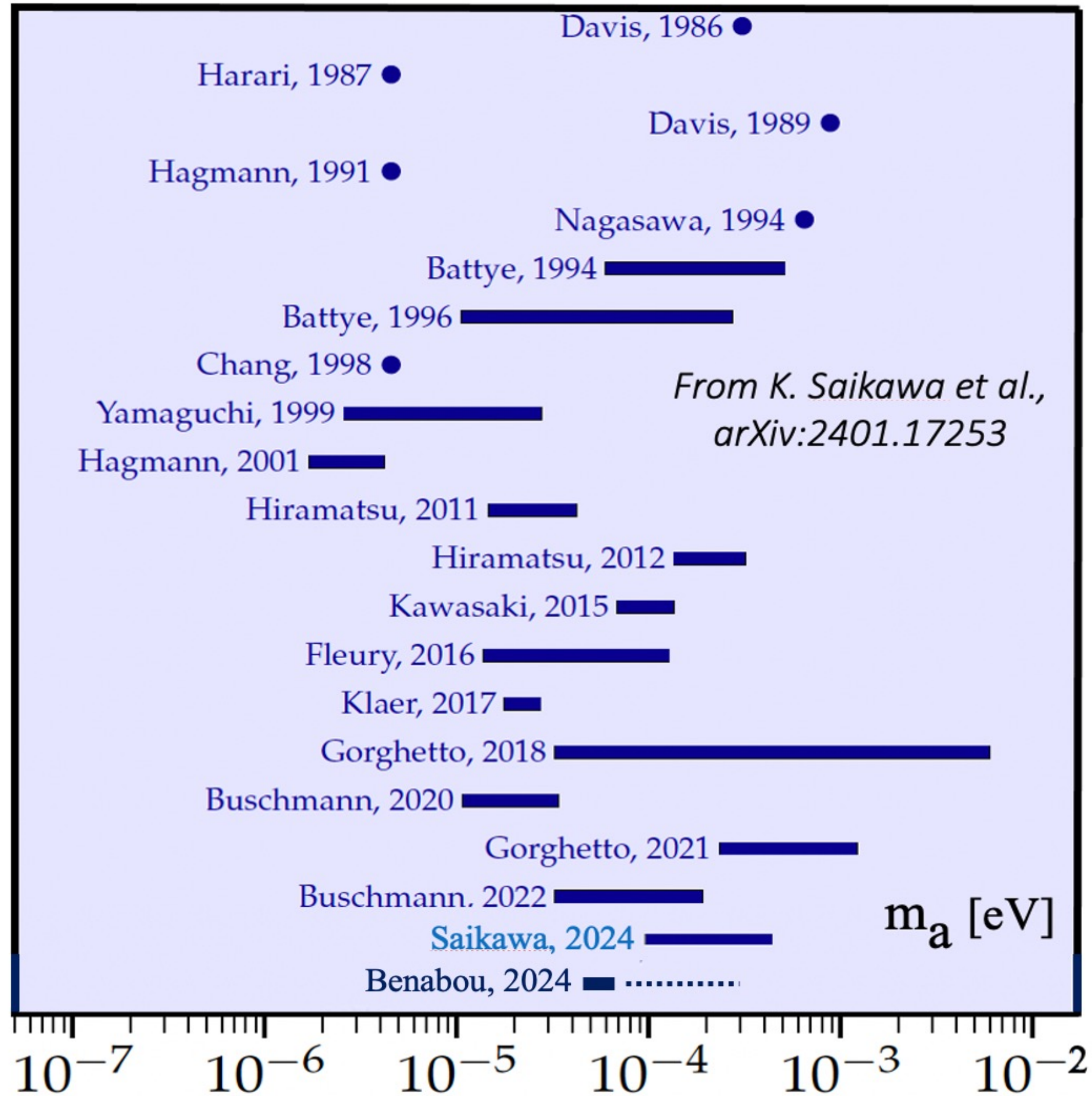

The mass of the post-inflation axion is in principle calculable, but challenging

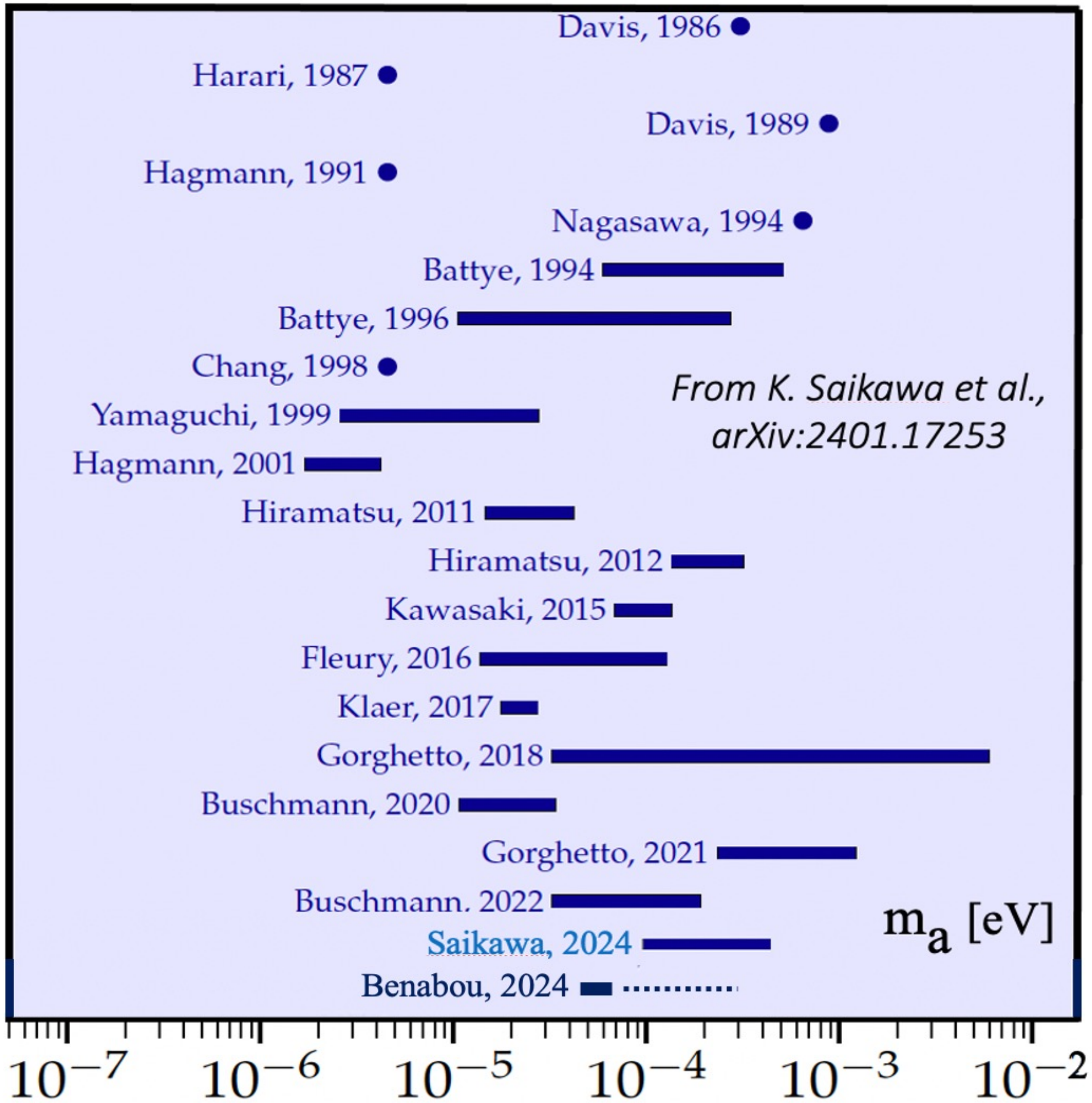

And the theorists’ challenges of course get handed on to the experimentalists !

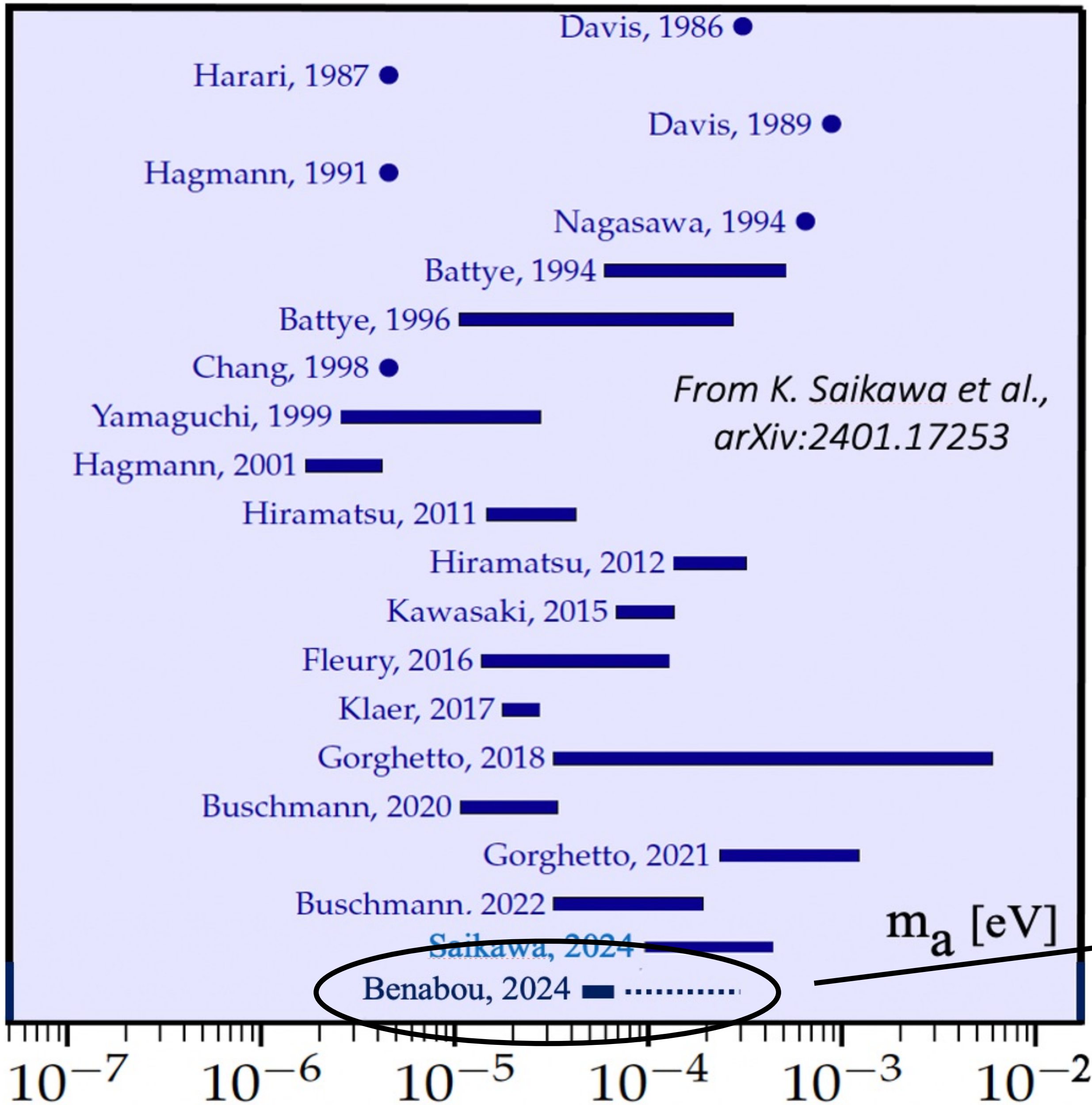

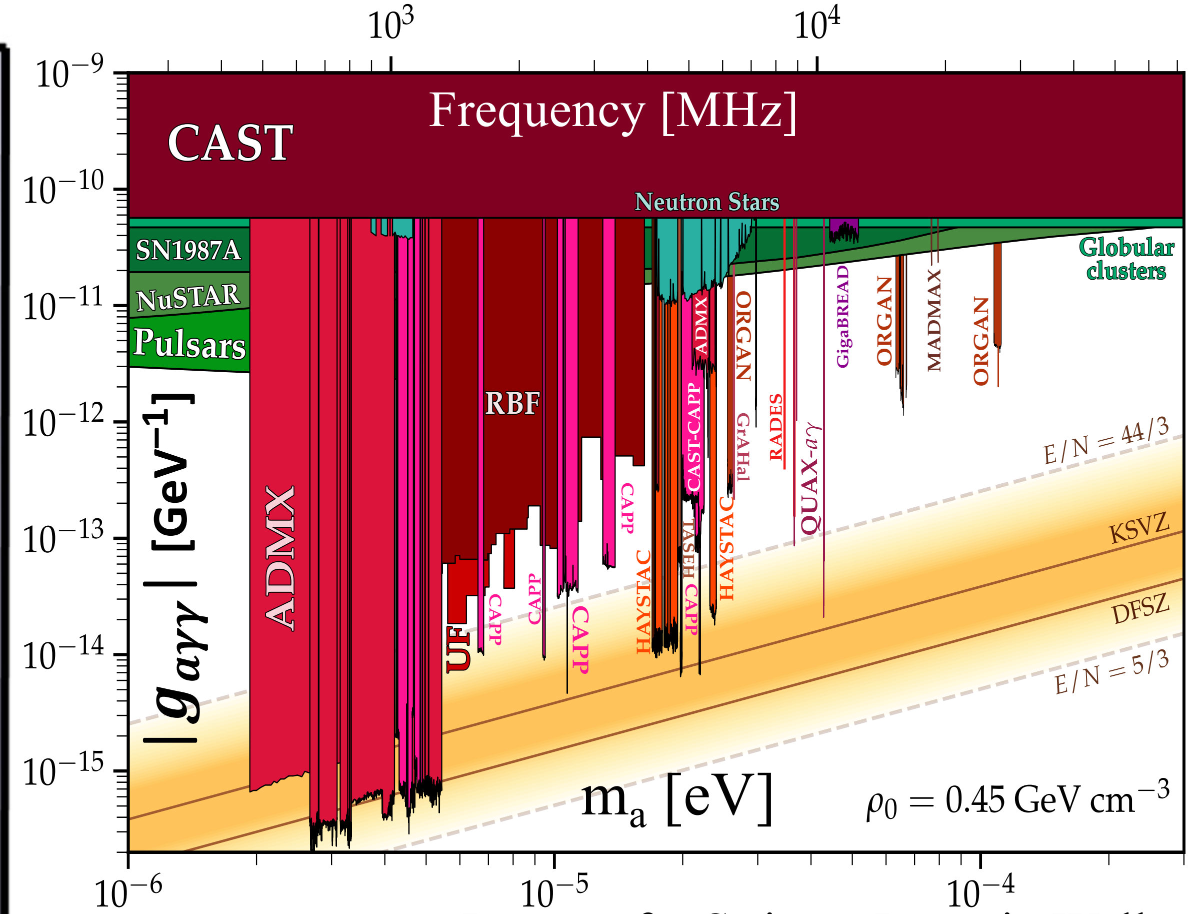

J.N. Benabou et al.,
134 (2025) 241003

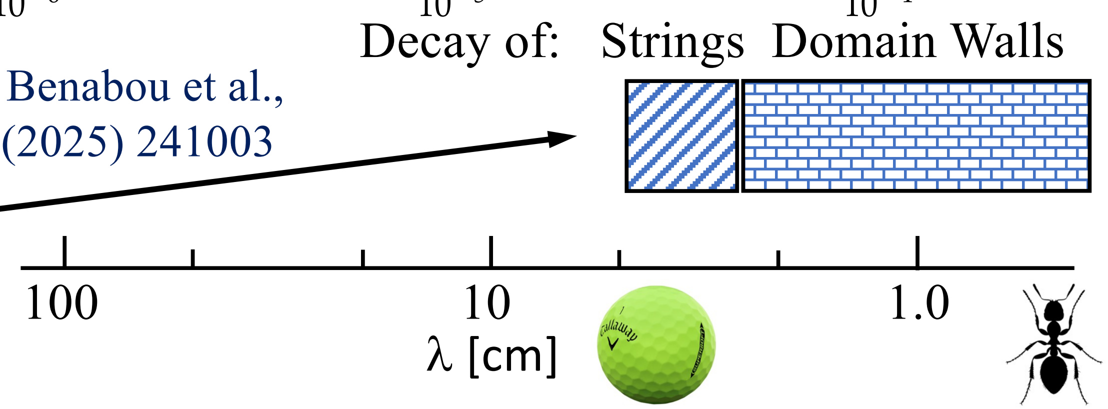

A brief tour through HAYSTAC (Yale-Berkeley-Johns Hopkins)

JPA-based Squeezed-State Receiver

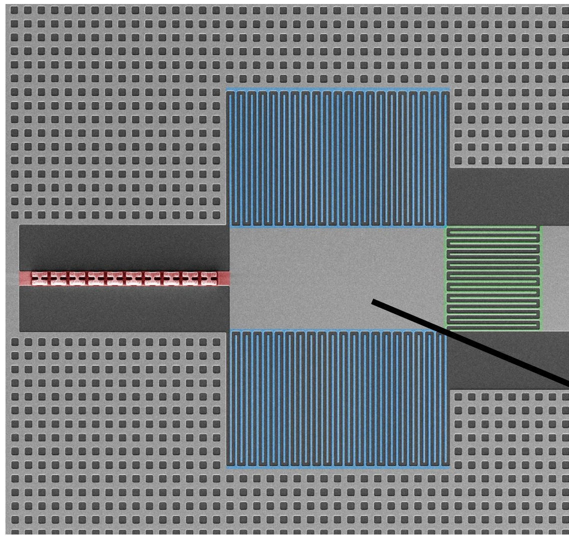

Microwave Cavity (copper)

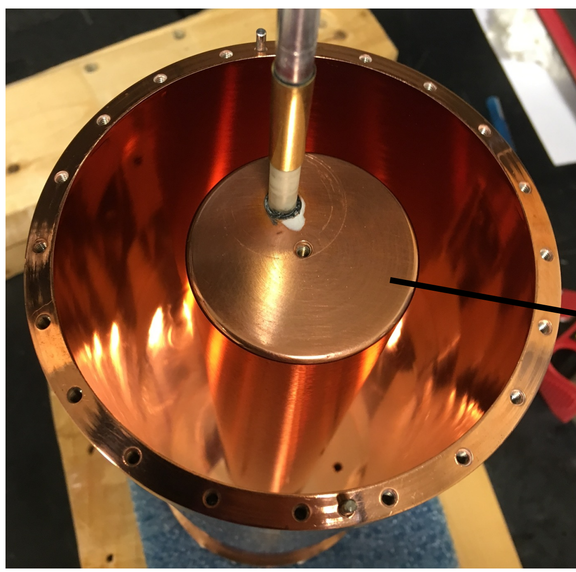

^{3}He/^{4}He Dilution Refrigerator

9.4 Tesla, 10 Liter Magnet

The Microwave Cavity Dark Matter Experiment

$$\mathcal{L} \supset -\frac{1}{4} g_{a\gamma\gamma} a \tilde{F}_{\mu\nu} F^{\mu\nu} = g_{a\gamma\gamma} a \mathbf{E} \cdot \mathbf{B}$$

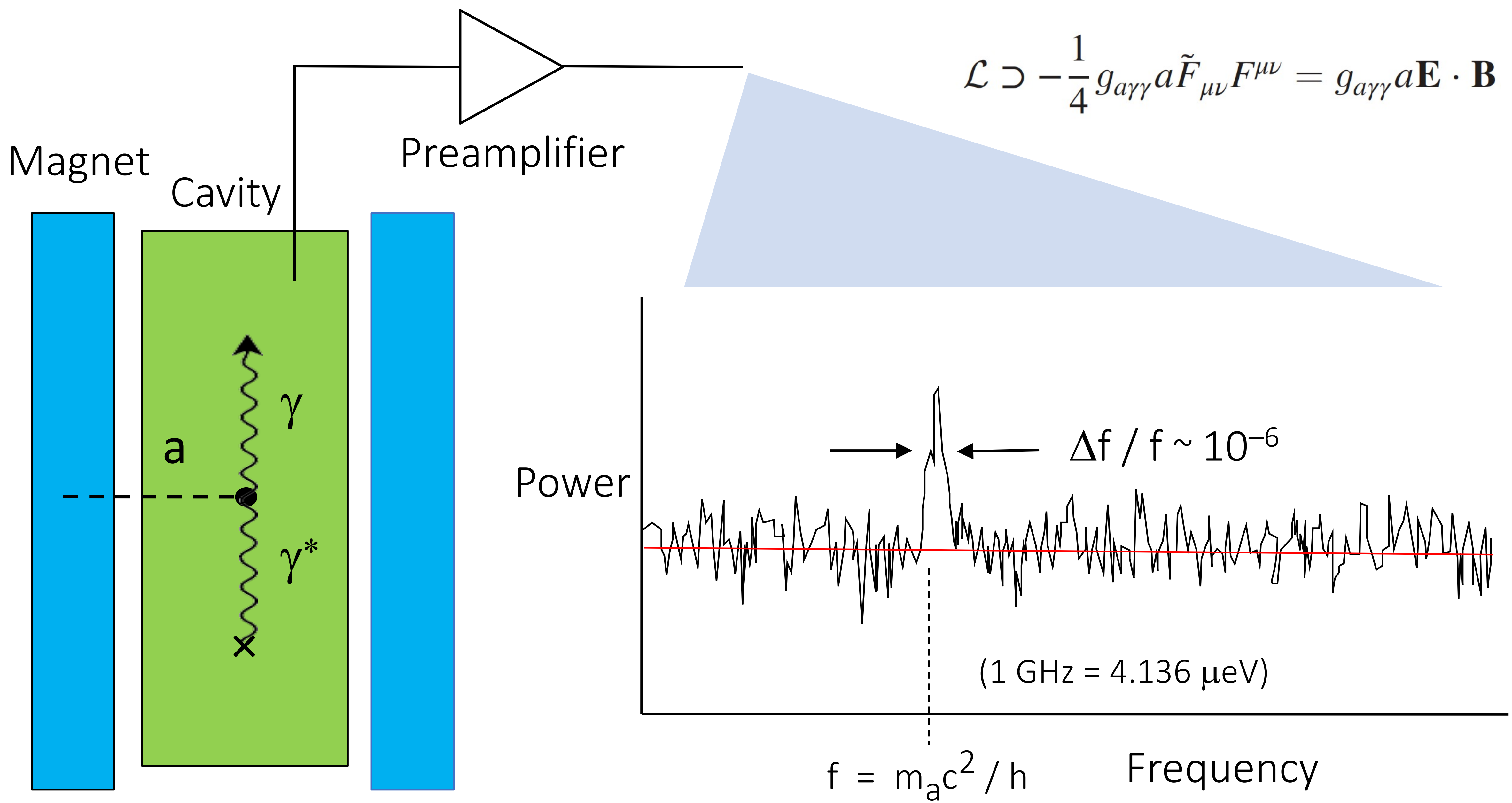

Conversion power, scan rate

Signal power

$$P_{ax} = \left(\frac{g_\gamma^2 \alpha^2 \rho_a}{\pi^2 \Lambda^4}\right) \omega_c B_0^2 V C_{\mathrm{mnl}} Q_L \times \frac{\beta}{1+\beta} \frac{1}{1+(2\delta_\nu/\Delta\nu_c)^2}$$

Q_L	=	$Q_0/(1+\beta)$	Loaded Q-value; β coupling
δf	=	$f - f_0$	Offset from central
C_{lmn}			Cavity form factor

Scanning rate

$$\frac{\mathrm{d}\nu}{\mathrm{d}t} \approx \frac{4}{5} \frac{Q_L Q_a}{\Sigma^2} \left(g_\gamma^2 \frac{\alpha^2}{\pi^2} \frac{\hbar^3 c^3 \rho_a}{\Lambda^4}\right)^2 \times \left(\frac{1}{\hbar \mu_0} \frac{\beta}{1+\beta} B_0^2 V C_{mn\ell} \frac{1}{N_{\mathrm{sys}}}\right)^2$$

Δf	Cavity bandwidth
f_{step}	Frequency tuning steps
n	Overlapping tuning steps

Form factor & Quality Factor

$$C_{\mathrm{lmn}} = \frac{\left(\int_V \boldsymbol{B}(\boldsymbol{x}) \cdot \boldsymbol{E}_{lmn}(\boldsymbol{x})\, \mathrm{d}^3\boldsymbol{x}\right)^2}{B_0{}^2 V \int_V \varepsilon_r(\boldsymbol{x}) \boldsymbol{E}_{lmn}(\boldsymbol{x})^2\, \mathrm{d}^3\boldsymbol{x}}$$

$$Q = O \frac{(Volume)}{(Surface\ Area) \cdot (Skin\ Depth)}$$

Conversion power, scan rate

Signal power

$$P_{ax} = \left(\frac{g_\gamma^2 \alpha^2 \rho_a}{\pi^2 \Lambda^4}\right) \omega_c B_0^2 V C_{\mathrm{mnl}} Q_L \cdot \times \frac{\beta}{1+\beta} \frac{1}{1+(2\delta_\nu/\Delta\nu_c)^2}$$

Q_L	=	$Q_0/(1+\beta)$	Loaded Q-value; β coupling
δf	=	$f - f_0$	Offset from central
C_{lmn}			Cavity form factor

Scanning rate

$$\frac{d\nu}{dt} \approx \frac{4}{5} \frac{Q_L Q_a}{\Sigma^2} \left(g_\gamma^2 \frac{\alpha^2}{\pi^2} \frac{\hbar^3 c^3 \rho_a}{\Lambda^4}\right)^2 \times \left(\frac{1}{\hbar\mu_0} \frac{\beta}{1+\beta} B_0^2 V C_{mn\ell} \frac{1}{N_{\mathrm{sys}}}\right)^2$$

Δf	Cavity bandwidth
f_{step}	Frequency tuning steps
n	Overlapping tuning steps

Form factor & Quality Factor

$$C_{\mathrm{lmn}} = \frac{\left(\int_V \boldsymbol{B}(\boldsymbol{x}) \cdot \boldsymbol{E}_{lmn}(\boldsymbol{x})\, \mathrm{d}^3\boldsymbol{x}\right)^2}{B_0{}^2 V \int_V \varepsilon_r(\boldsymbol{x}) \boldsymbol{E}_{lmn}(\boldsymbol{x})^2\, \mathrm{d}^3\boldsymbol{x}}$$

$$Q = O\frac{(Volume)}{(Surface\ Area)\cdot(Skin\ Depth)}$$

System noise temperature, Figure-of-merit

System Noise Temperature

Dicke radiometer equation:

$$SNR = \frac{P}{k_B T_{SYS}} \sqrt{\frac{t}{\Delta\nu_a}}$$

$$k_B T_{SYS} = h\nu \left(\frac{1}{e^{h\nu/k_B T} - 1} + \frac{1}{2} \right) + k_B T_A$$

T	Physical temperature
T_A	Amplifier noise temperature
t	Integration time

The Standard Quantum Limit for Linear Amplifiers

$$T_A > T_{SQL}$$

where

$$k_B T_{SQL} = h\nu$$

$$FOM \propto \frac{B^4 V^2 C^2 Q}{T_{SYS}}$$

HAYSTAC Phase I (2015-18) – single Josephson Parametric Amplifier (JPA) @ SQL

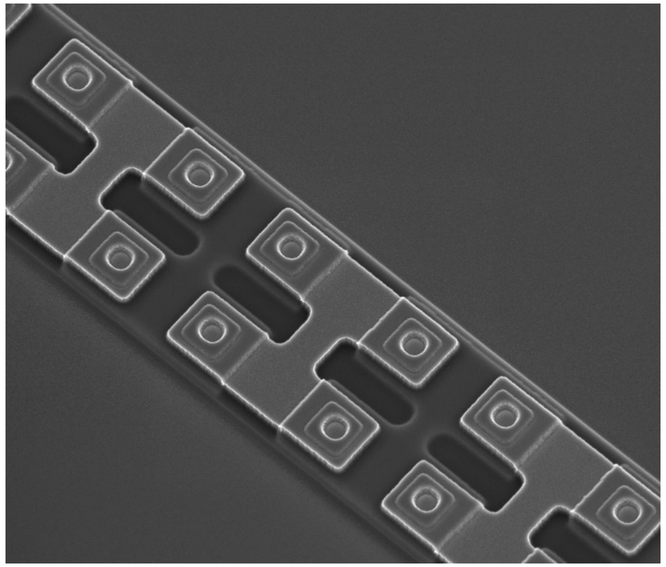

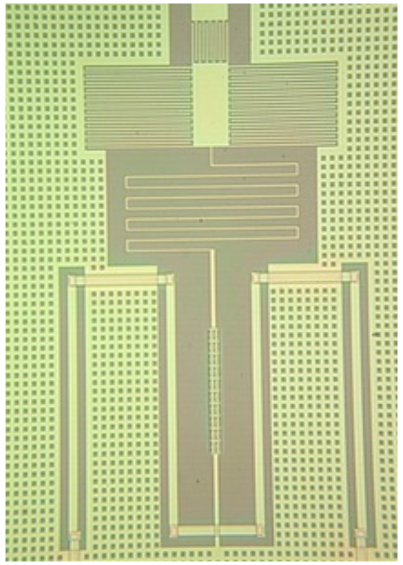

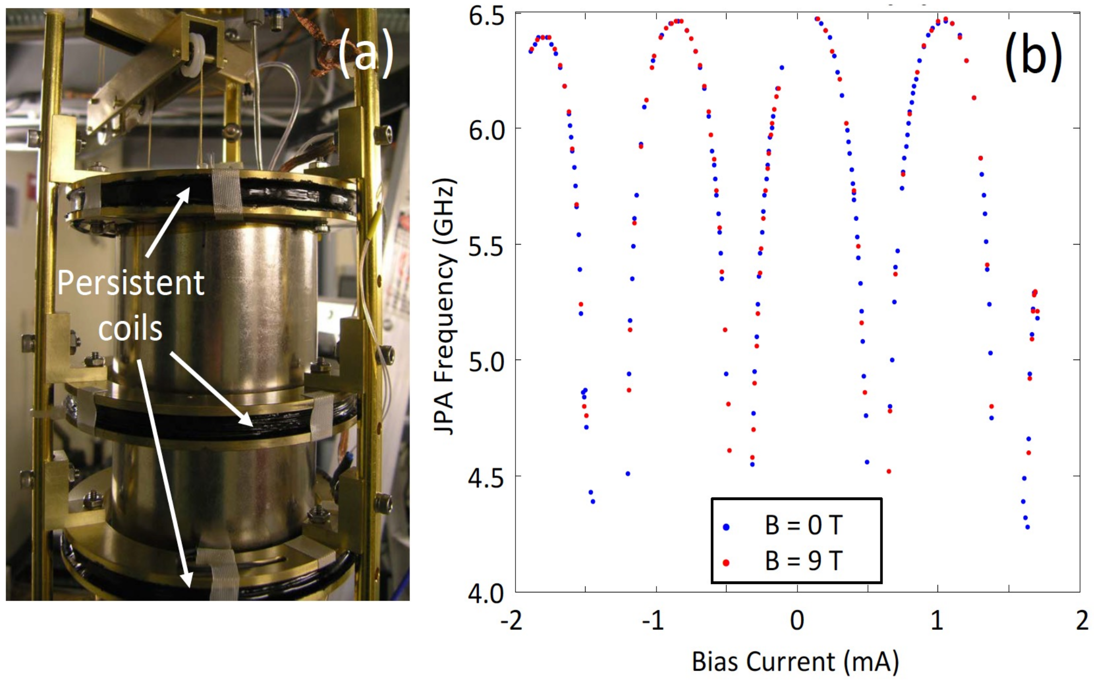

- Flux-pumped JPAs developed for HAYSTAC began operation at $T_A \sim T_{SQL}$ in 2015
  - B. Brubaker *et al.*, PRL 118 (2017) 061302
  - L. Zhong *et al.*, PRD 97 (2018) 092001
- Reduction of fringe field at the JPA to less than 0.01 of a flux quantum was essential
  - S. Al Kenany et al., NIM A 854 (2017) 11
- New analysis procedure for JPA-based system
  - B. Brubaker *et al.*, PRD 96 (2017) 123008

HAYSTAC Phase II – Squeezed State Receiver: Routine operation < T_{SQL} (2019 –)

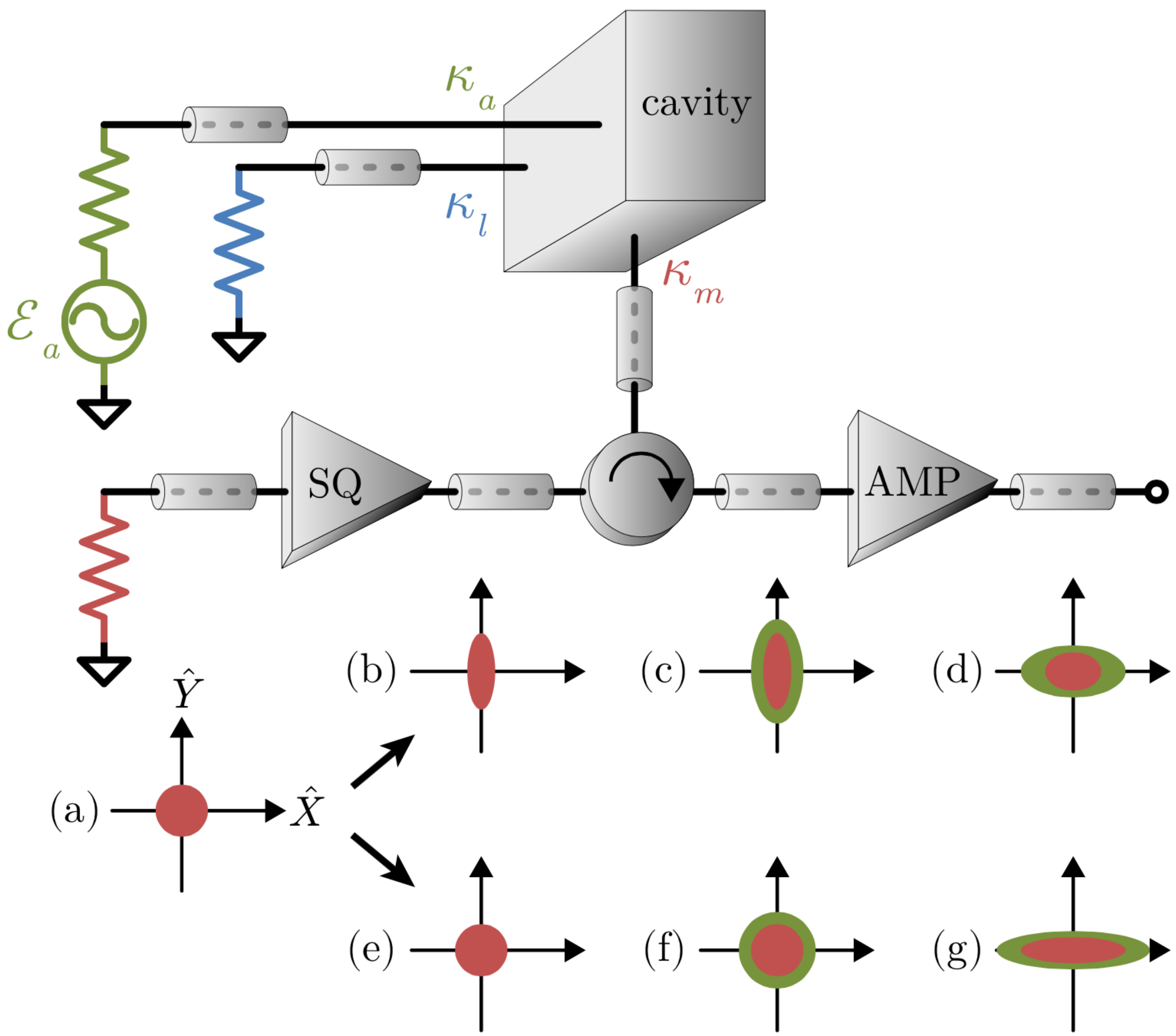

M. Malnou *et al.*, PRX9 (2019) 021023

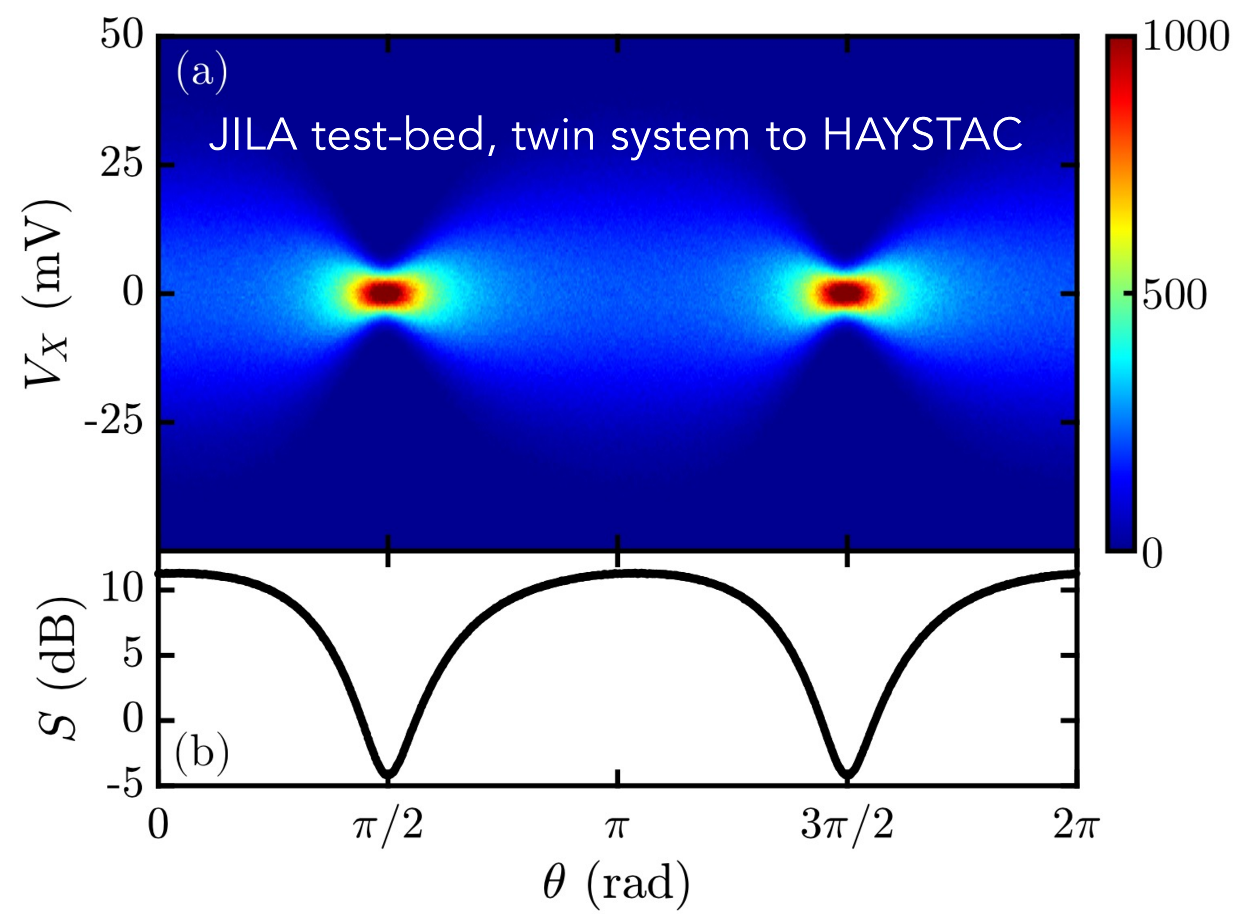

Squeezing and amplifying in the same quadrature yielded –4.5 ± 0.1 dB, just as predicted by modeling

In more detail

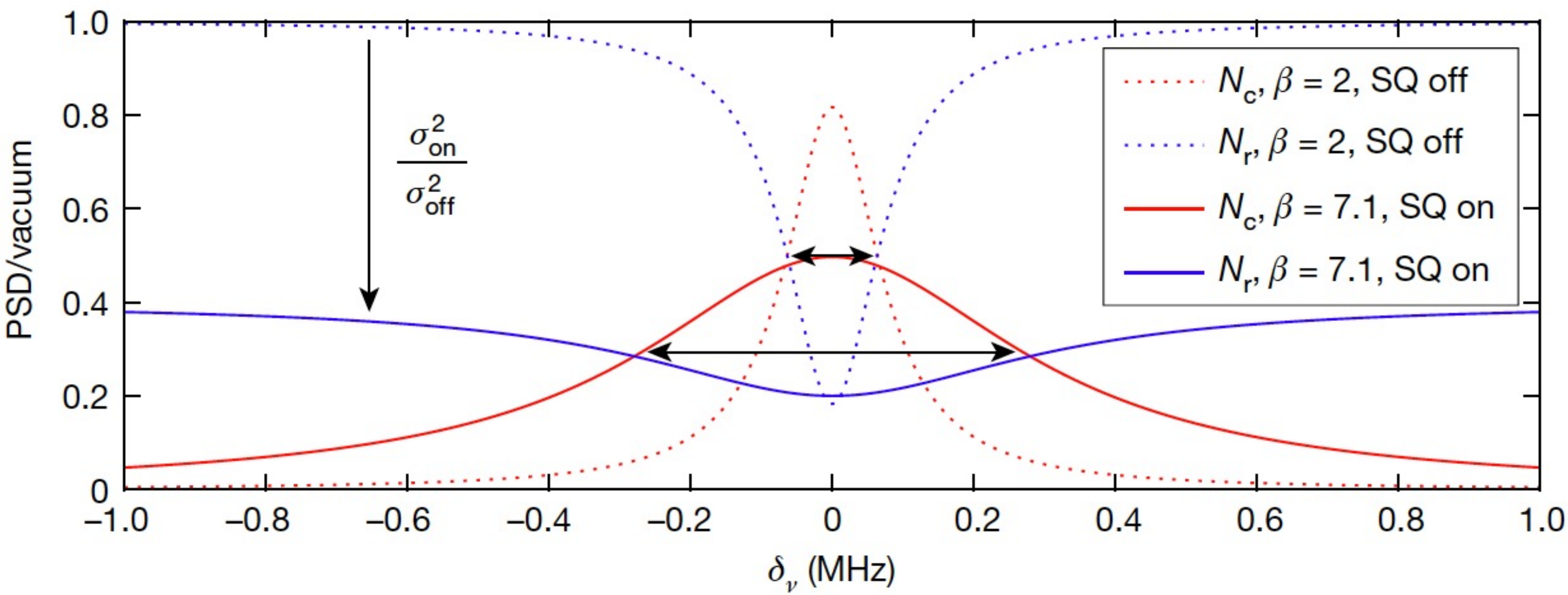

Overcoupling is essential to the acceleration

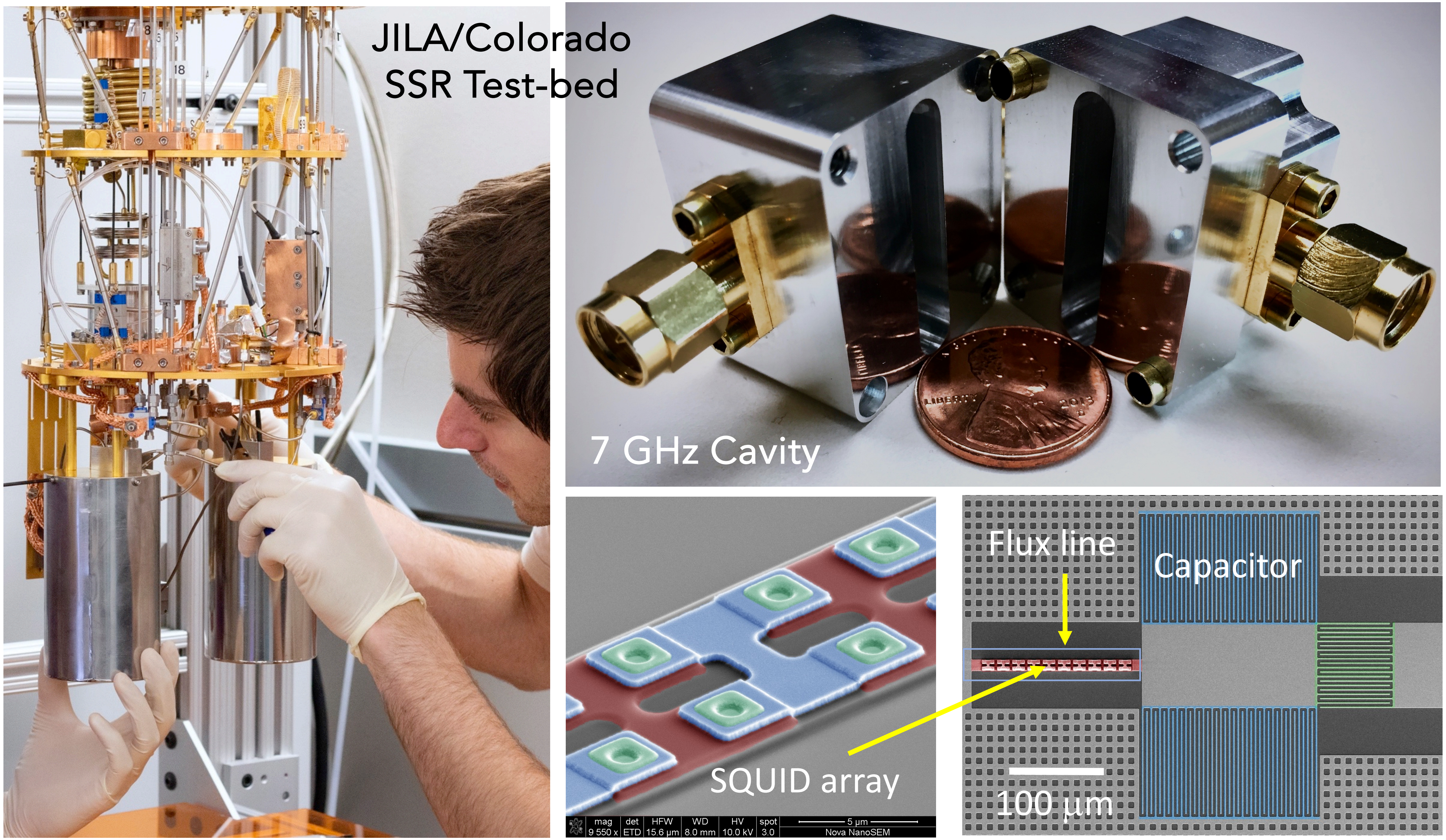
JILA/Colorado
SSR Test-bed
7 GHz Cavity
Flux line
Capacitor
SQUID array
100 μm
mag 9 550 x
det ETD
HFW 15.6 μm
WD 8.0 mm
HV 10.0 kV
spot 3.0
5 μm
Nova NanoSEM

HAYSTAC with Squeezed State Receiver in routine operation for 5 years

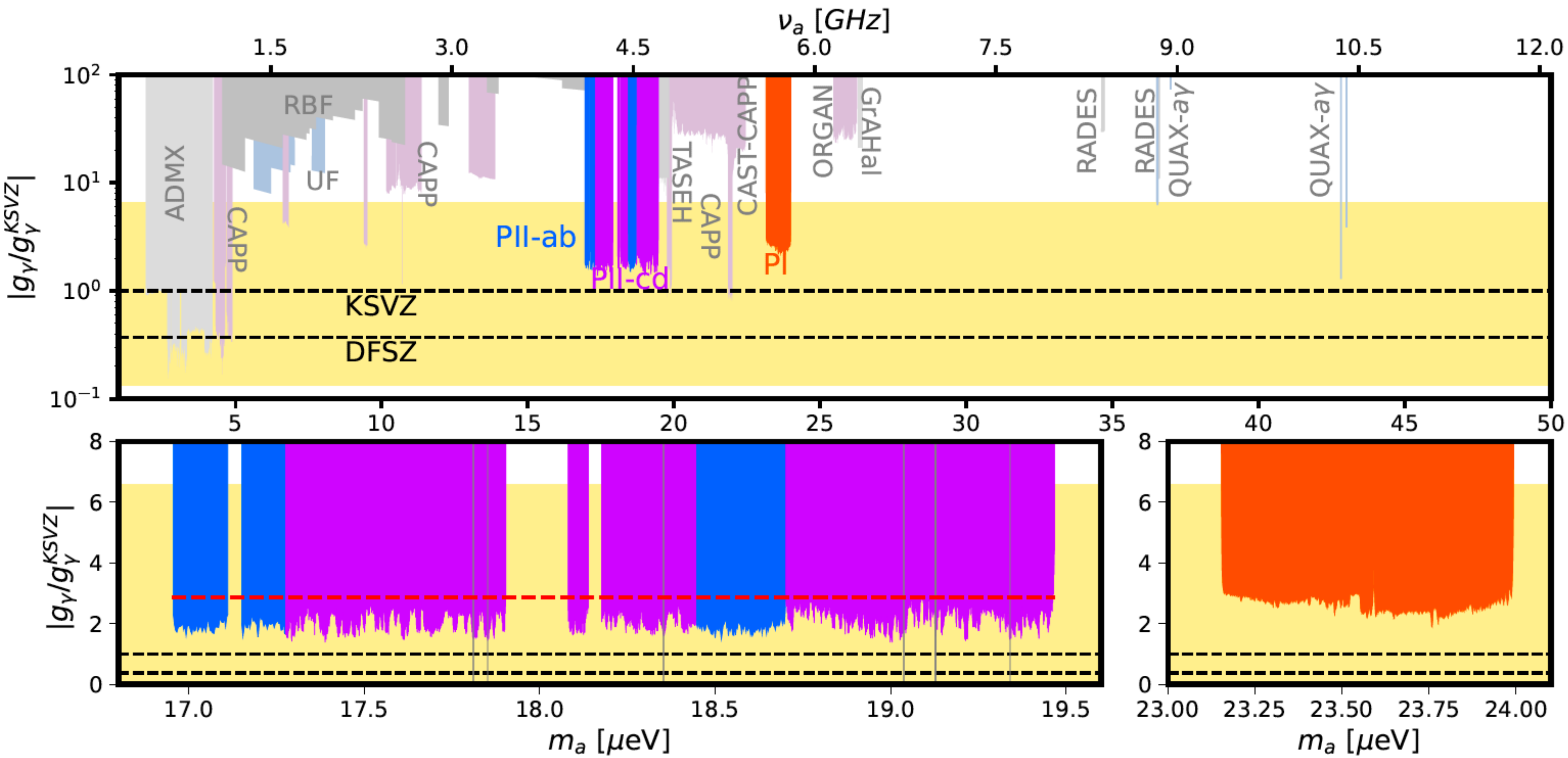

K.M. Backes *et al.*, Nature 590 (2021) 238 ; M.J. Jewell *et al.*, PRD 107 (2023) 072007 ; Xiran Bai *et al.*, PRL 134 (2025) 151006; D. Palken *et al.*, Phys. Rev. D 101 (2020) 123011 introduced Bayesian analysis to the microwave cavity experiment field

CEASEFIRE: Cavity Entanglement and State Exchange for Improved Readout Efficiency

K. Wurtz *et al.*, PRX Quantum 2 (2021) 040350
Y. Jiang *et al.*, PRX Quantum 4 (2023) 020302

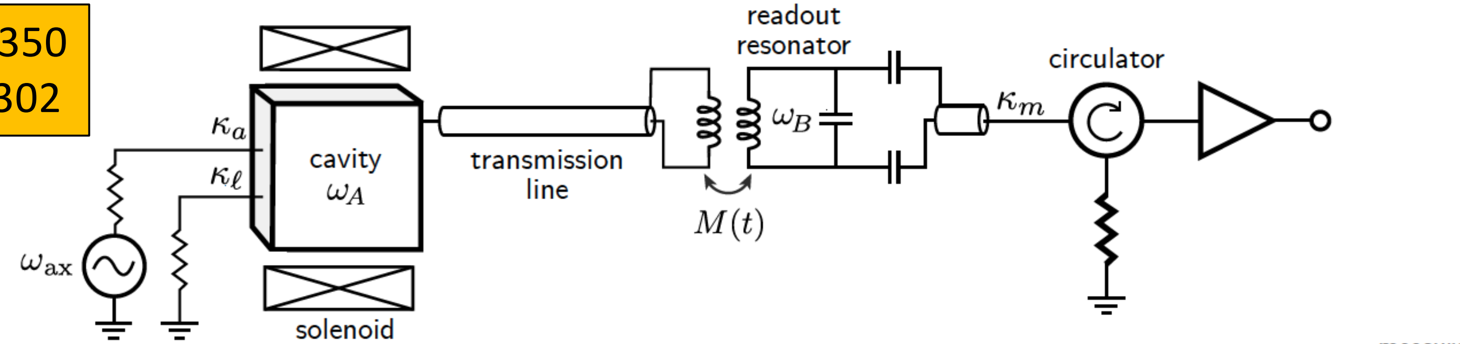

Following the same pattern of prototype-experiment twins

Will deploy for Phase IIIc HAYSTAC for in mid-2026

Projected x 10 scan speedup

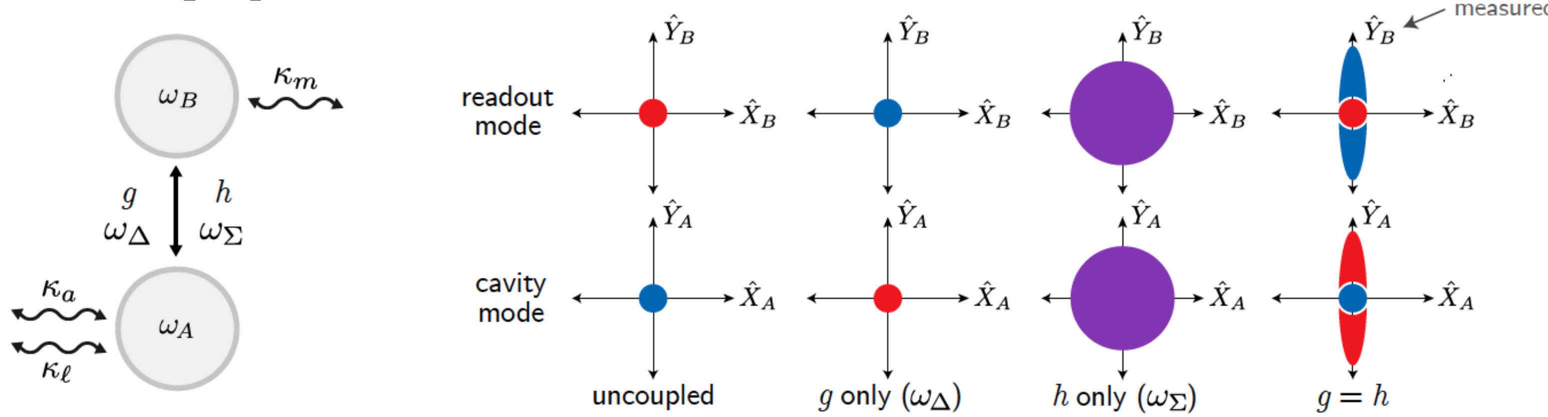

(a) Linear amplifier

(b) Squeezing

(c) Squeezing with state exchange

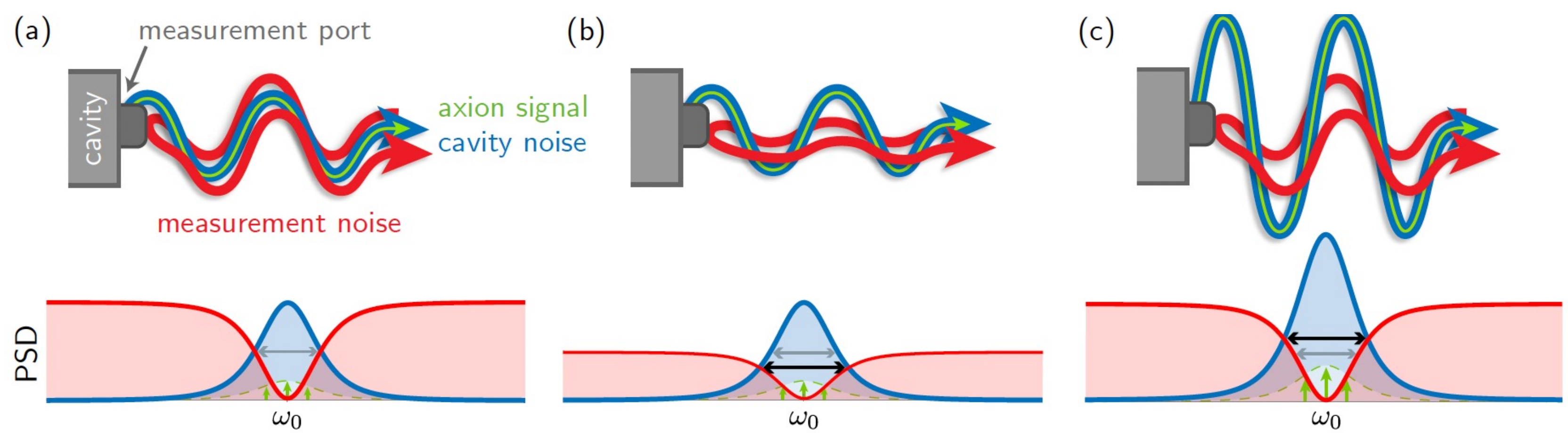

Axion Conversion Cavity

Cavity on a Chip

Modulate *M(t)* @

ω_Σ : Entangle

ω_Δ : Exchange

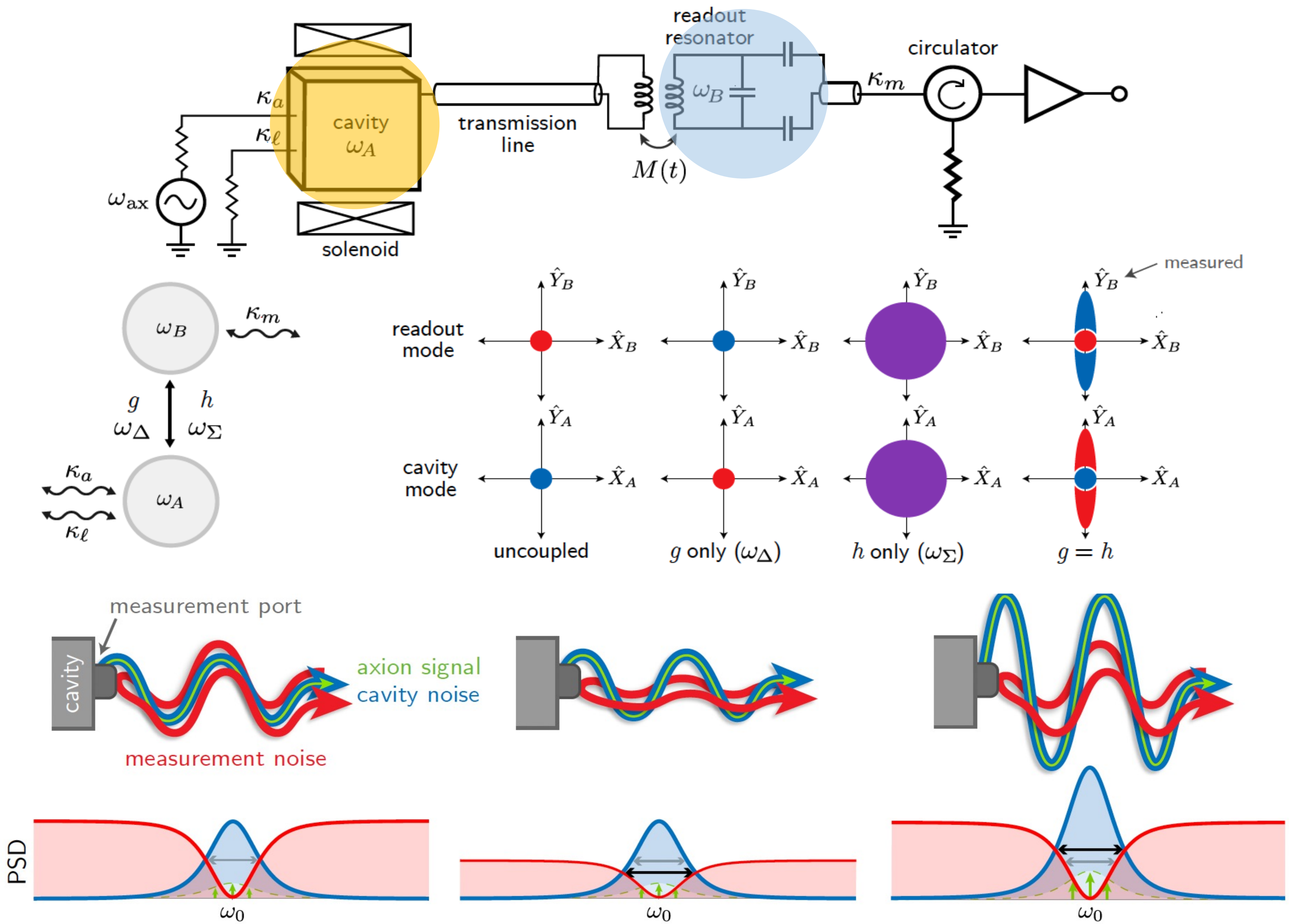

Crossover point between Linear Amplifiers etc. and Single Quantum Detection

- There will be a frequency above which single quantum detection will be more sensitive and the advantage will grow with frequency:
  - S.K. Lamoreaux *et al.*, PRD 88 (2013) 035020
  - E. Graham *et al.*, PRD 109 (2024) 032009
- The RAY (Rydberg Atoms @ Yale) is working toward the potential implementation in HAYSTAC and ALPHA.

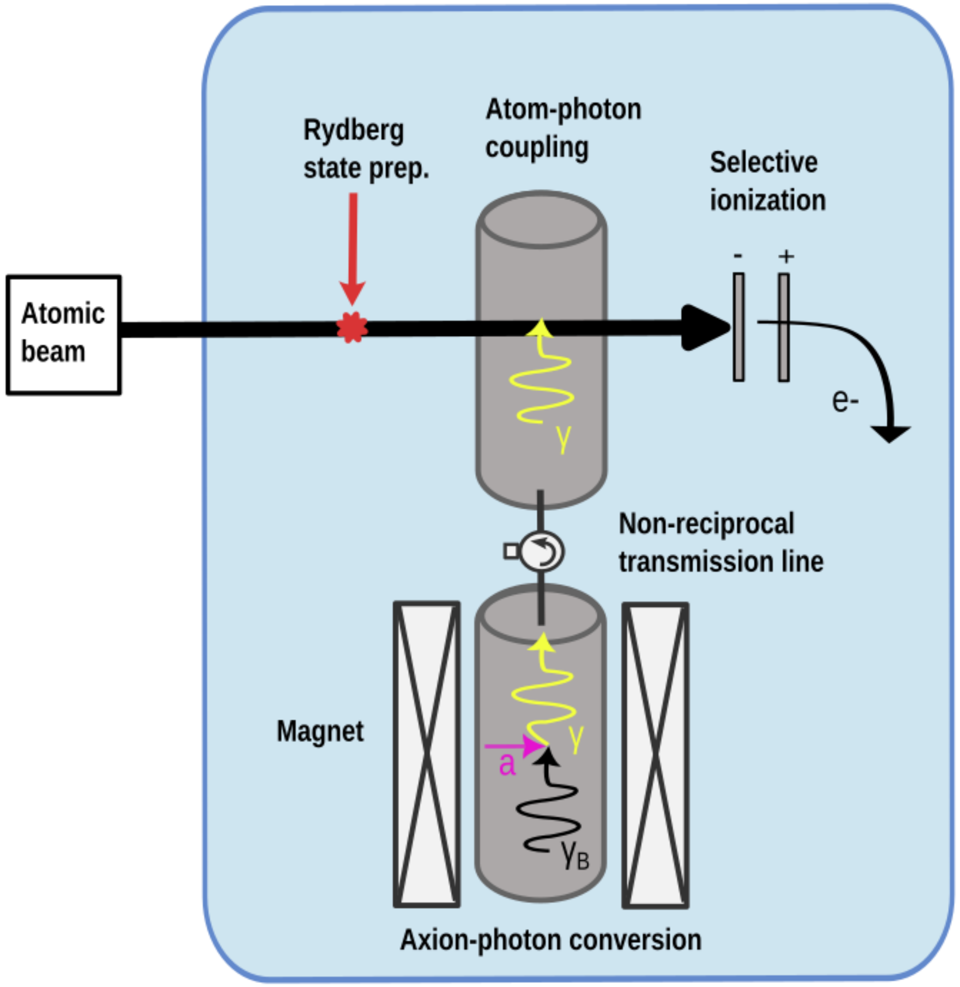

The CARRACK (Kyoto) Rydberg-atom Single Photon Detector (S. Matsuki *et al.*)

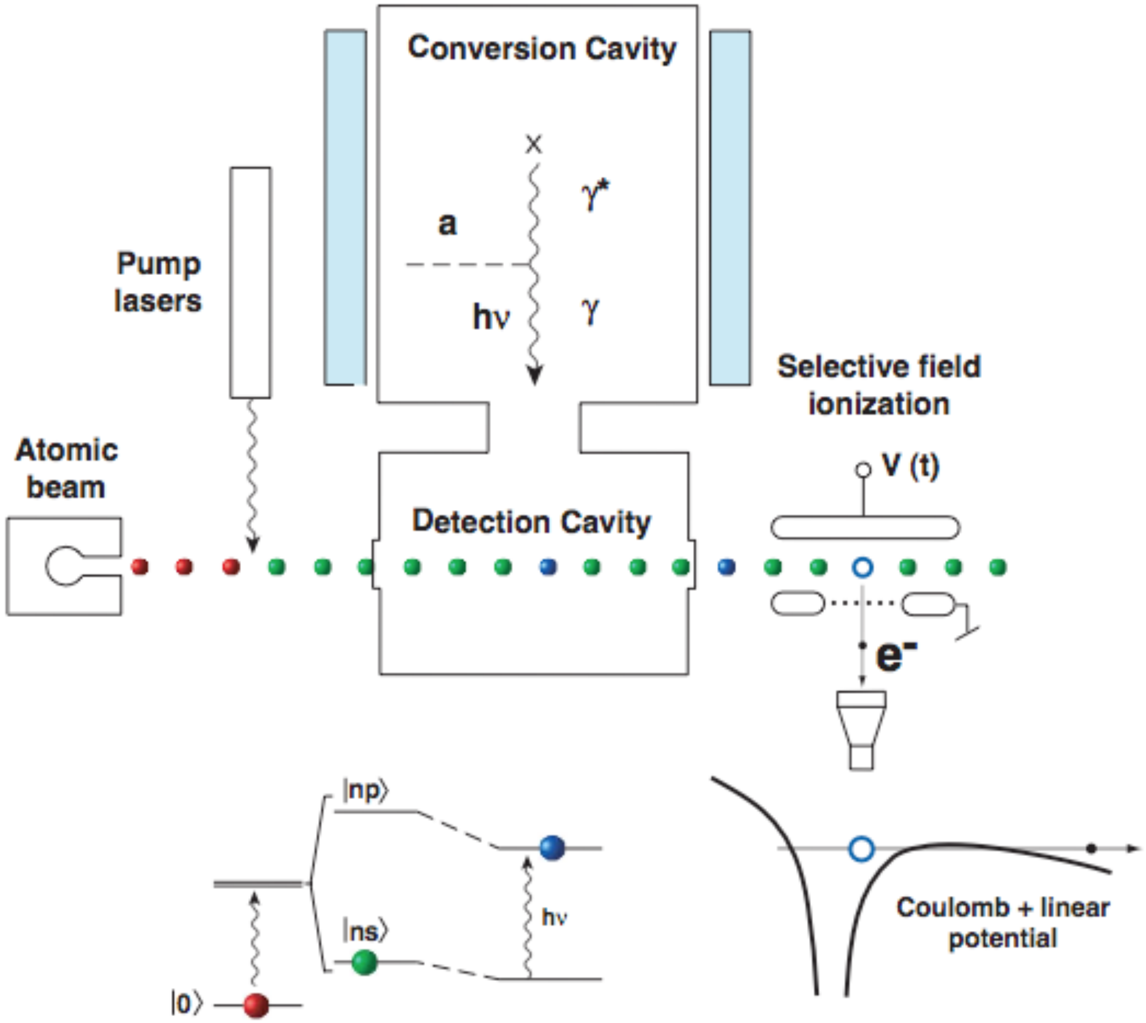

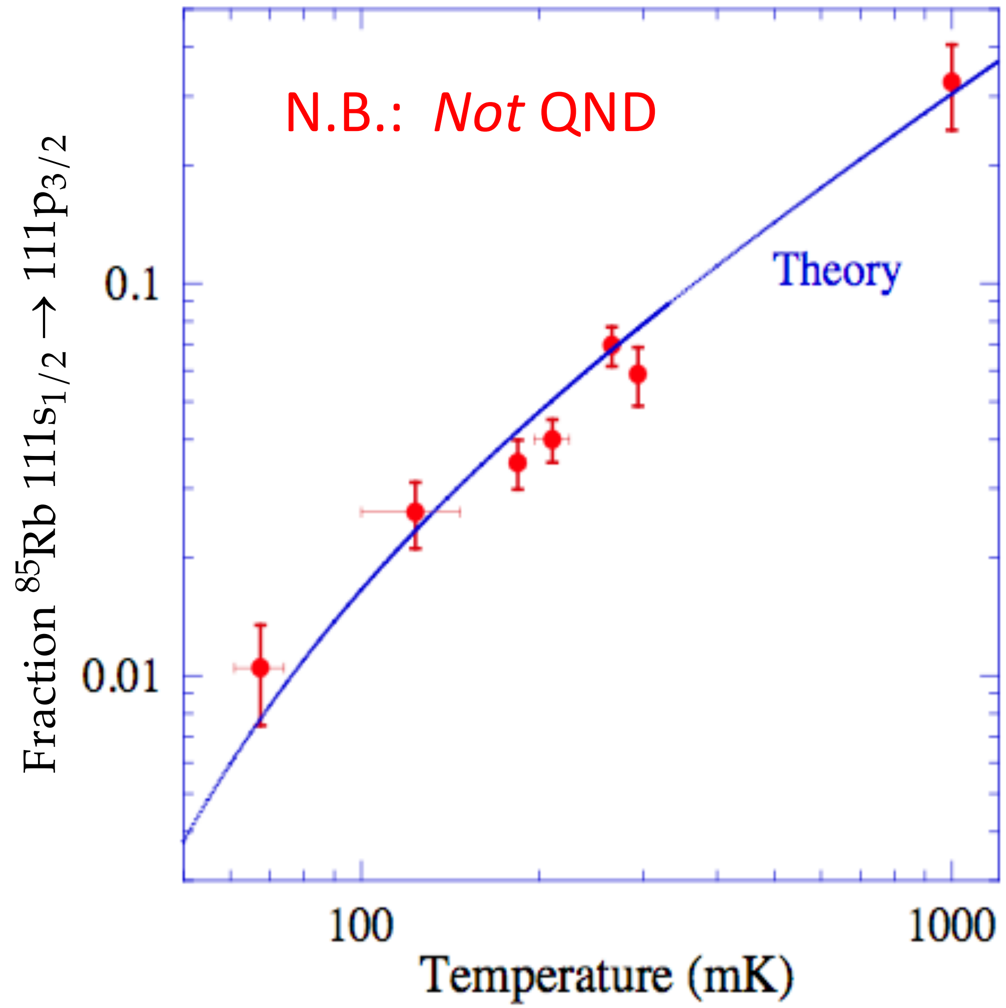

Tada *et al. Phys. Lett. A* 349:488 (2006) demonstrated a receiver a factor ~2 below SQL at 2.527 GHz (~120 mK).
DFSZ exclusion at ~10 μeV presented at conference (Matsuki, 1997), but never published in a refereed journal.

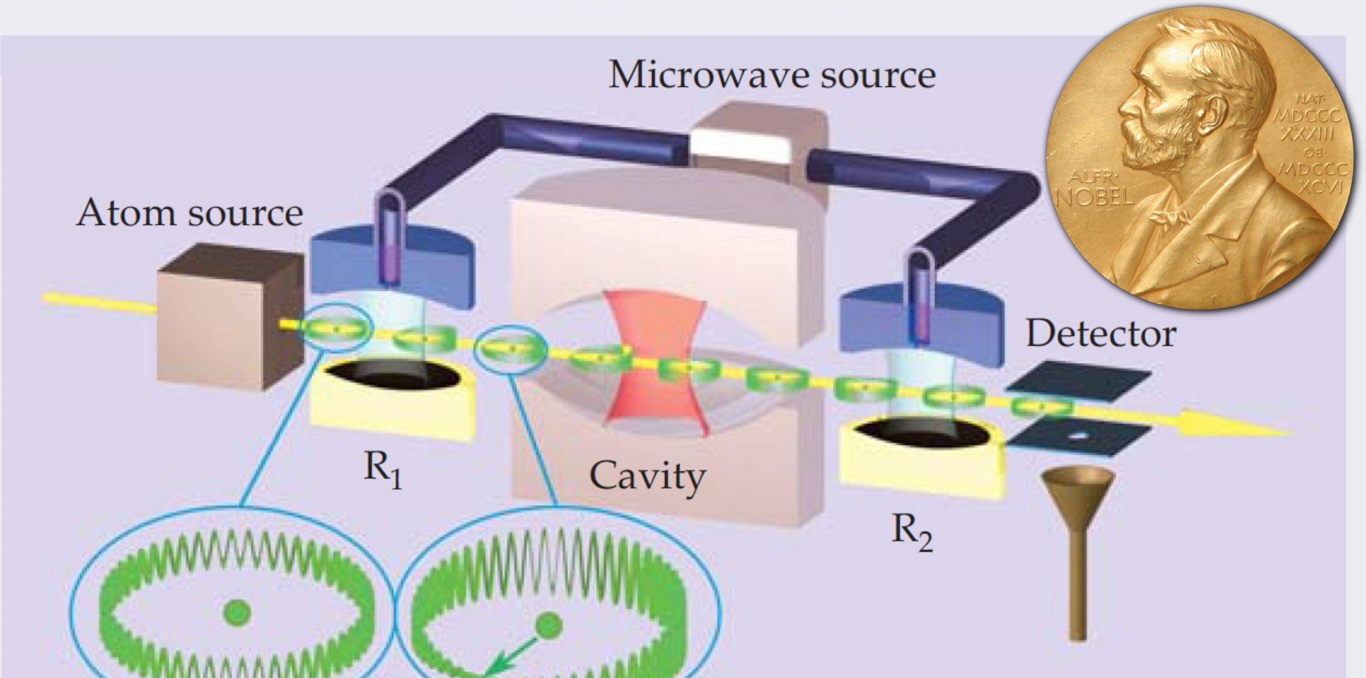

S. Gleyzes *et al.*, Nature 446 (2007) 297

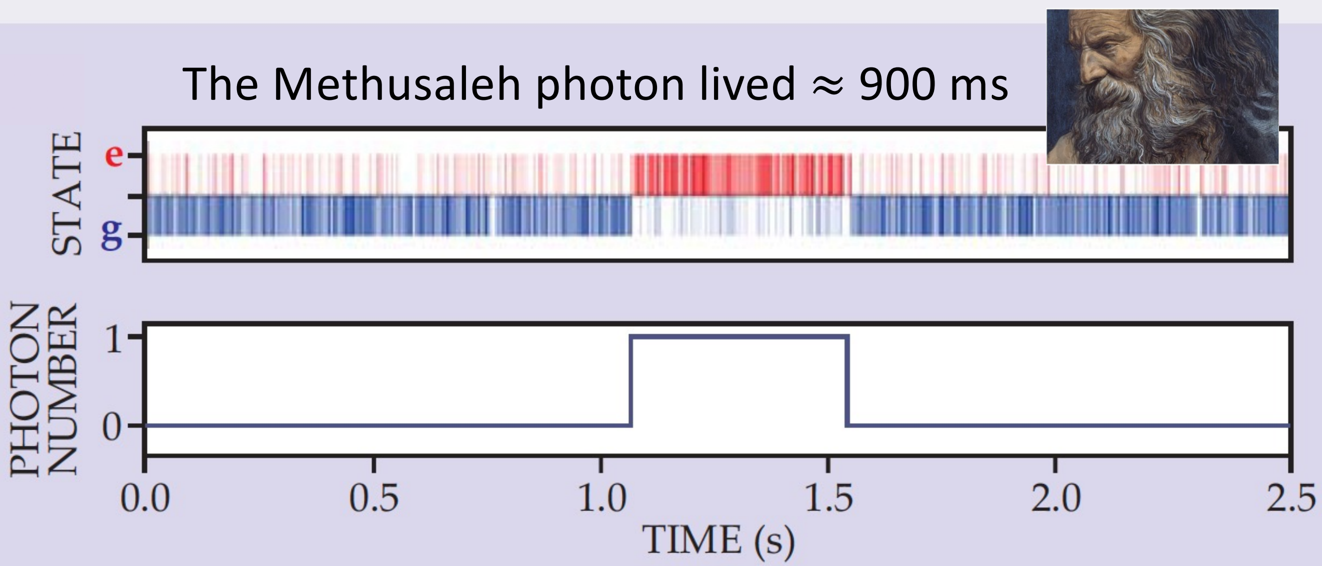

QND Measurement of Single Photons

- Serge Haroche's Quantum Non-Demolition observation of individual photons, based on a Ramsey interferometer.
- A microwave source is tuned close to the $n = 50 \rightarrow 51$ ($p \rightarrow s$) transition energy, creating a superposition which evolves at the phase difference between the microwave transition frequency, resulting in a large rotating dipole moment.
- An off-resonant photon in the optical cavity perturbs the atomic potential, thus shifting the phase & changing the g , e measurement probabilities at the detector. Individual photons are thus detected without destroying them.
- A R&D program at Yale is ramping up to look at the applicability of Rydberg atom as a single-quantum detector (non-QND) for HAYSTAC and beyond ("RAY" – Reina Maruyama, PI).

HAYSTAC – Phase III and beyond

P-IIIa

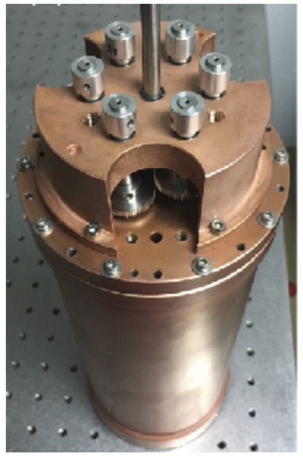

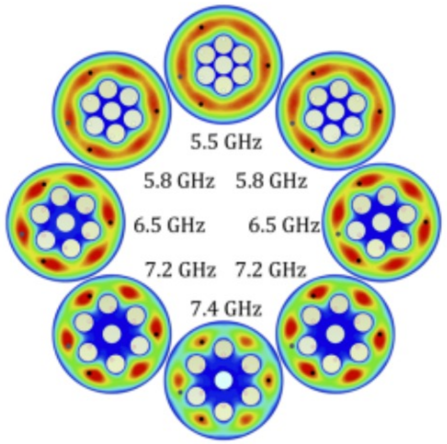

Rev.Sci.Instrum. 92 (2021)

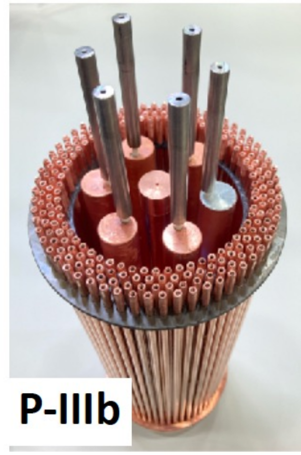

arXiv:2411.18914 (2024)

Lehnert Group:
Y. Jiang et al., PRX Quantum 4 (2024)

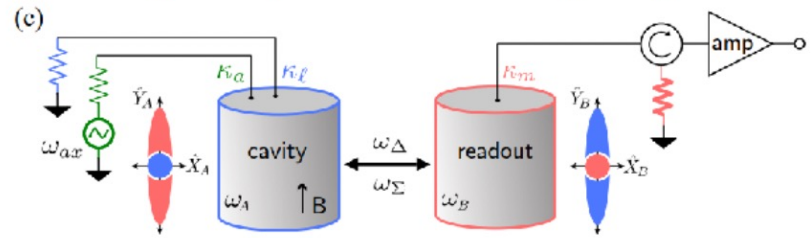

P-IV

van Bibber group:

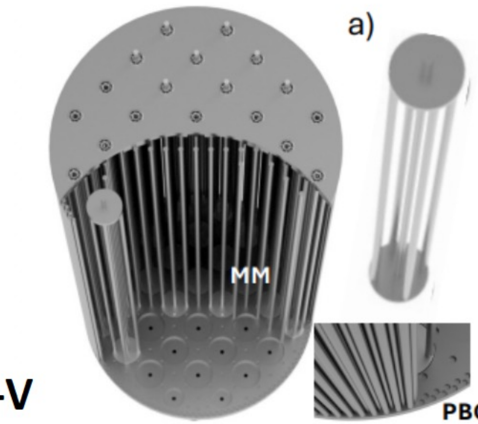

P-V

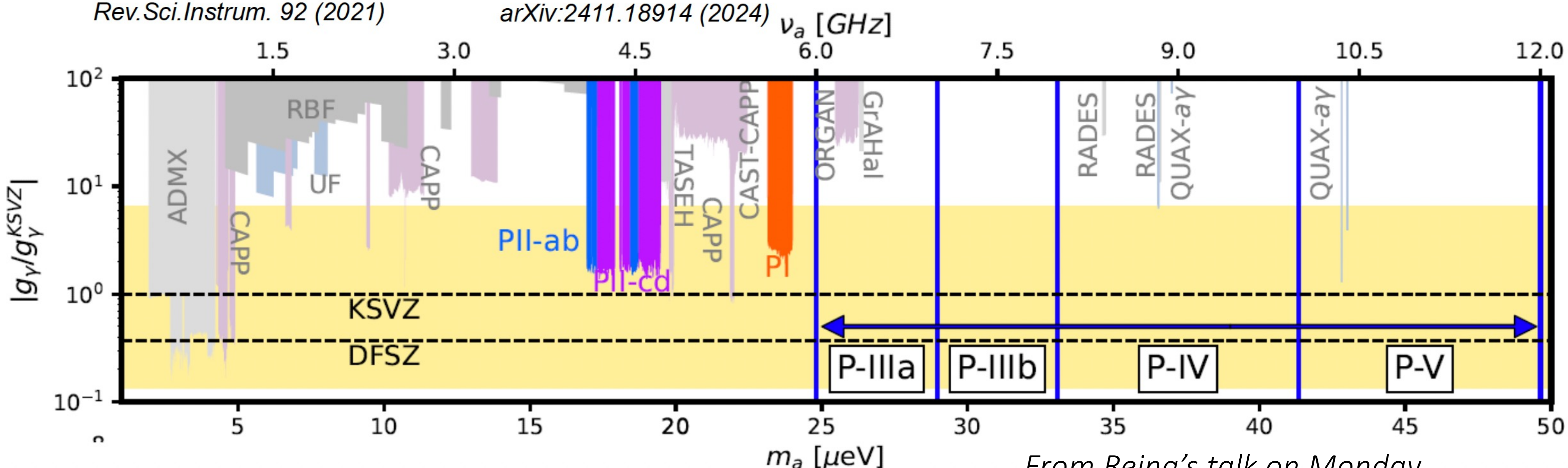

From Reina's talk on Monday

Axion **L**ongitudinal **P**lasma **Ha**loscope

Small-Scale Experiments That Advance Fundamental Physics

Yale University [1]
University of California Berkeley [2]
Colorado University
Johns Hopkins University
Massachusetts Institute of Technology
Wellesley College
Arizona State University
Oak Ridge National Laboratory
Stockholm University
Iceland University [3]
ITMO University
Cambridge University

[1] *Host Institution*
[2] *PI Institution*
[3] *Inaugural Spokesperson: Jón Gudmundsson*

Together, Math and Science Foundations Fund 'Tabletop' Physics That Could Transform Our Understanding of the Universe

December 11, 2023

University of California, Berkeley graduate student Heather Jackson performs research on metamaterial resonators to be used in the plasma haloscope search for dark matter axions. AJ Gubser, UC Berkeley

The Tunable Plasma Haloscope *M. Lawson et al., PRL 123 (2019) 141802*

Microwave Cavity

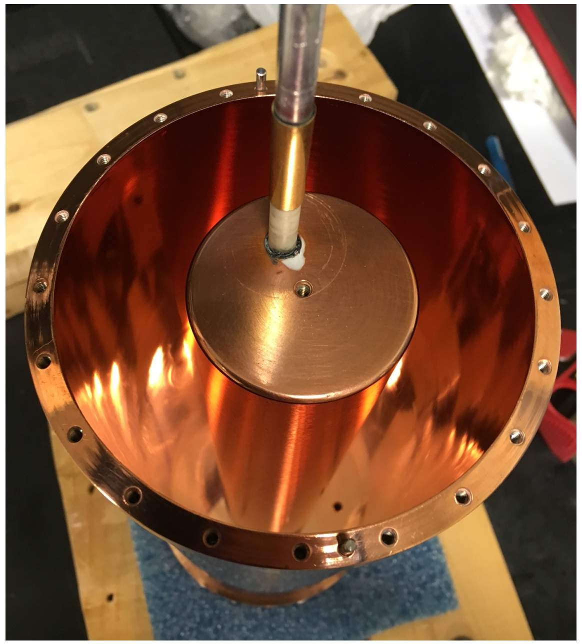

Frequency determined by boundary conditions (size)

Metamaterial Resonator

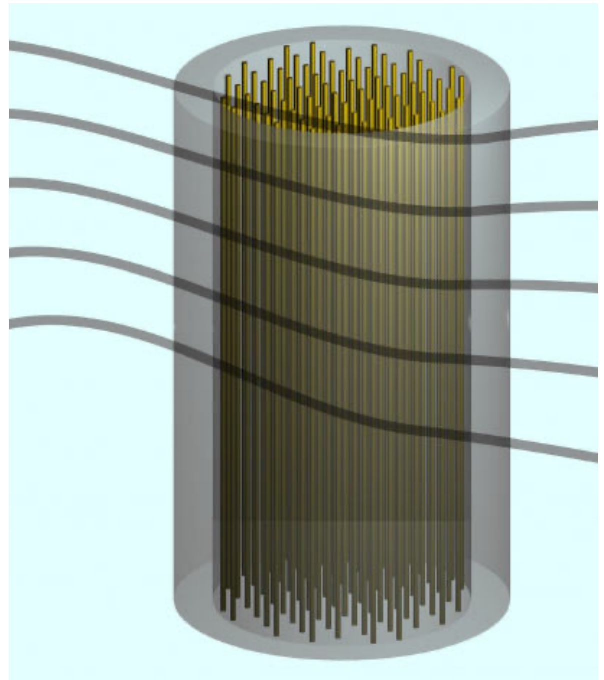

Frequency determined by bulk property (unit cell)

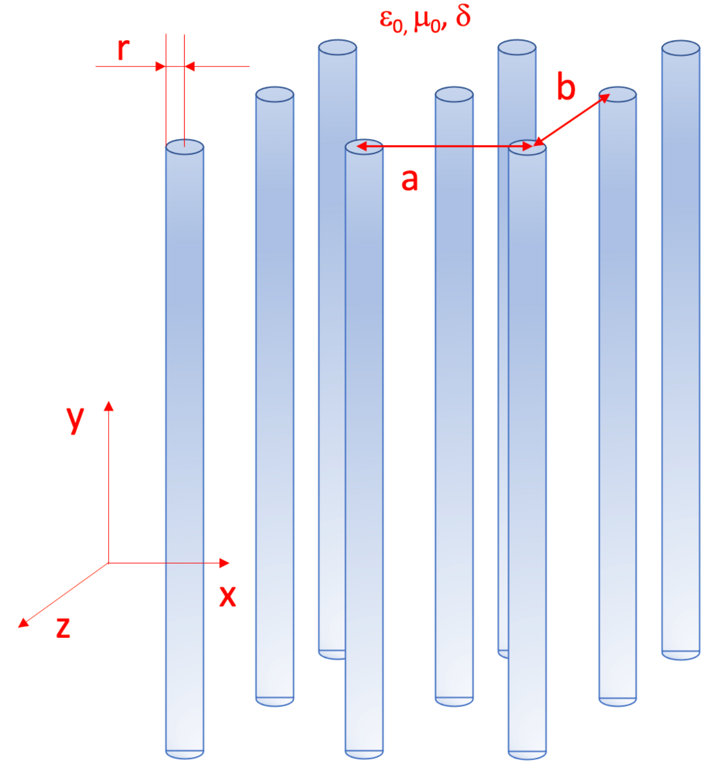

For square lattice of wires, radius *r*, spacing *a* :

$$\boxed{\omega_p^2 = \frac{n_e e^2}{m_{eff}} = \frac{2\pi}{a^2 \log(a/r)}}$$

r = 25 μm, *a* = 5 mm → ν_{pl} = 10 GHz

J.B. Pendry *et al.*, J. Phys.: Condens. Matter 10 (1998) 4785

Fulfills promise of a resonator that is both arbitrarily high in frequency and arbitrarily large in volume!

Metamaterials @ Berkeley: S_{21} measurements of basic properties & tuning

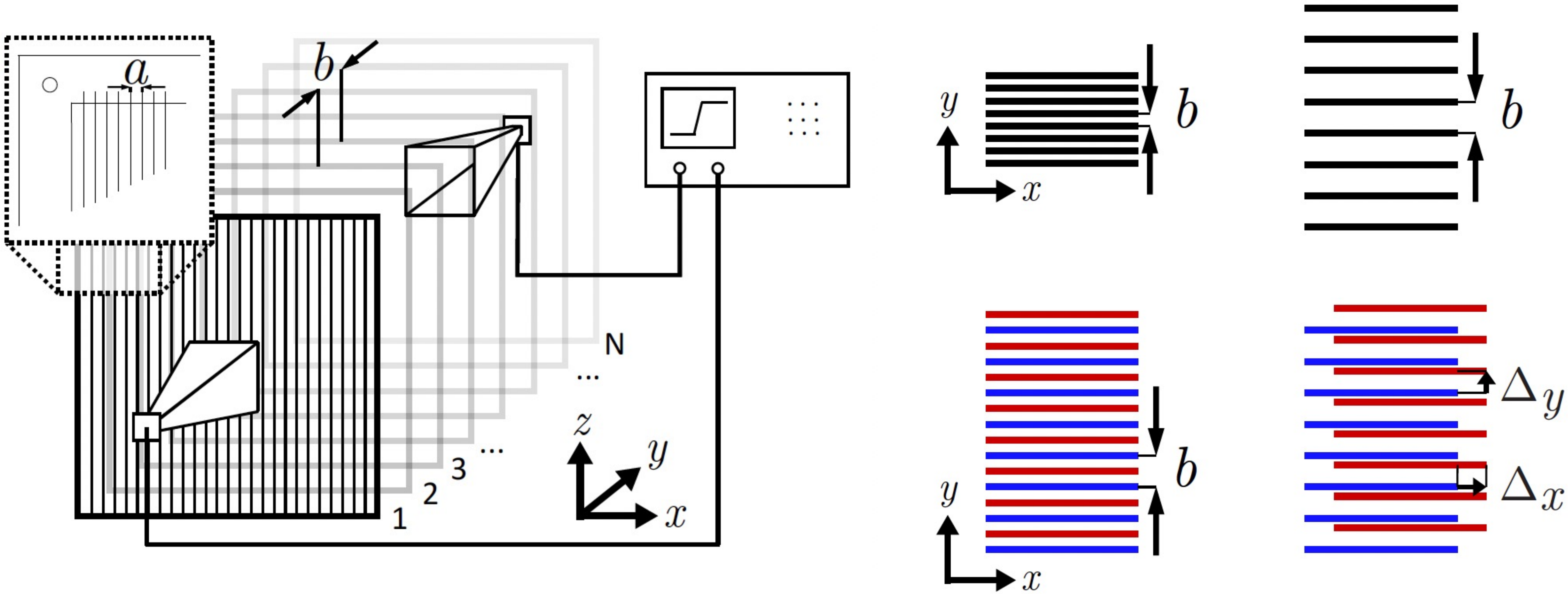

Make planes of thin wires, stack them, and study the microwave transmission spectrum as a function of number, spacing and relative positioning

The wire frames & array

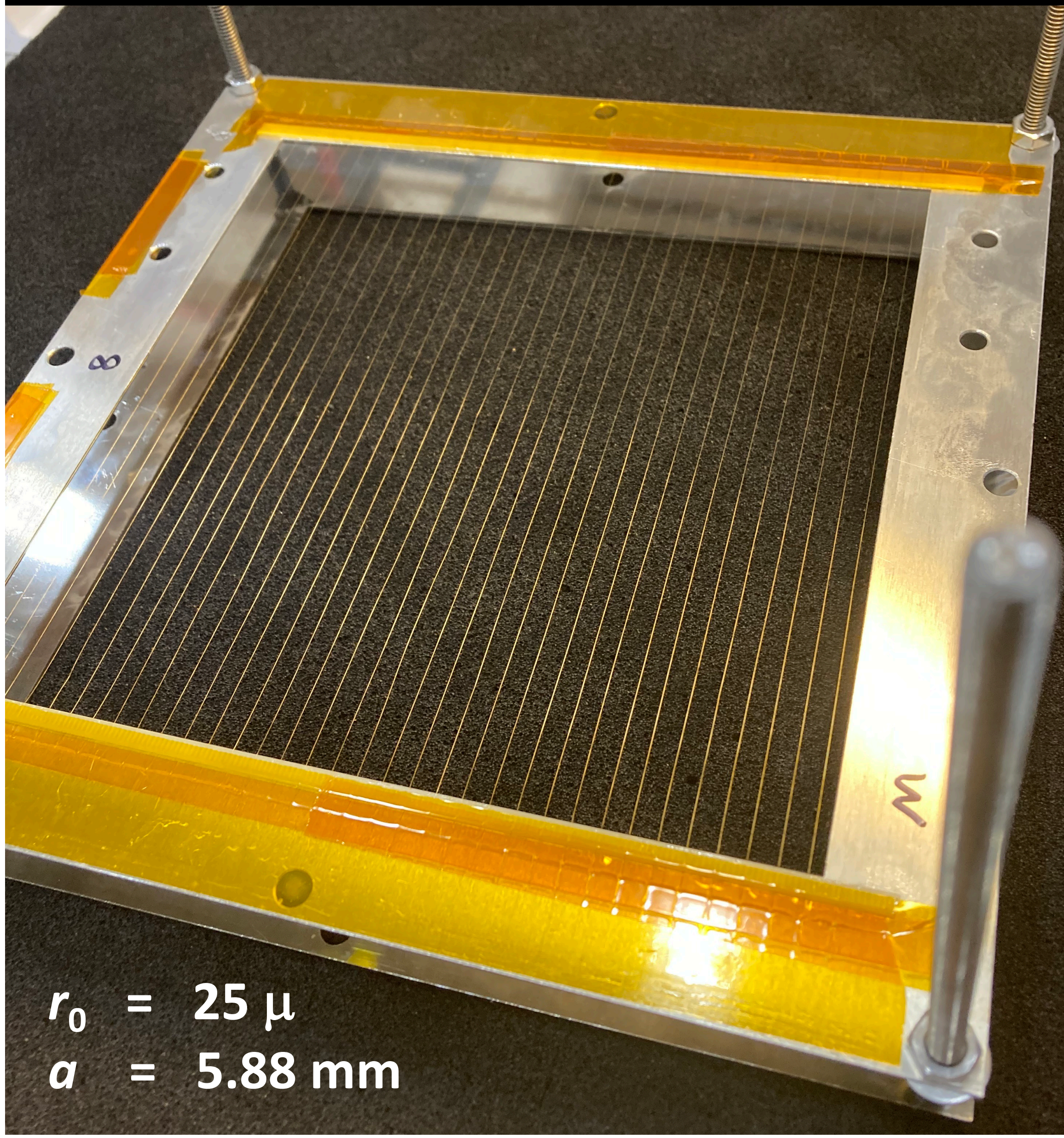

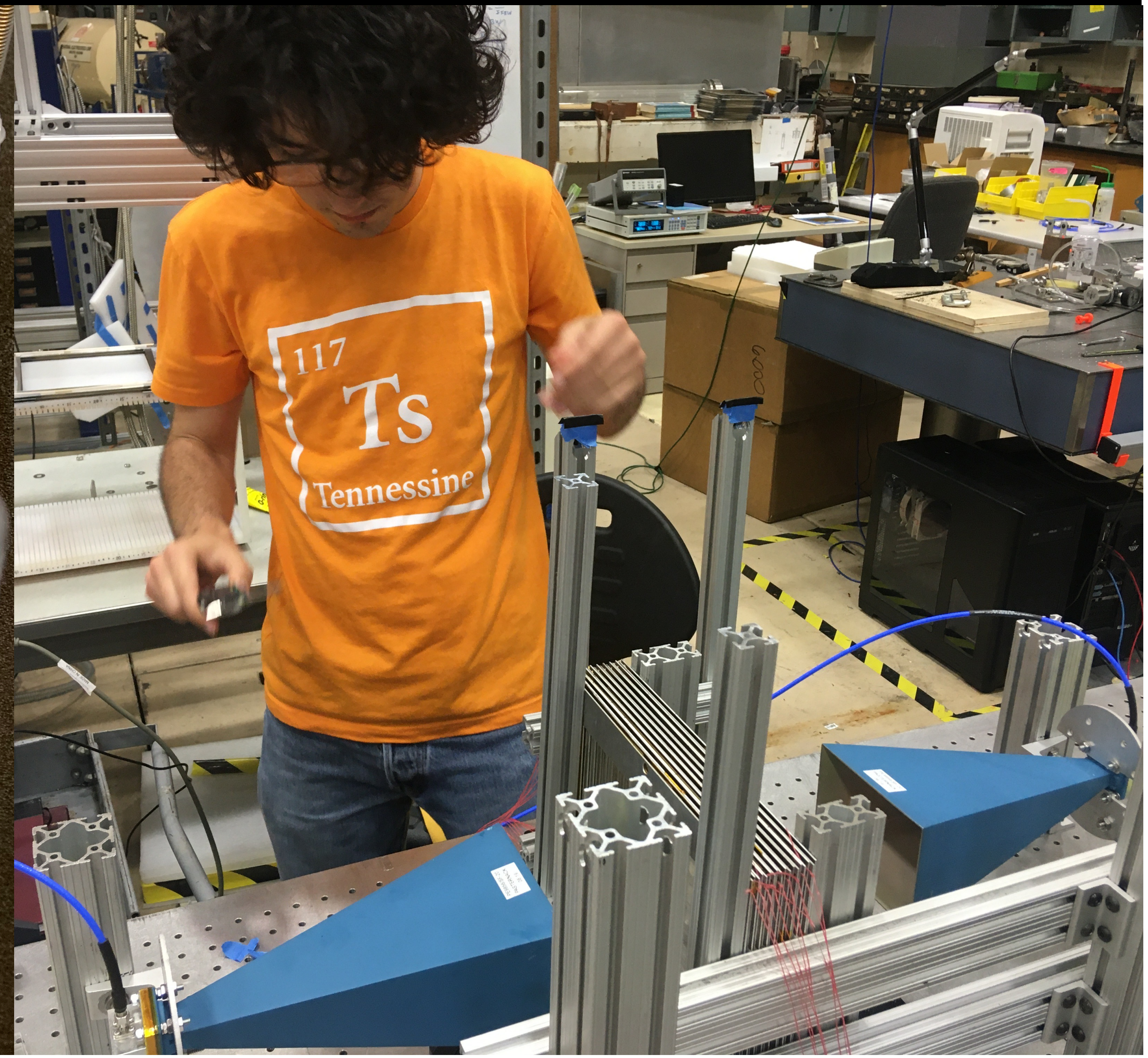

Extracting parameters from S_{21} for a complex, frequency dependent medium

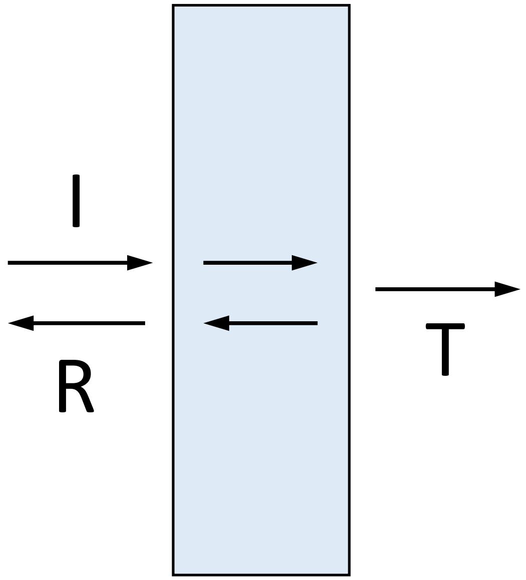

$$\epsilon' = \left(1 - \frac{\omega_p^2}{\omega^2 + \Gamma^2}\right)$$

$$\epsilon'' = \left(\frac{\Gamma}{\omega}\right)\frac{\omega_p^2}{\omega^2 + \Gamma^2}$$

$\longrightarrow$ S_{21} (= t)

$\longrightarrow$ ν_{pl} , Γ, d

Fix: ν_{pl} = 8.4 GHz, Γ = 0.01 GHz
Vary: d = 0 – 196 mm

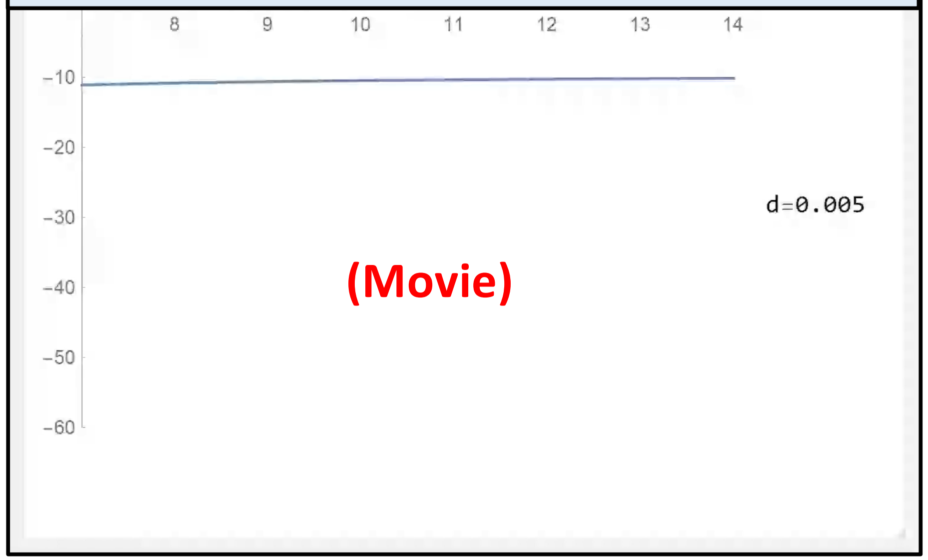

Fix: ν_{pl} = 8.4 GHz, d = 88 mm
Vary: Γ = 0.0 – 0.50 GHz

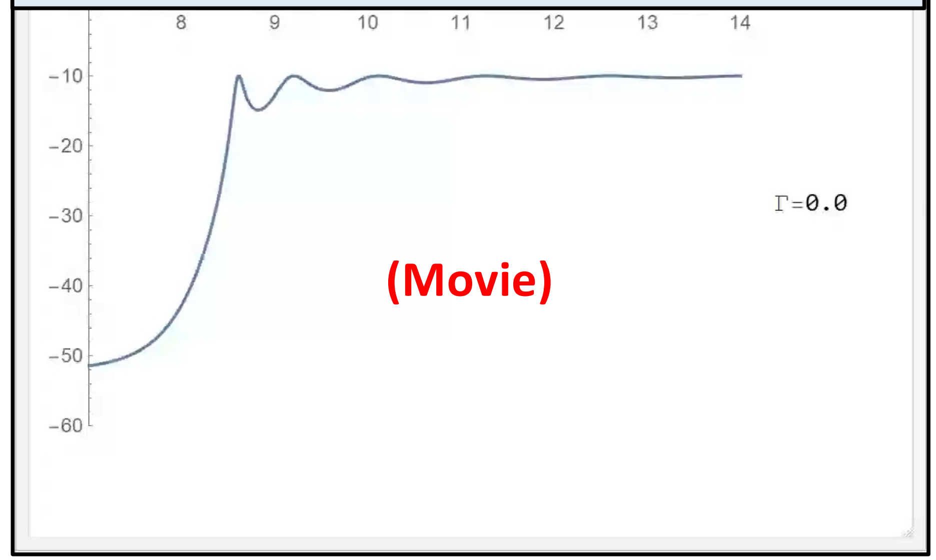

Spectra are fit with the semianalytic theory of
P. Belov *et al.*, Phys. Rev. B 67, 113103 (2003)

Early onset of plasmonic behavior & systematics *M. Wooten et al., Ann. Phys. (2023) 2200479*

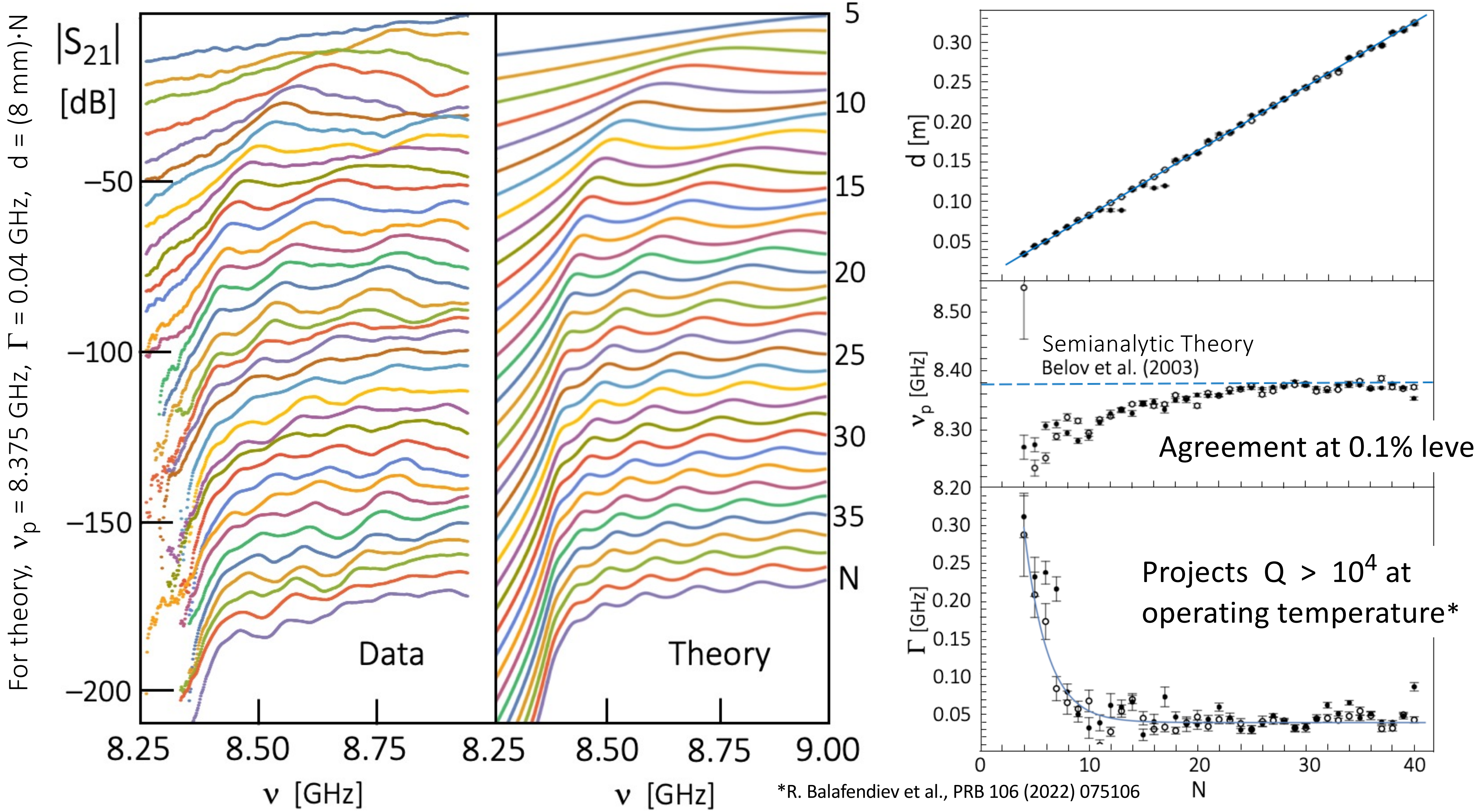

*R. Balafendiev et al., PRB 106 (2022) 075106

Resonator broadly tunable by changing the metamaterial's unit cell

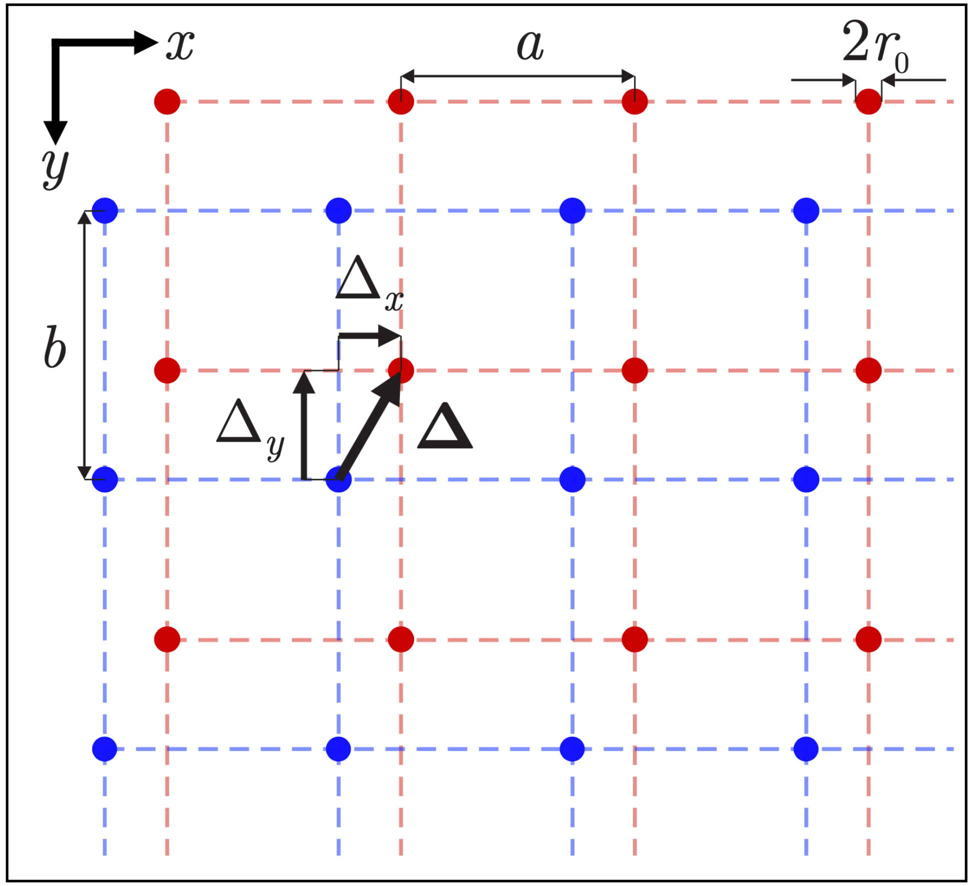

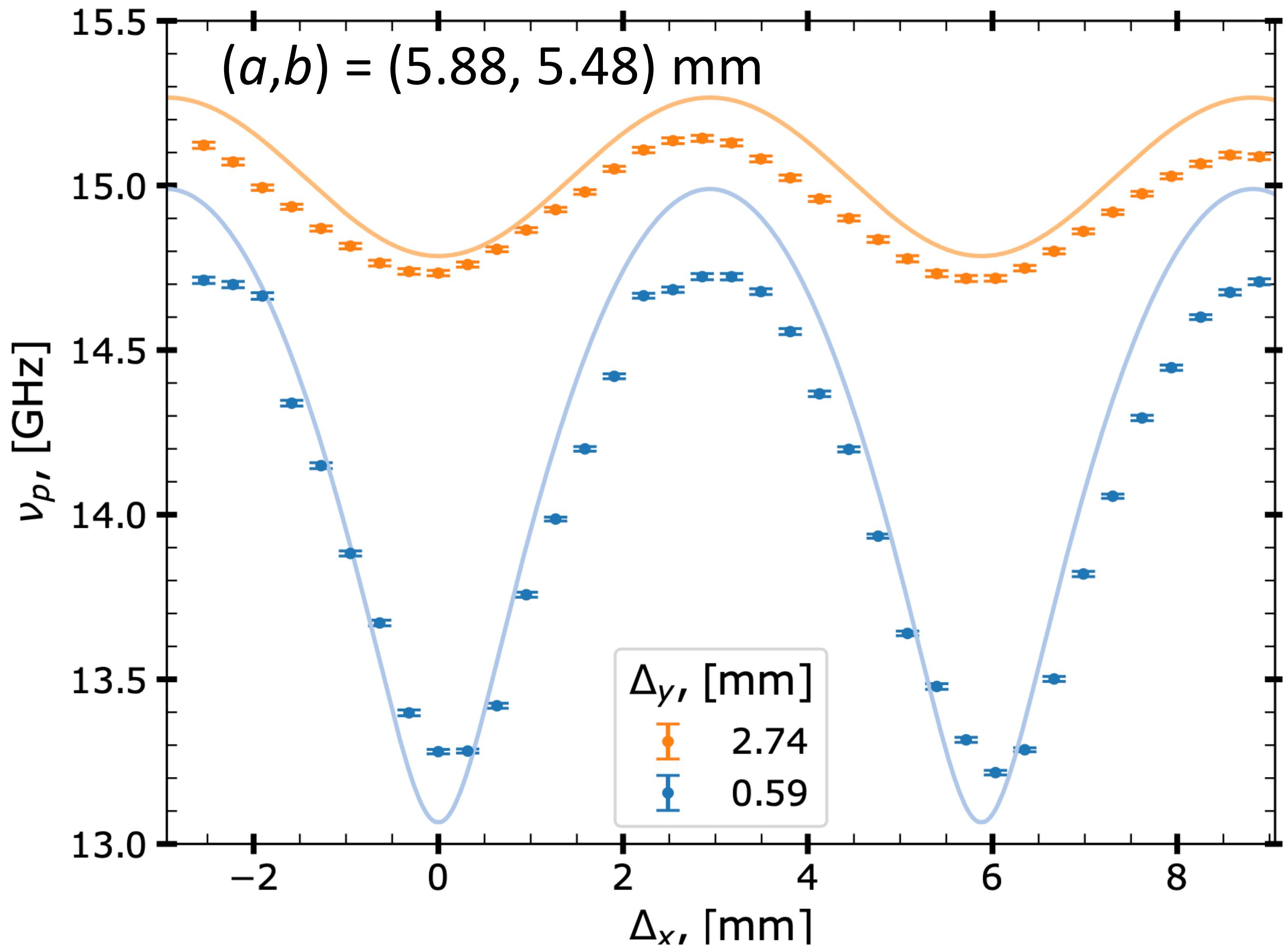

N. Kowitt *et al.*, Phys. Rev. Appl. 20 (2023) 044051

Symmetric 6-rod tuner with conventional b.c.

Spectrum is dominated by forest of TE modes; TM_{010} mode of interest completely fragmented and lost

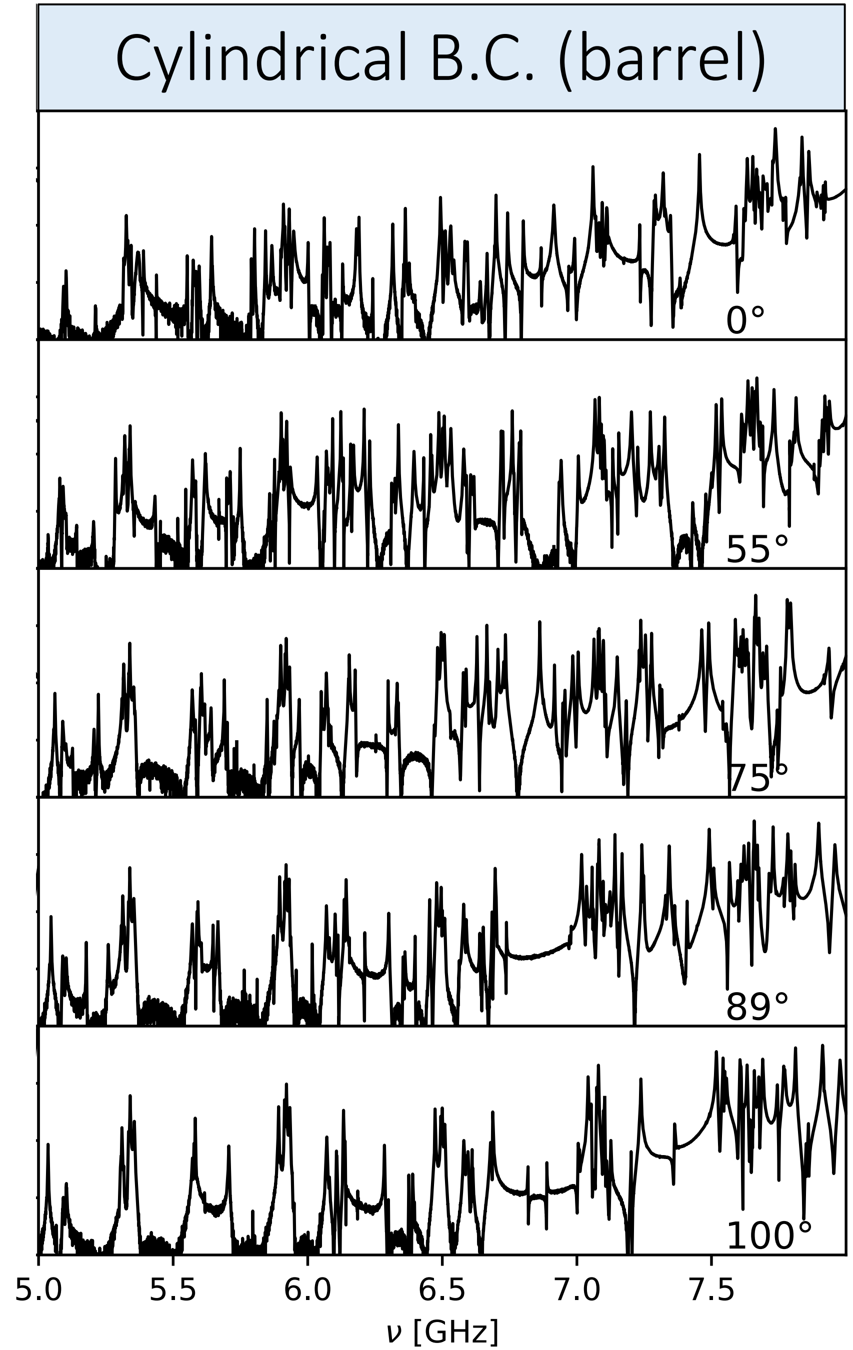

Field Mapping – Bead Perturbation method

$$\frac{\Delta\omega}{\omega} = \frac{-(\epsilon-1)}{2}\frac{V_{\text{bead}}}{V_{\text{cav}}}\frac{E(r)^2}{\langle E(r)^2\rangle_{\text{cav}}}$$

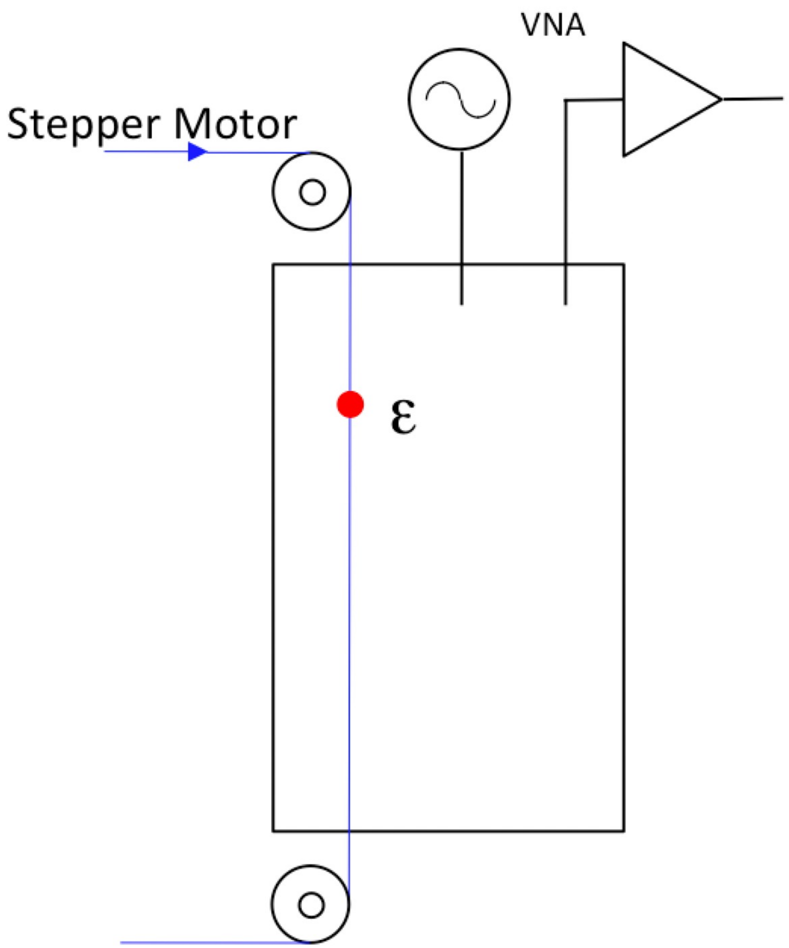

Discontinuities in Waveguides, J. Schwinger & D. Saxon (1968)

Example: TEM (n = 19)

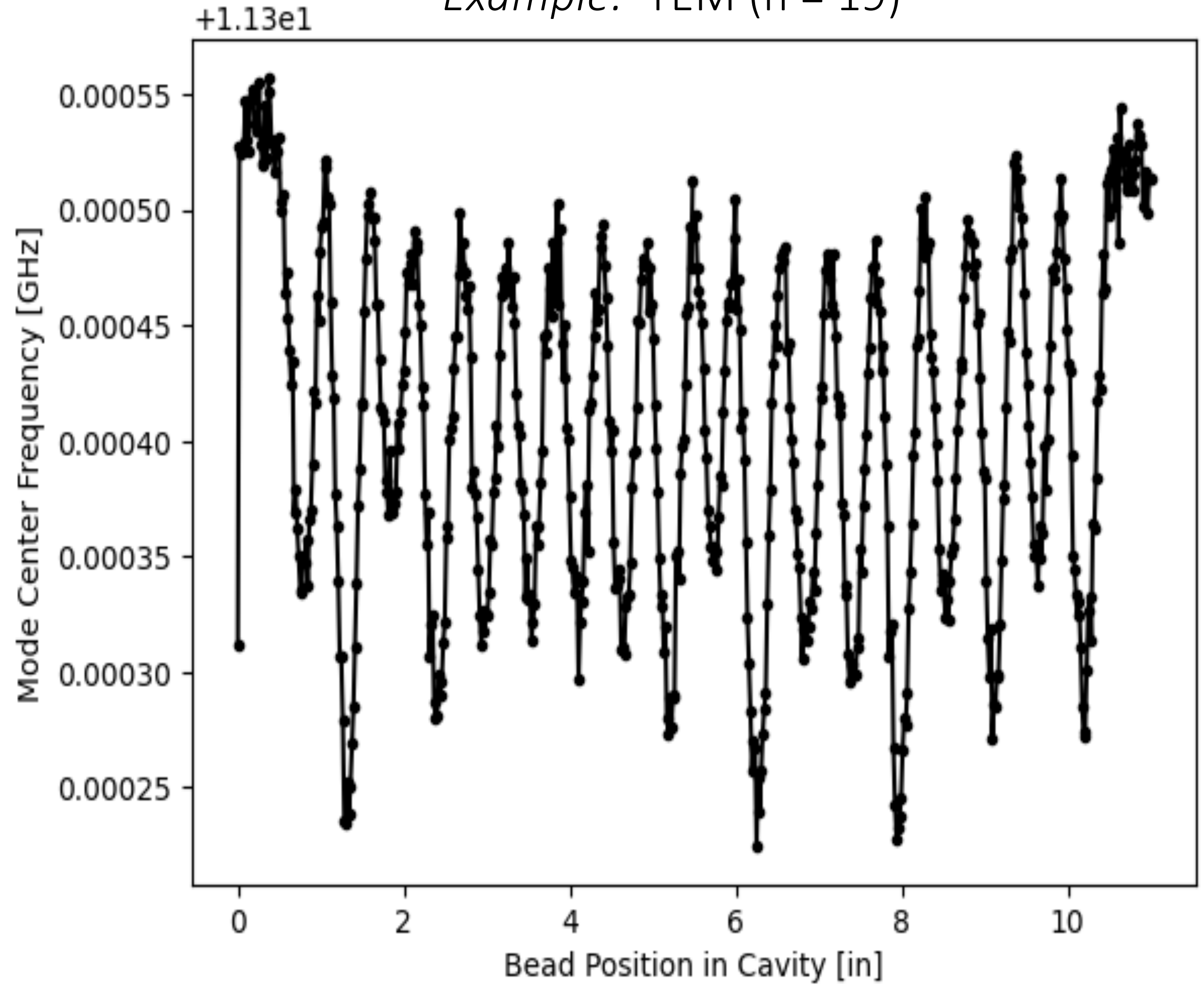

Mode hybridization is a serious problem & ultimately fatal at higher frequencies

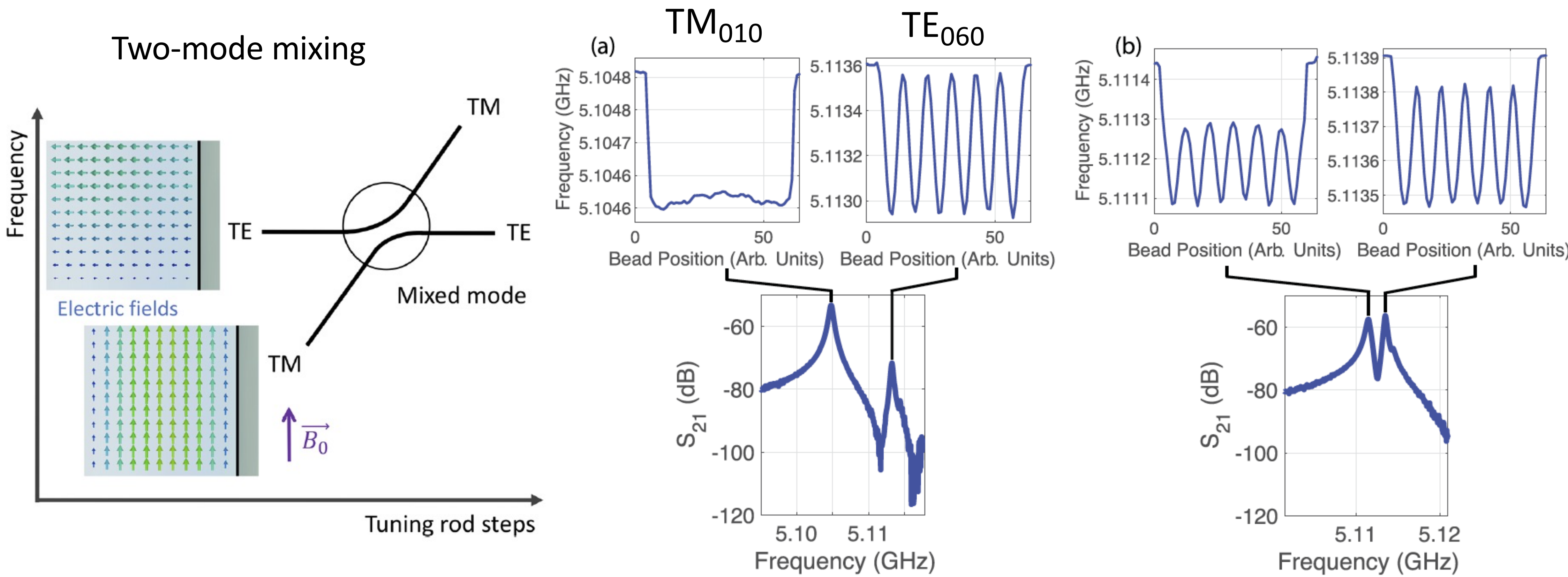

Some crossings benign; most require excision of a large notch in frequency

Photonic Band Gap Resonators (Yablonovitch, Kroll, Temkin, ...)

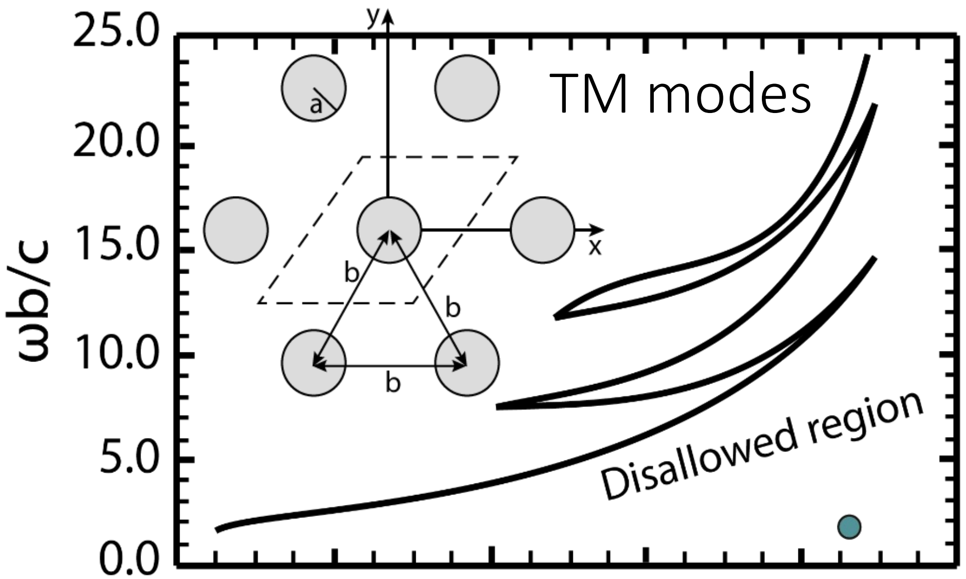

E. Smirnova et al., J. App. Phys. 91 (2002) 960

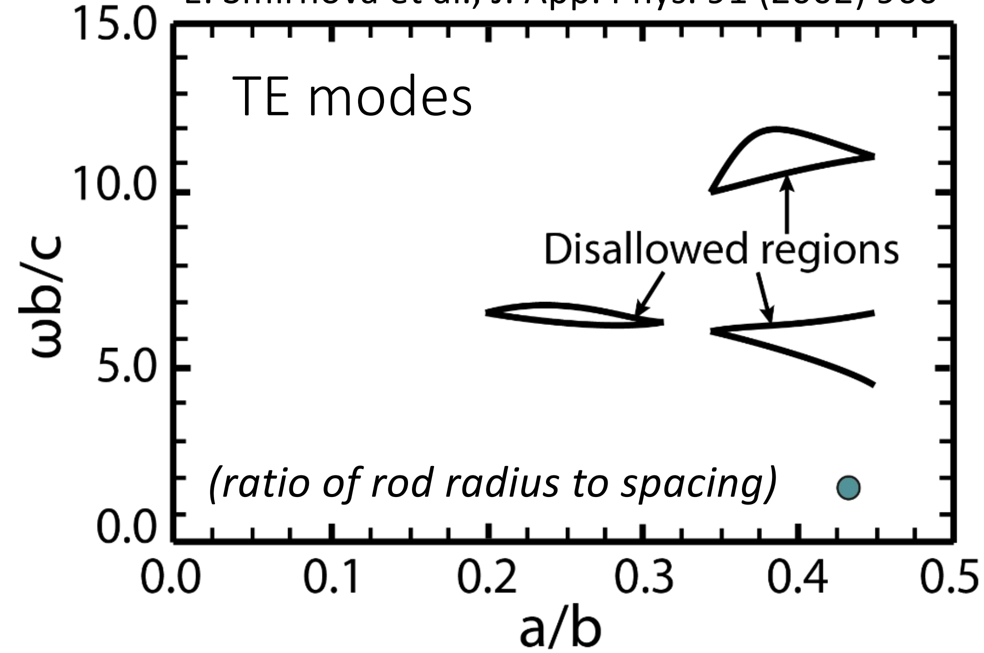

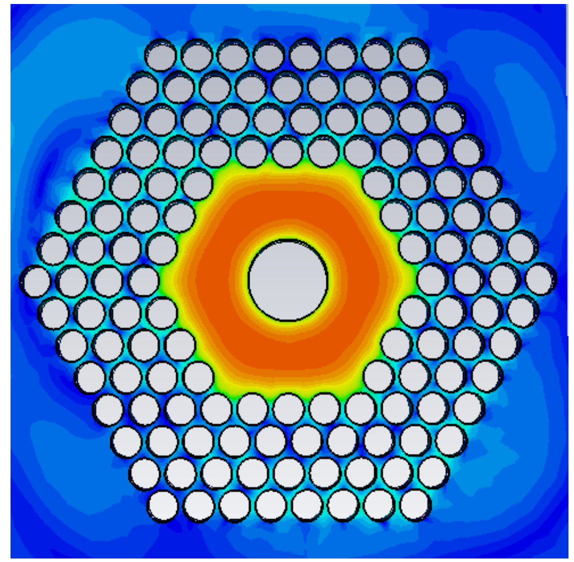

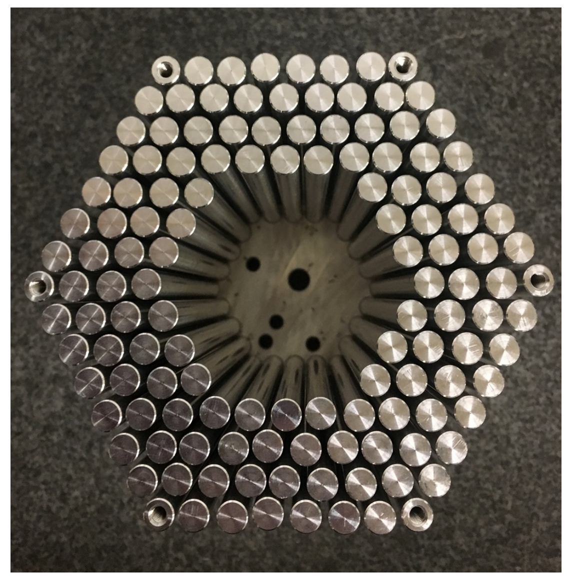

S.M. Lewis *et al.*, 2408.03861, in revision PRD

Thin circular Photonic Band Gap structures to suppress forest of TE modes

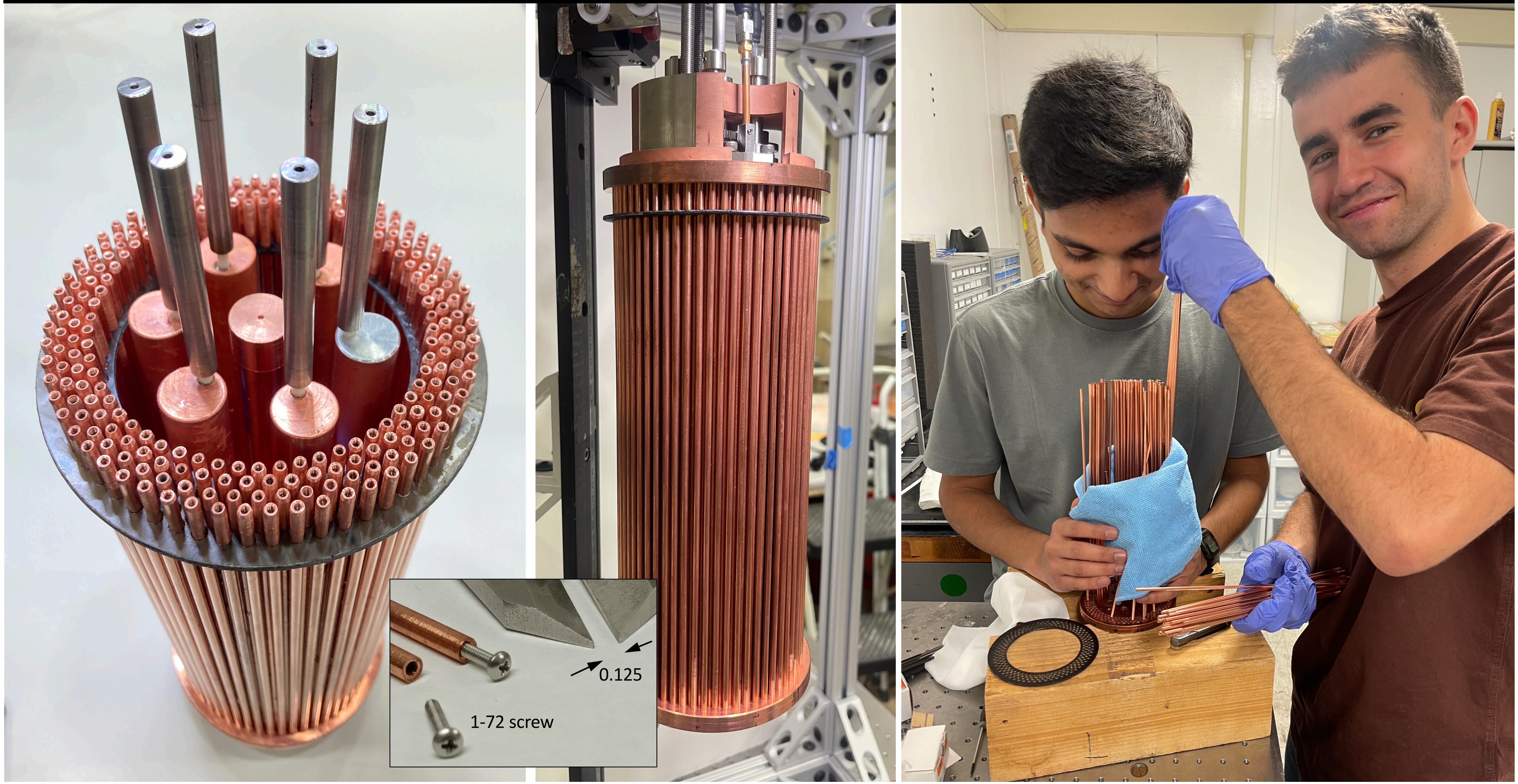

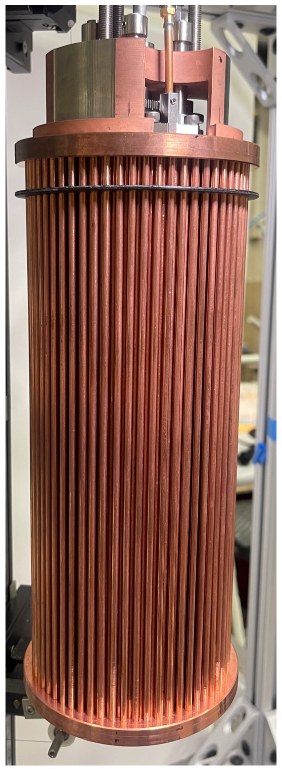

6-Rod
PBG

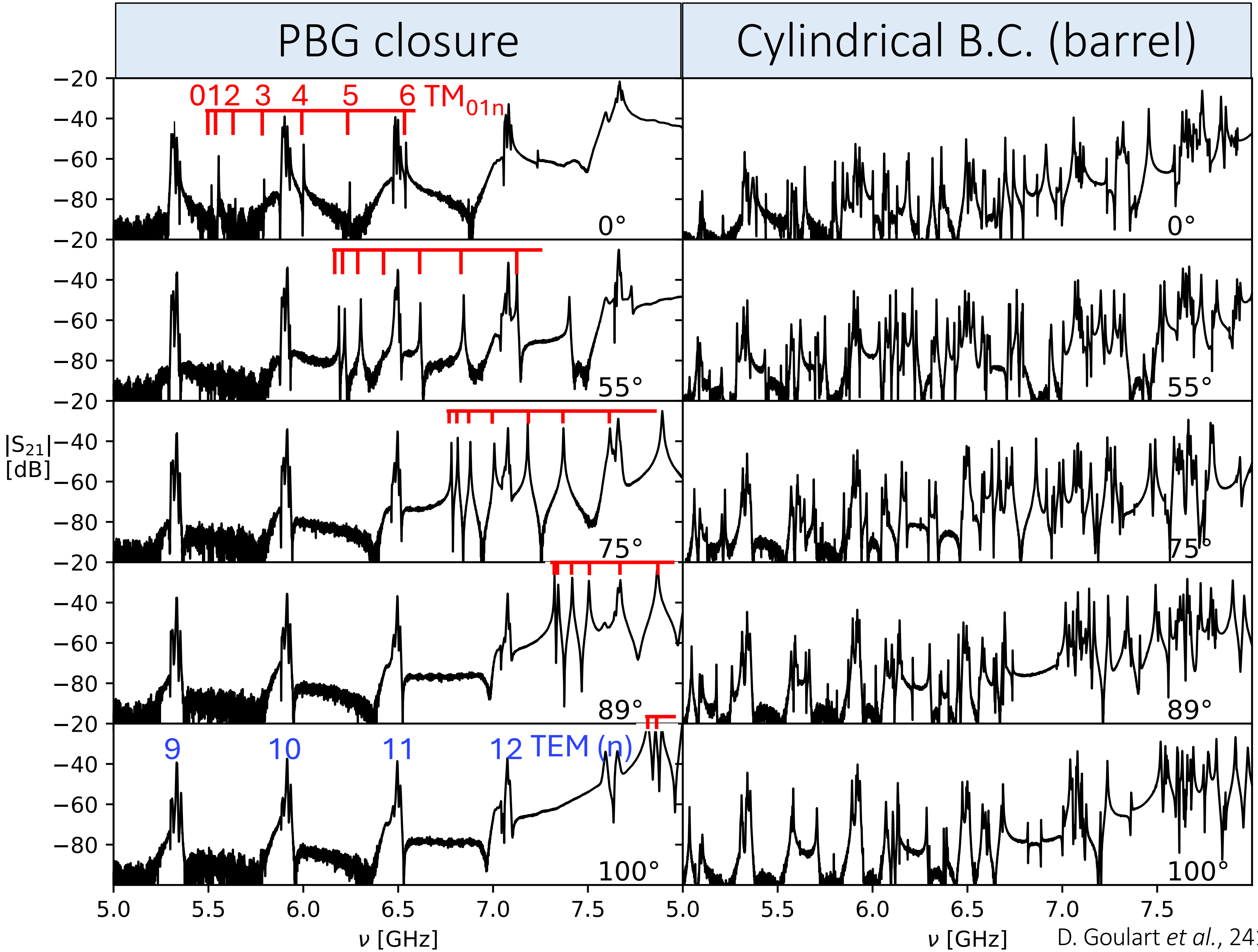

6-Rod
Barrel

D. Goulart *et al.*, 2411.18914, in revision RSI

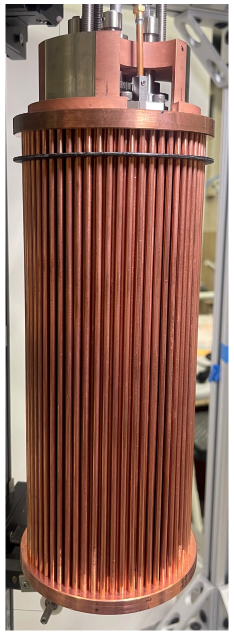

6-Rod
PBG

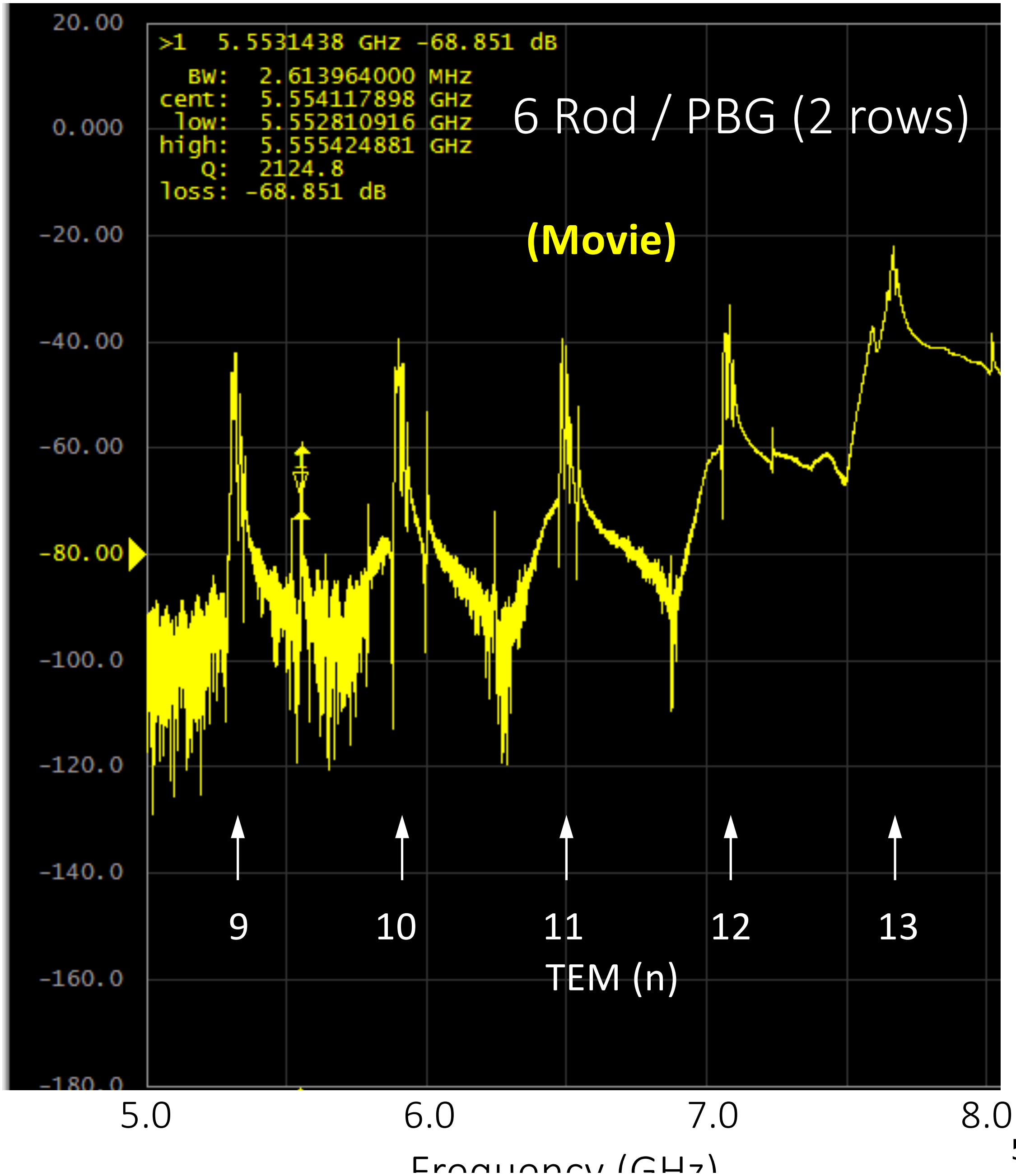

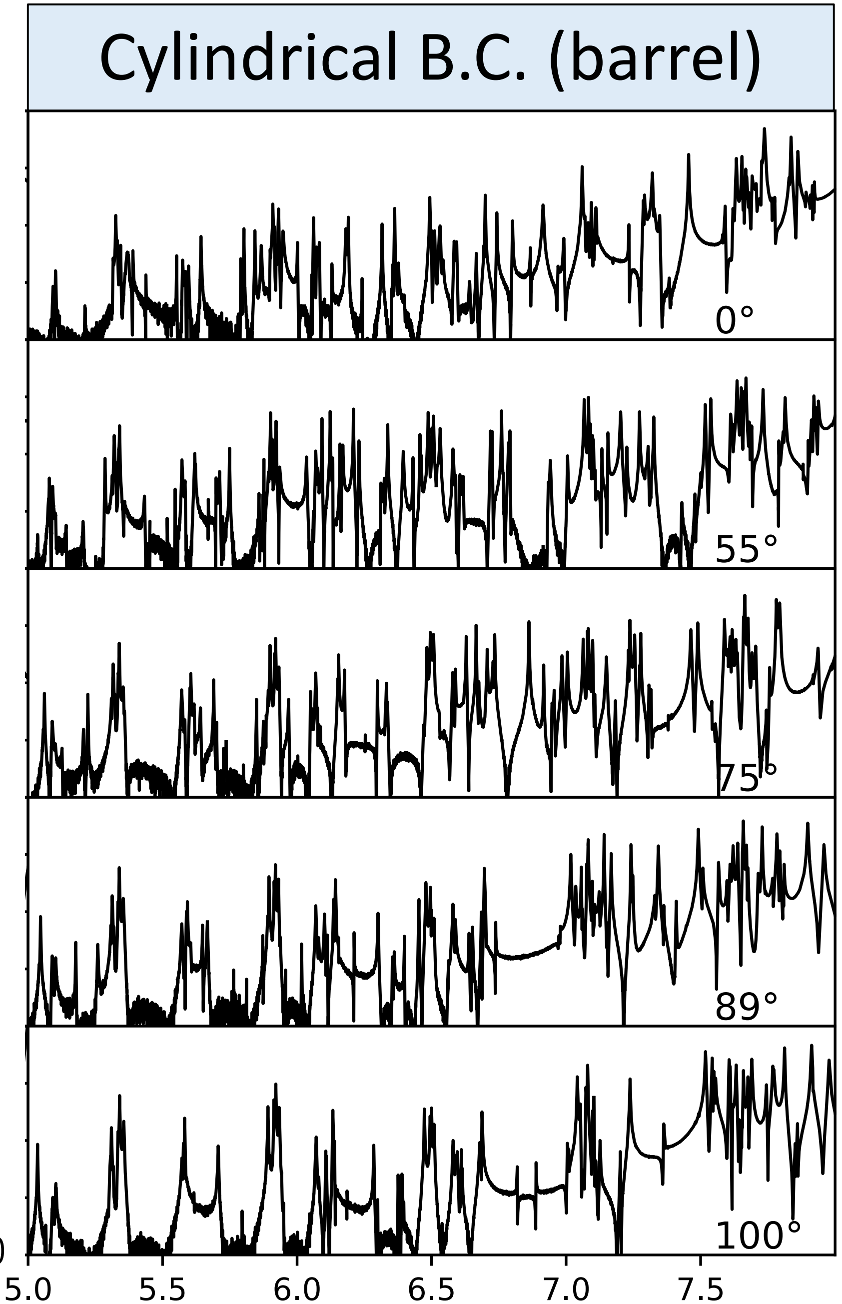

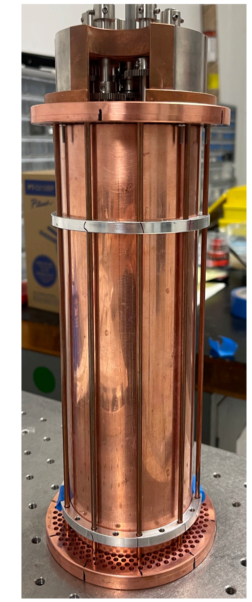

6-Rod
Barrel

Superconducting wire-array metamaterials

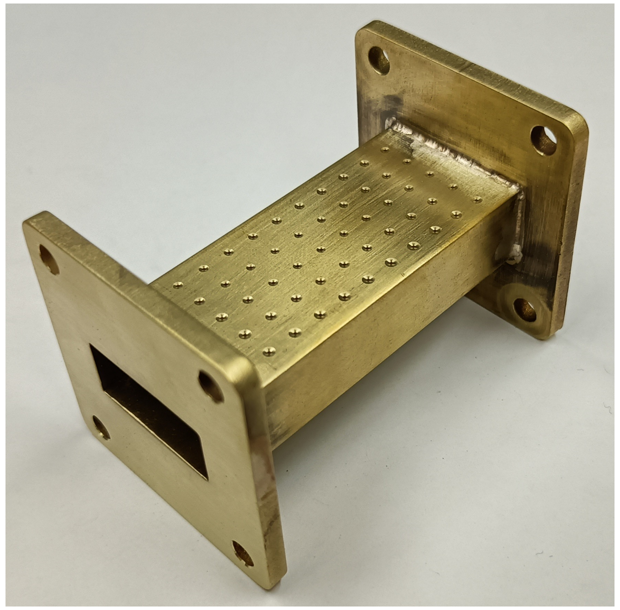

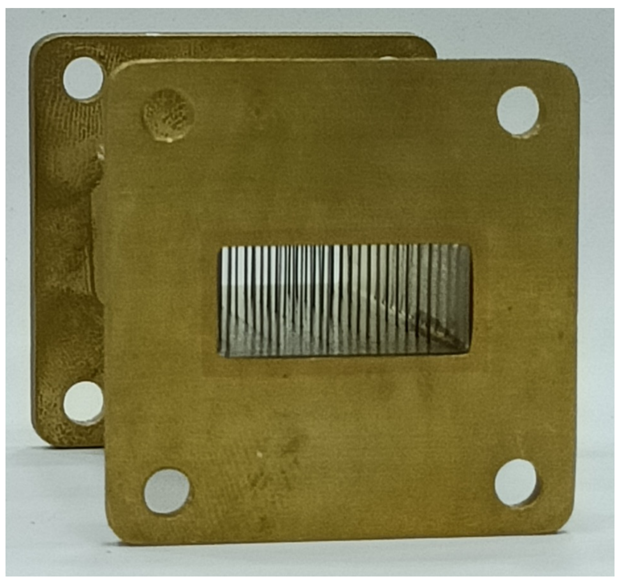

Superconducting wire-array metamaterials, for 25 - 50 GHz

Builds on work by Anlage et al. on Nb metamaterials in waveguides for B = 0: M. Ricci, N. Orloff, S.M. Anlage, *Superconducting Materials*, Appl. Phys. Lett. 87 (2005) 034102

Measurements of S_{21} for square arrays of Cu, Nb & MgB_2 wire of 250 μ diameter, with lattice a = 4.50 mm and 6.36 mm

First measurements have been performed at B = 0; later tests to be made with fields parallel to the wires up to B = 9 T

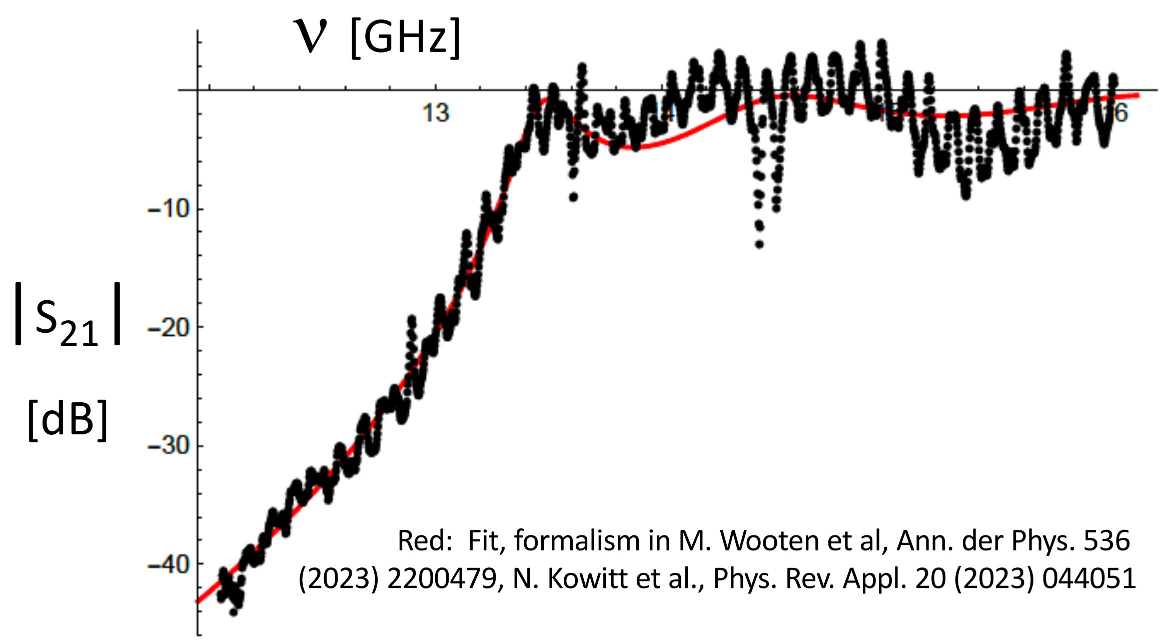

Nb & MgB_2 transitions observed in waveguide-mounted metamaterial

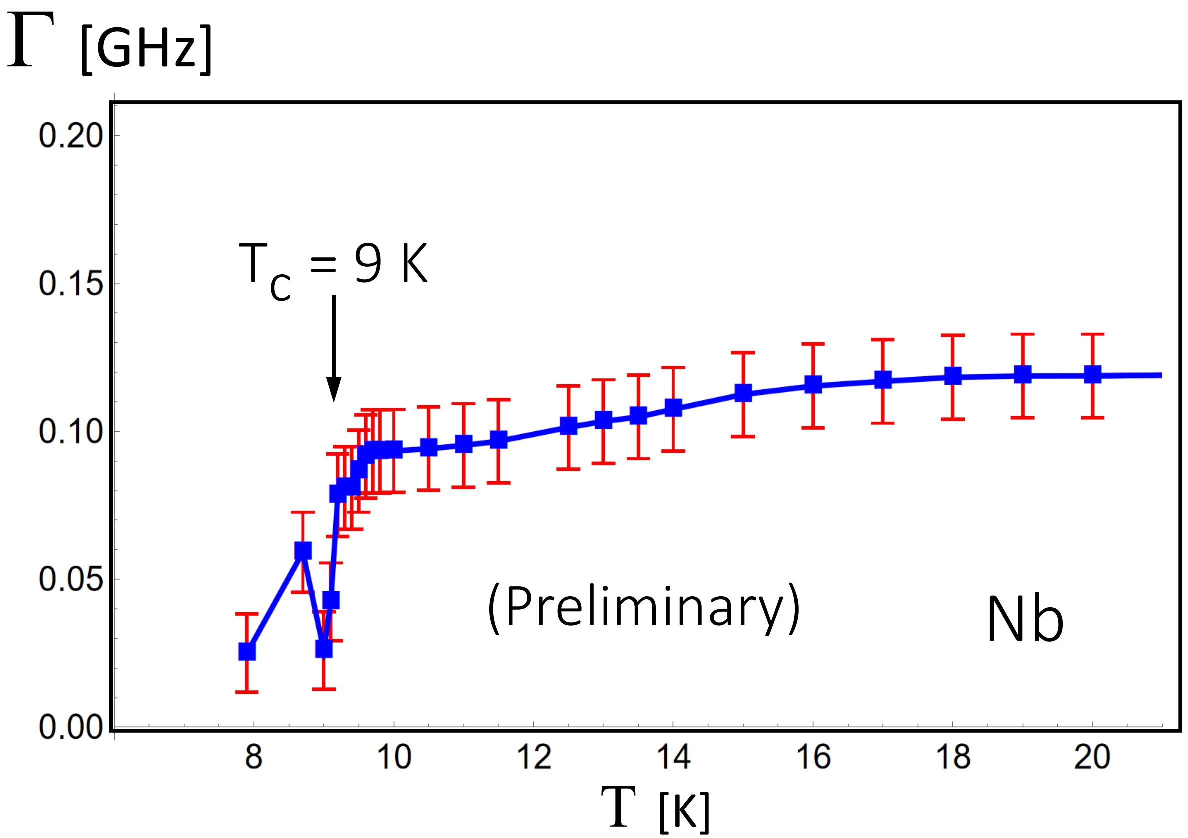

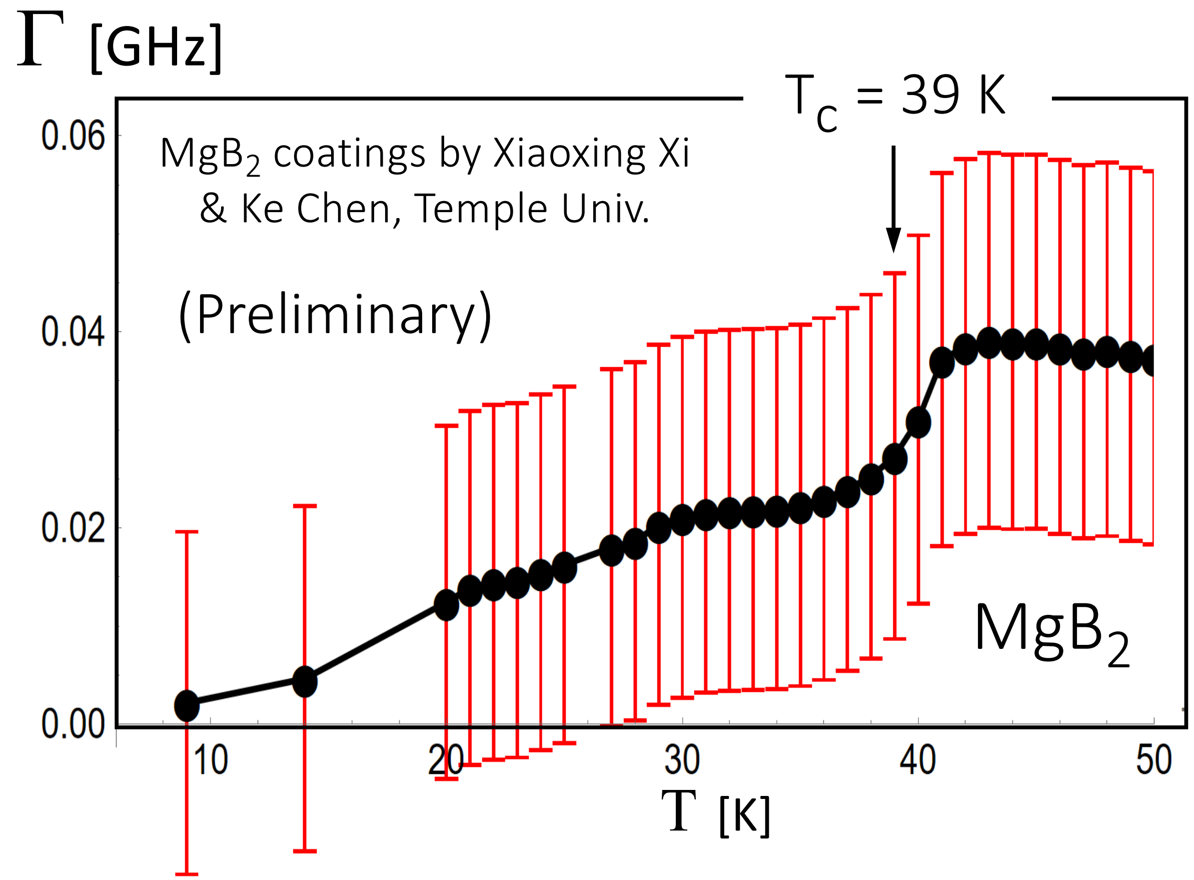

Magnesium Diboride: Advantages

- T_C = 39 K
- $H_{c2}(||)$ = 14 T, 74 T in thin films
- Carbon doping pins vortices, reduces RF loss
- $H_{c2}(||$, 5% Carbon doped) = 36 T
- Easy to deposit on wires, rods, surfaces

Only disadvantage: It should be stored in vacuum or dessicator to minimize exposure to moisture. It can be passivated, and micron-thick MgB_2 films do self-passivate, but don't leave out indefinitely.

ALPHA Phase Ia Resonator – UC Berkeley

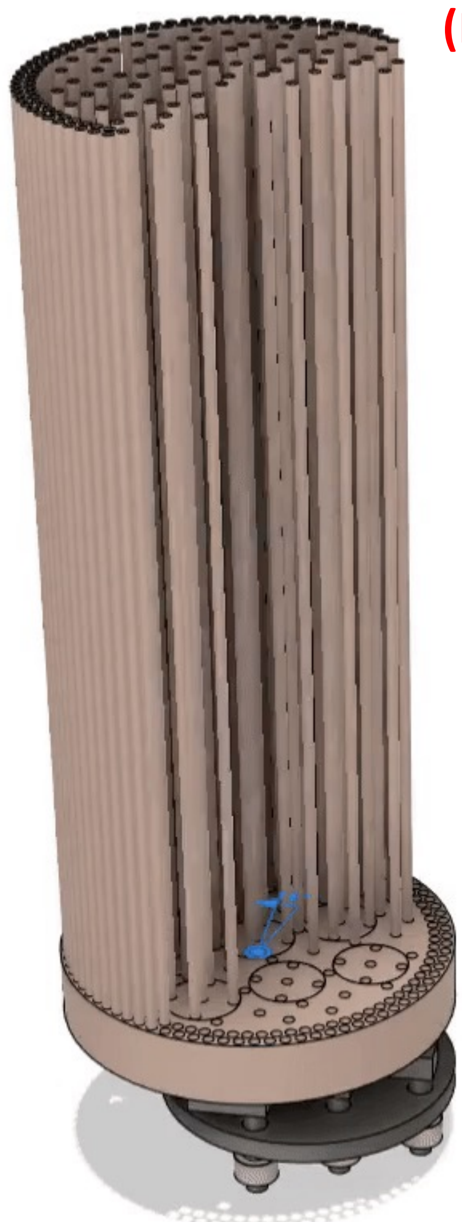

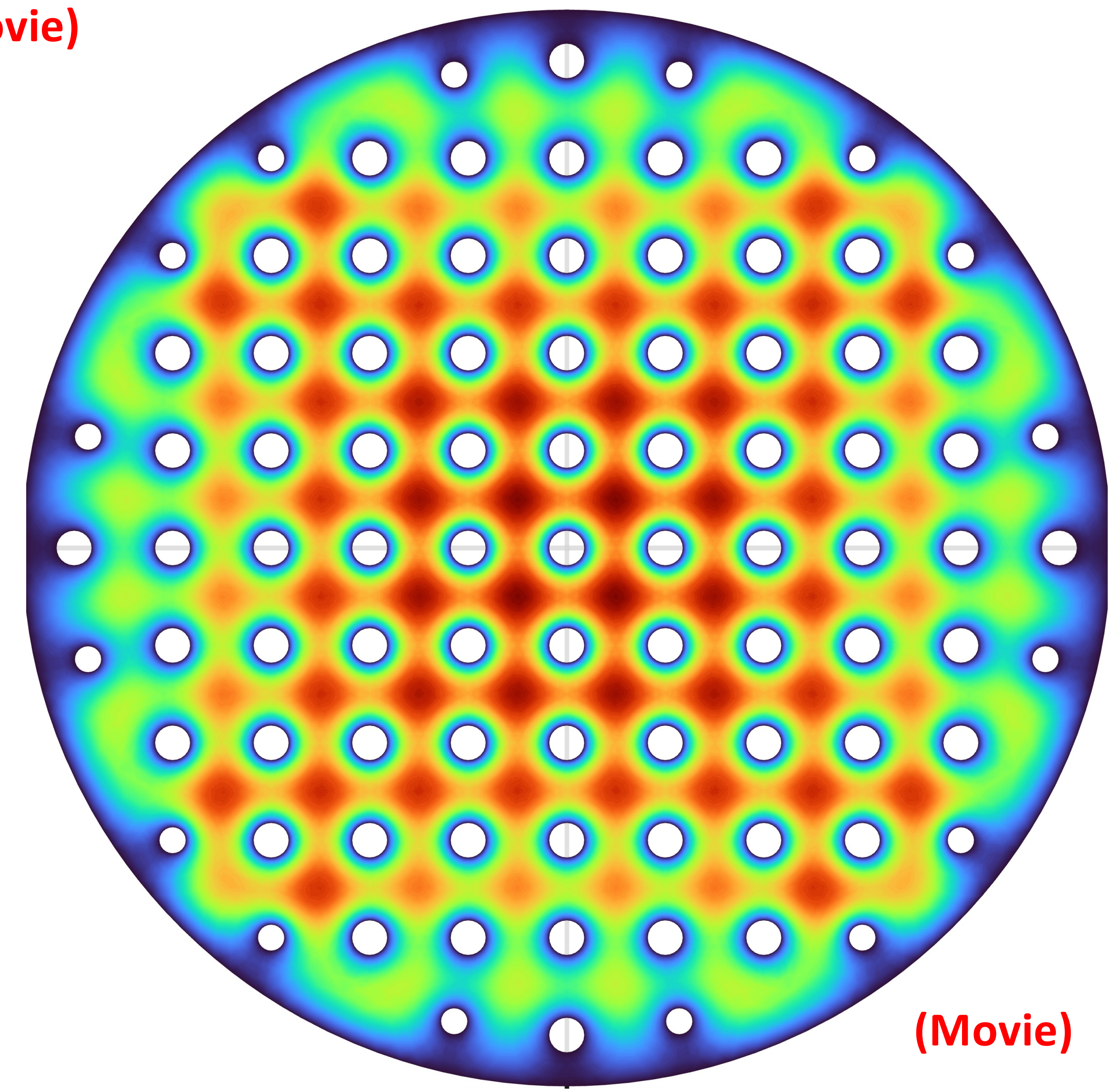

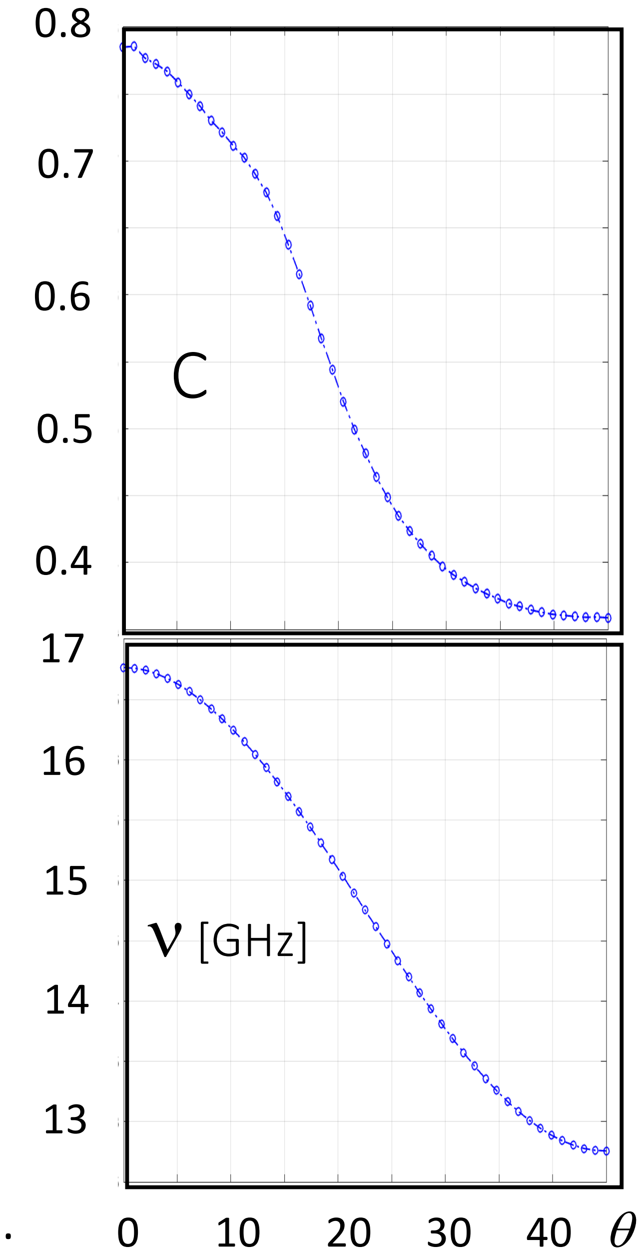

HAYSTAC format prototype; ALPHA x1.7 linear dim.

Phase I resonator development - Stockholm

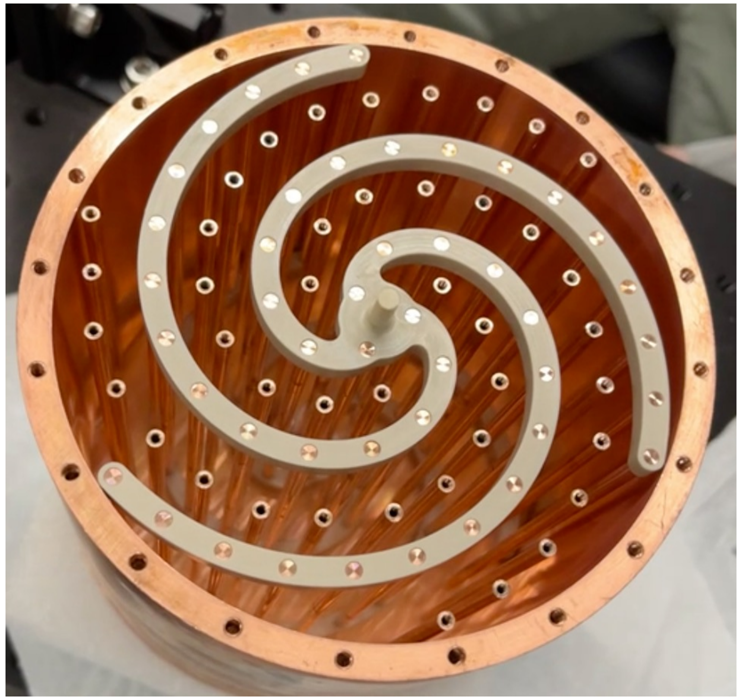

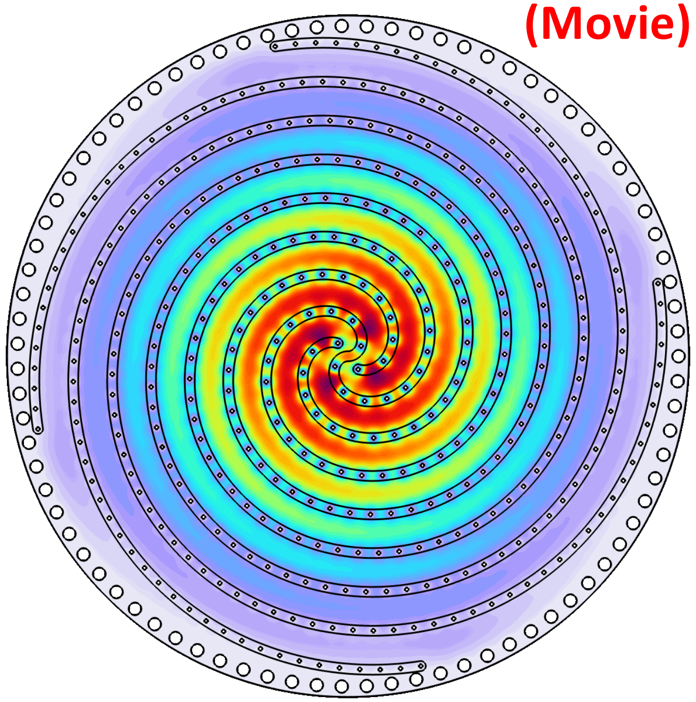

Multiarm spiral resonator

- Single rotational motion
- Design covers 9-12 GHz
- With flat form factor, C > 0.5

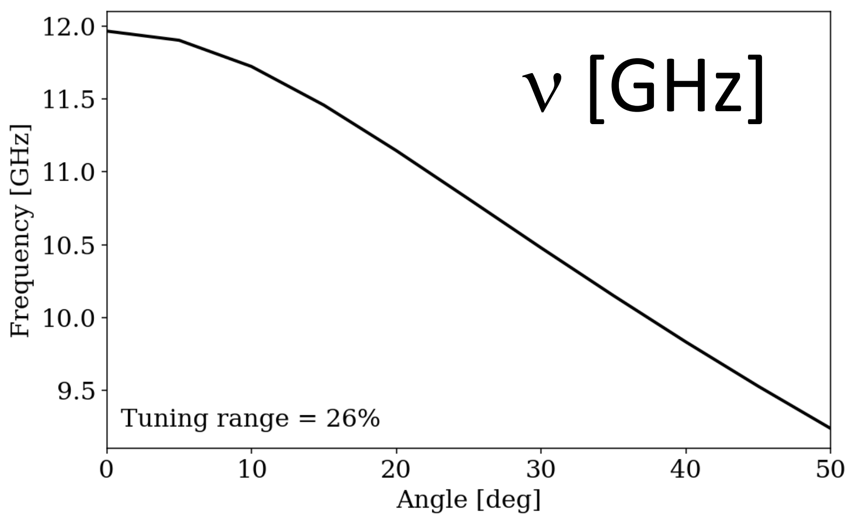

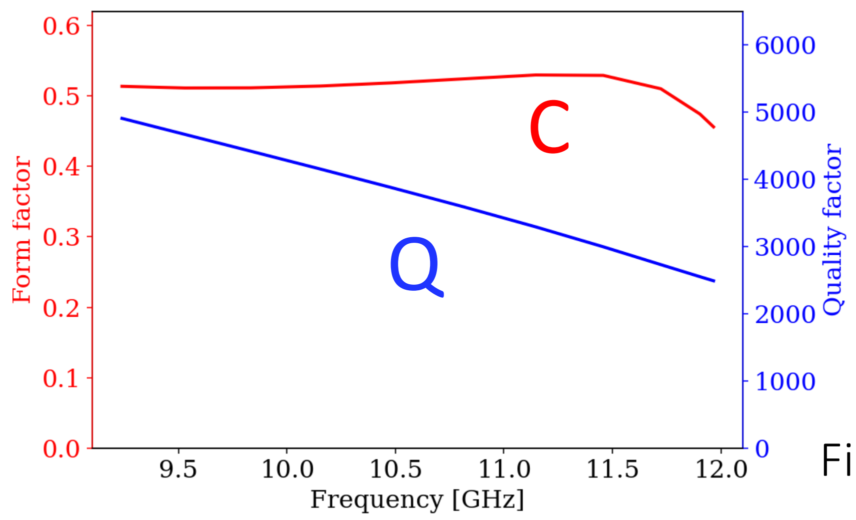

Figures courtesy of Jun-Woo Jeoung

ALPHA Phase I (commission 2027) and Phase II (begin > 2029) goals & projections

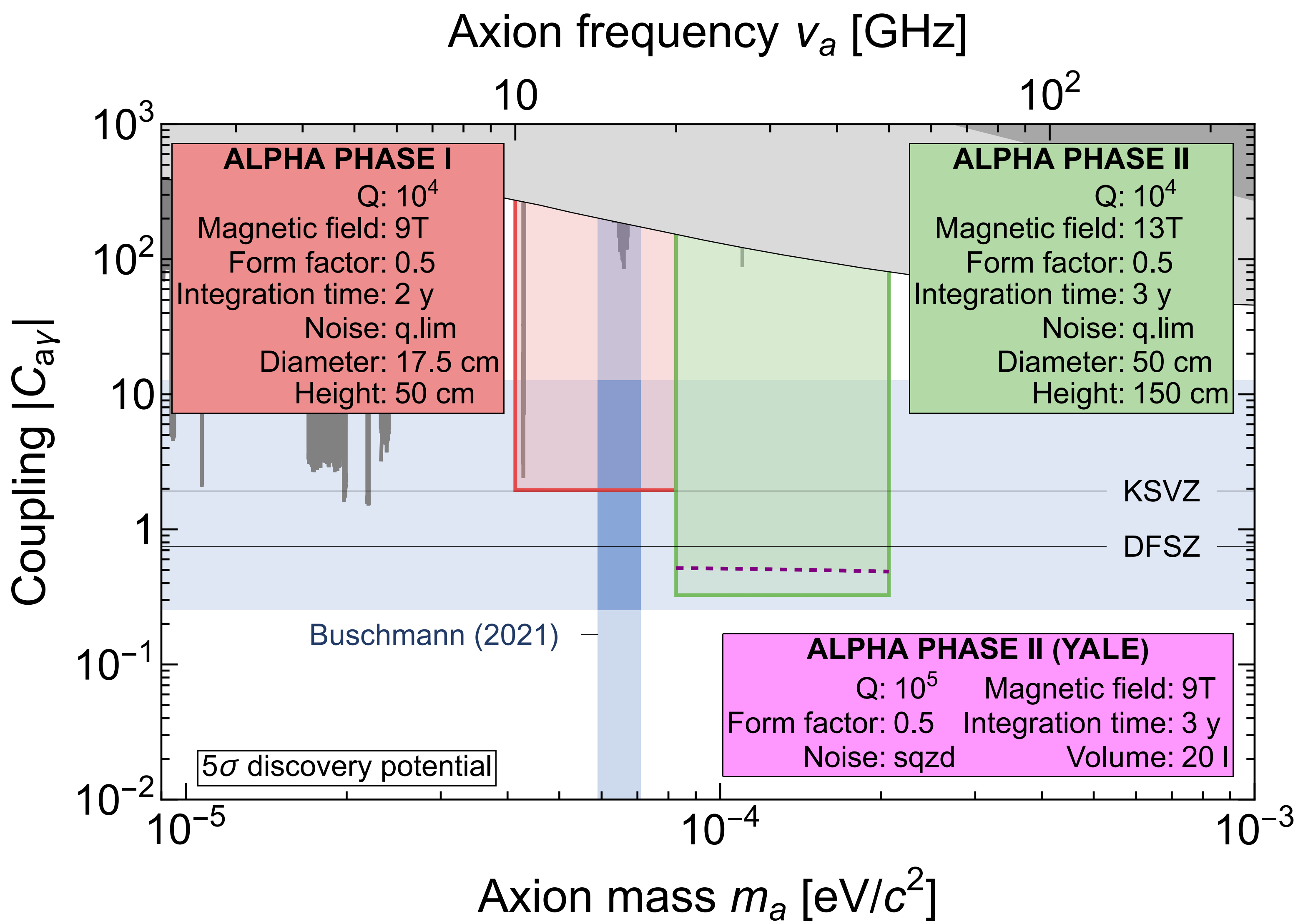

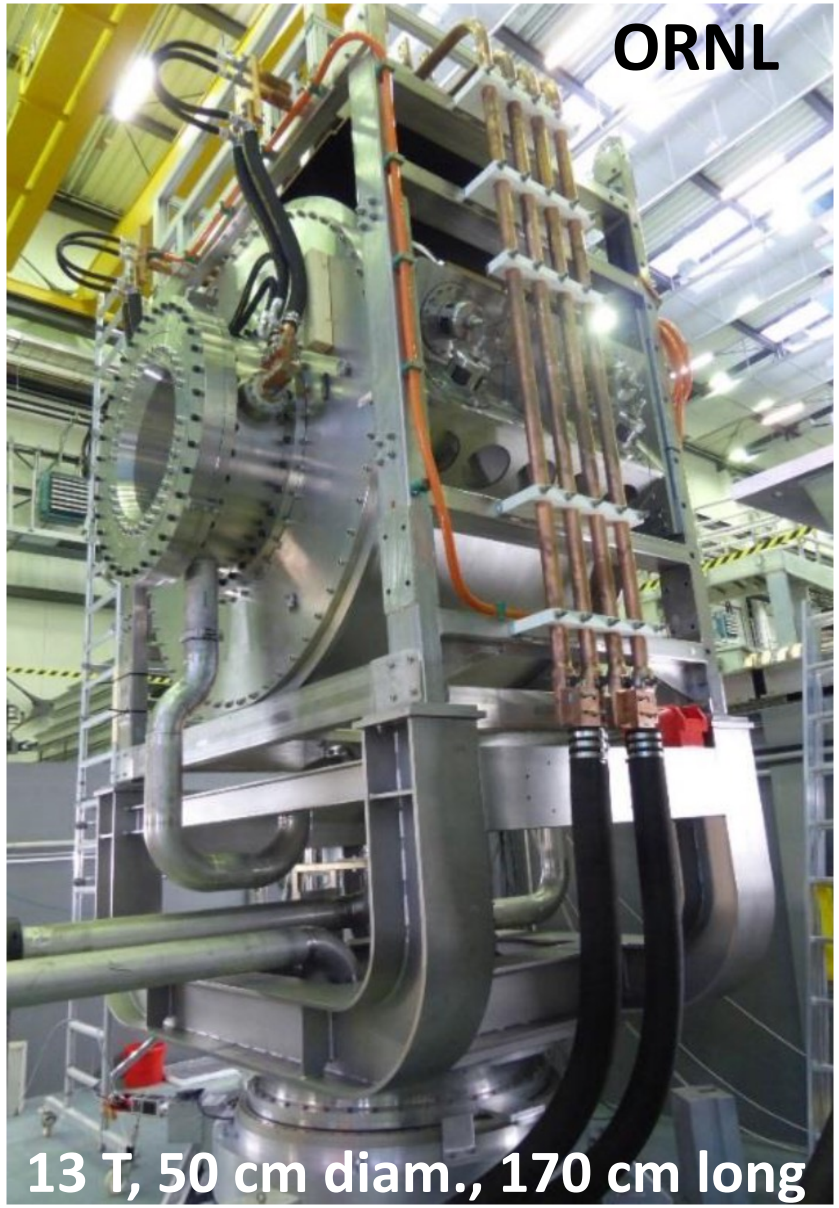

ALPHA Project - Status

PHYSICAL REVIEW D **107,** 055013 (2023)

Searching for dark matter with plasma haloscopes

Alexander J. Millar,[1,2,3,*] Steven M. Anlage,[4] Rustam Balafendiev,[5] Pavel Belov,[6] Karl van Bibber,[7] Jan Conrad,[1] Marcel Demarteau,[8] Alexander Droster,[7] Katherine Dunne,[1] Andrea Gallo Rosso,[1] Jon E. Gudmundsson,[1,5] Heather Jackson,[7] Gagandeep Kaur,[9,1] Tove Klaesson,[1] Nolan Kowitt,[7] Matthew Lawson,[1,2] Alexander Leder,[7] Akira Miyazaki,[10] Sid Morampudi,[11] Hiranya V. Peiris,[1,12] Henrik S. Røising,[13] Gaganpreet Singh,[1] Dajie Sun,[7] Jacob H. Thomas,[14] Frank Wilczek,[1,11,15,16] Stafford Withington,[17] Mackenzie Wooten,[7]

(Endorsers)

Jens Dilling,[8] Michael Febbraro,[8] Stefan Knirck,[3] and Claire Marvinney[8]

[1]*The Oskar Klein Centre, Department of Physics, Stockholm University, AlbaNova, SE-10691 Stockholm, Sweden*
[2]*Nordita, KTH Royal Institute of Technology and Stockholm University, Roslagstullsbacken 23, 10691 Stockholm, Sweden*
[3]*Fermi National Accelerator Laboratory, Batavia, Illinois 60510, USA*
[4]*Quantum Materials Center, Physics Department, University of Maryland, College Park, Maryland 20742-4111, USA*
[5]*Science Institute, University of Iceland, 107 Reykjavik, Iceland*
[6]*Narxoz University, Zhandossov street 55, 050035 Almaty, Kazakhstan*
[7]*Department of Nuclear Engineering, University of California Berkeley, Berkeley, California 94720, USA*
[8]*Physics Division, Oak Ridge National Laboratory, Tennessee 37831*
[9]*Centre for Lasers and Photonics, Indian Institute of Technology Kanpur; Kanpur, 208016, India*
[10]*Department of Physics and Astronomy, Uppsala University, Uppsala 75237, Sweden*
[11]*Center for Theoretical Physics, MIT, Cambridge, Massachusetts 02139, USA*
[12]*University College London, Gower Street, London WC1E 6BT, United Kingdom*
[13]*Niels Bohr Institute, University of Copenhagen, DK-2200 Copenhagen, Denmark*
[14]*X1, Department of Physics, Illinois Institute of Technology, Chicago, Illinois 60616, USA*
[15]*T.D. Lee Institute and Wilczek Quantum Center, Shanghai Jiao Tong University, Shanghai 200240, China*
[16]*Arizona State University, Tempe, Arizona 85287, USA*
[17]*Department Physics, University of Oxford, Clarendon Laboratory Parks Road, Oxford OX1 3PU, United Kingdom*

(Received 11 November 2022; accepted 2 February 2023; published 10 March 2023; corrected 27 March 2023)

Following the Lawson et al. PRL, an R&D consortium formed to provide all supporting theory, simulations & data

These including working groups on theory, wire array metamaterials, superconducting wires and cavities, quantum amplifiers and antennas

After four years, this work culminated in a published white-paper document *(A.J. Millar et al, Phys. Rev. D 107 (2023) 055013)*

A proposal to the Simons, Sloan, Templeton and Moore Foundations was selected for funding in June 2022; Swedish funding was already in place.

Project kickoff meeting with Simons & Templeton sponsors, September 25-27, 2023 at Yale

SIMONS FOUNDATION

JOHN TEMPLETON FOUNDATION

Inspiring Awe & Wonder

And once the axion is found: Dark matter Interferometry & Axio-astronomy

- Foster et al. [Phys. Rev. D 103 (2021) 076018] consider what can be learned by two or more haloscopes operating simultaneously within a few coherence lengths of the axion field and whose signal outputs are combined or time-stamped and recorded.

- Analogously to a global array of radio telescopes, not only can the coherence length of the axion field be measured, but its phase space structure at the earth precisely determined (i.e. vector velocity of the Sun through the galactic halo, cold flows in the axion substructure, etc. to better than 1^{o}, etc.)

Axion interferometry *J. Foster et al., Phys. Rev. D 103 (2021) 076018*

A recent spectacular example from radio astronomy (2019): The Event Horizon Telescope (EHT)

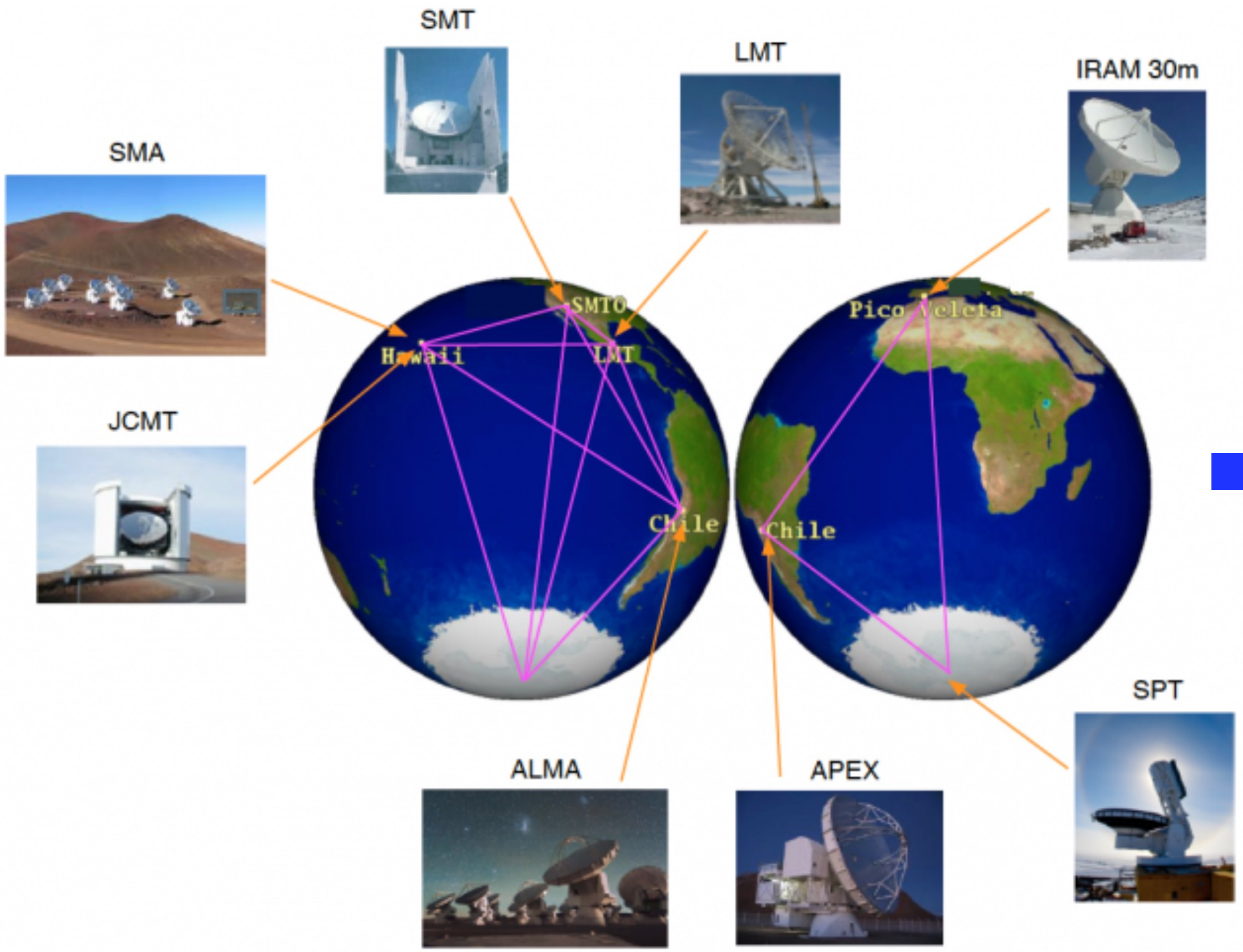

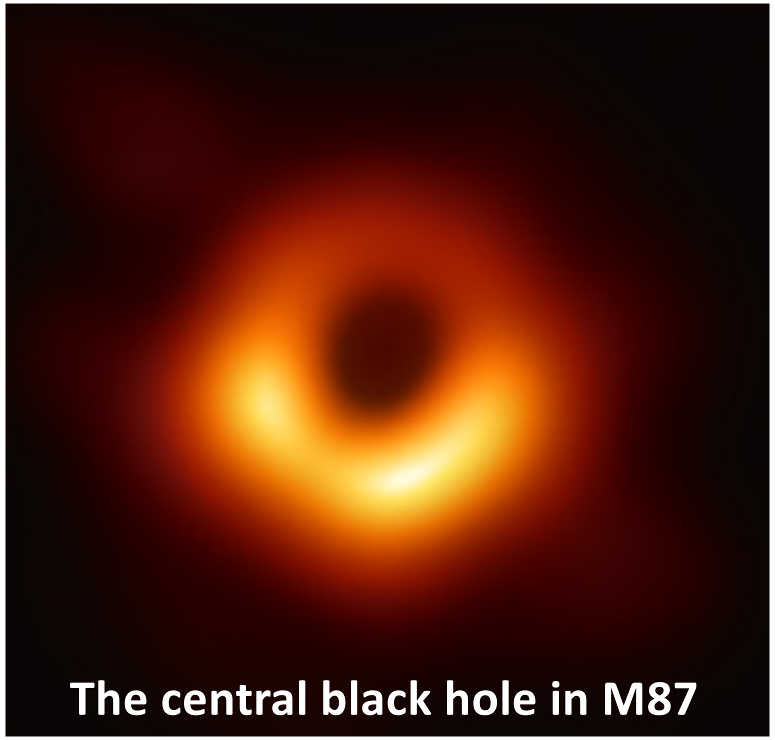

Analogously, one can carry out axion interferometry with multiple platforms located within a few coherence lengths

Example from Foster paper is explicitly based on the HAYSTAC laboratory

Coherence length & coherence time:

$$\boxed{\lambda_c \sim \frac{1}{m_{\rm DM} v_0}, \qquad \tau \sim \frac{1}{m_{\rm DM} \bar{v} v_0}}$$

m_{DM} = dark matter mass
v_0 = velocity dispersion
$\bar{v}$ = mean velocity
$\mathbf{x}_{12}$ = separation between detectors

Cosine & Sine components of the interference terms:

$$\mathcal{F}^c_{12}(v) = \int d^3\mathbf{v} f(\mathbf{v}) \cos(m_{\rm DM}\mathbf{v}\cdot\mathbf{x}_{12})\delta[|\mathbf{v}| - v]$$

$$\mathcal{F}^s_{12}(v) = \int d^3\mathbf{v} f(\mathbf{v}) \sin(m_{\rm DM}\mathbf{v}\cdot\mathbf{x}_{12})\delta[|\mathbf{v}| - v].$$

- m_{DM} = 25.2 μeV, "near the window where the HAYSTAC collaboration is searching for the axion"
- Lab is located at (41° N, 73° W), with the second detector $2\lambda_C \sim 20$ m north of the first detector
- In the example shown, the individual curves are taken 10 minutes apart beginning midnight January 1, 2020

The modulation due to the earth's rotation is clearly seen

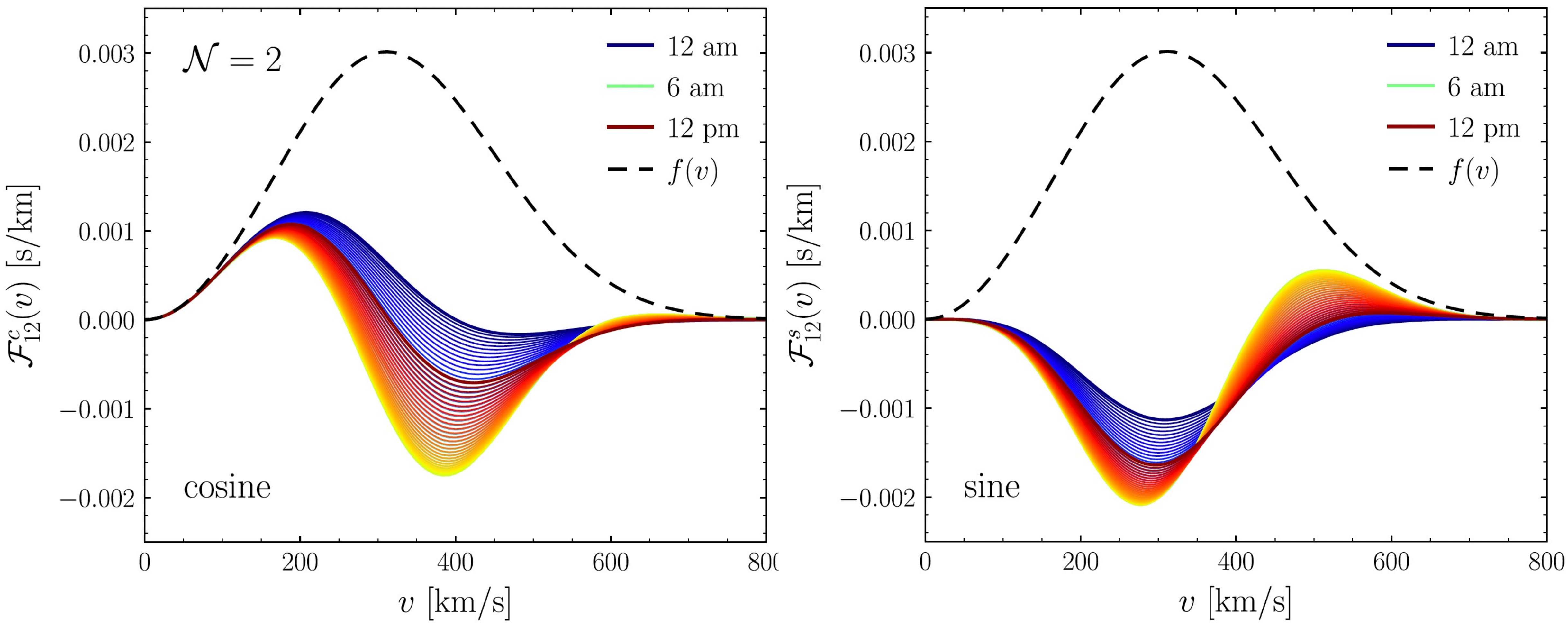

Summary

- HAYSTAC-ALPHA will probe deep into the post-inflation axion region this decade
- It is well supported both in quantum metrology and photonic dimensions
- It has an upgrade path to a large scale experiment at ORNL in the 50 GHz range
- Should the axion be discovered, the infrastructure is in place to promptly initiate a follow-on program of axion interferometry and axio-astronomy
- Many thanks to our sponsors!

NSF
Swedish Research Council
Rymdstyrelsen Swedish National Space Agency
Funded by the European Union
European Research Council Established by the European Commission
SIMONS FOUNDATION
JOHN TEMPLETON FOUNDATION
Knut and Alice Wallenberg Foundation
Wright Laboratory
Yale University

Additional slides

Tuning studies: Dependence of the plasma frequency on the unit cell (I)

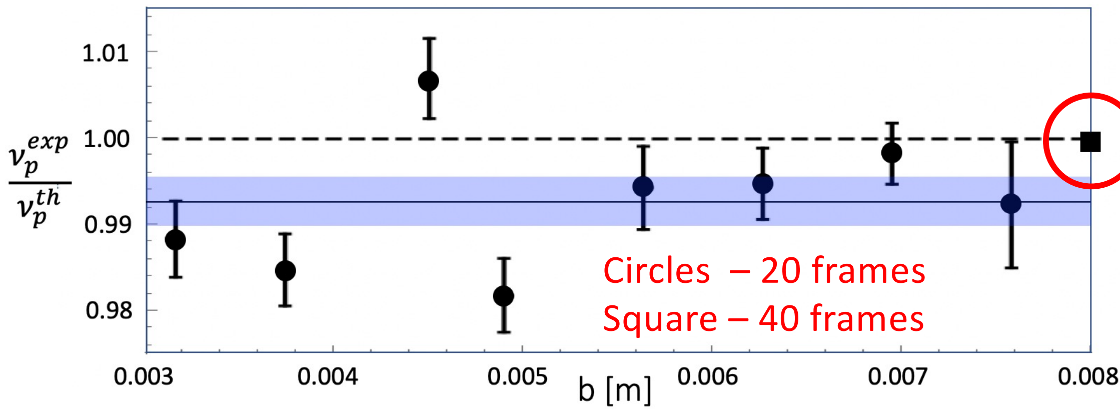

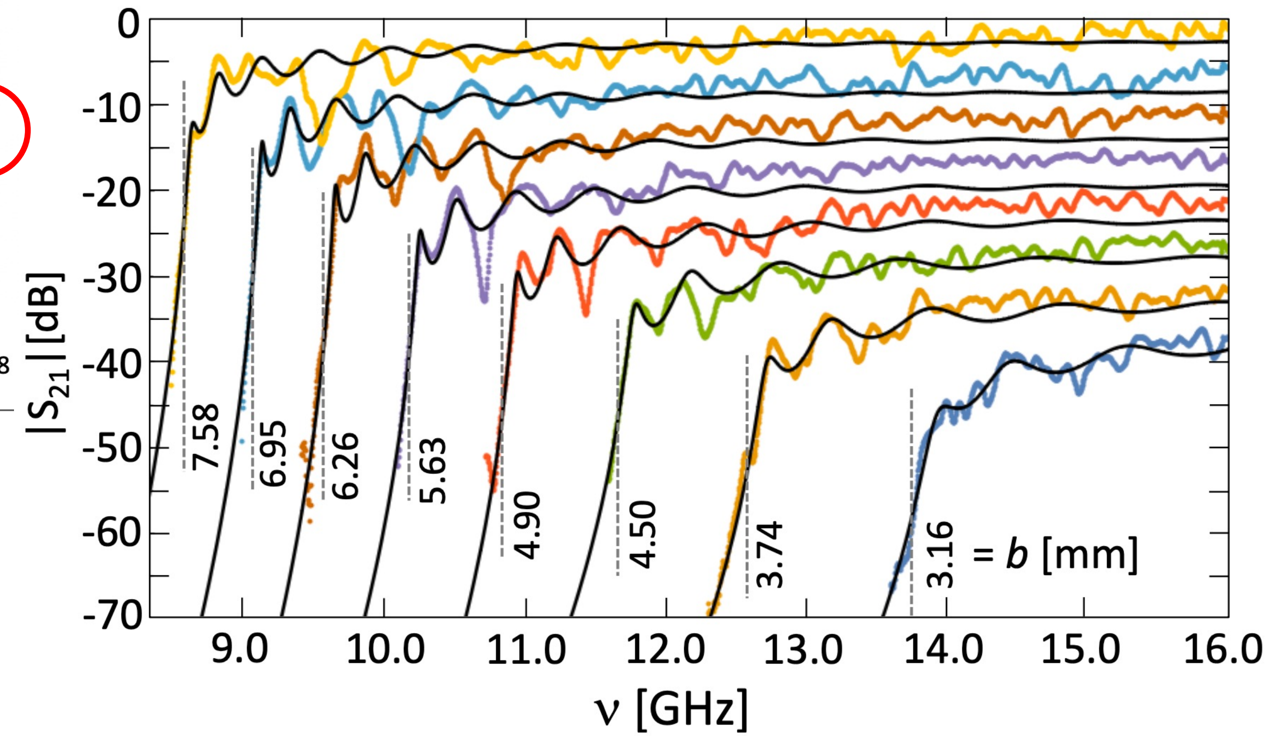

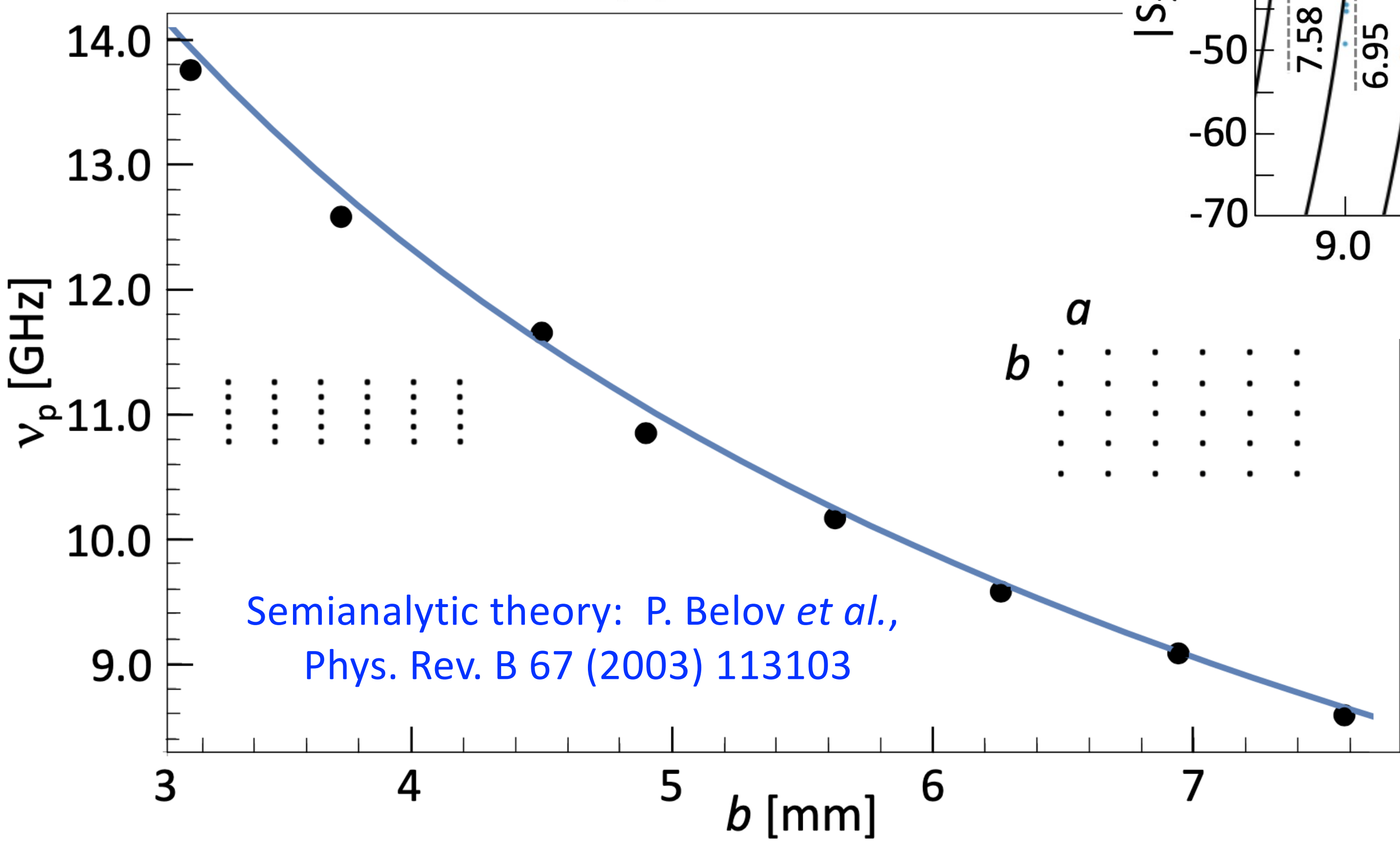

Belov et al. predictions for the asymptotic plasma frequency borne out at the 0.1% level

N. Kowitt *et al.*, Phys. Rev. Appl. 20 (2023) 044051, arXiv:2306.15734

Photonic Band Gap (PBG) structures *E. Yablonovich (1987); S. John (1987)*

- Basic idea: E&M in a periodic lattice (dots, metallic or dielectric rods, etc.) is completely analogous to solid state: Bloch functions, bands, gaps, etc.

- Furthermore, lattice defects can be created to confine modes of interest, while suppressing unwanted modes

- This idea has had a large impact in optical photonics, basic physics, and microwave and accelerator physics

- It may now be critically important in opening up axion searches at much higher masses

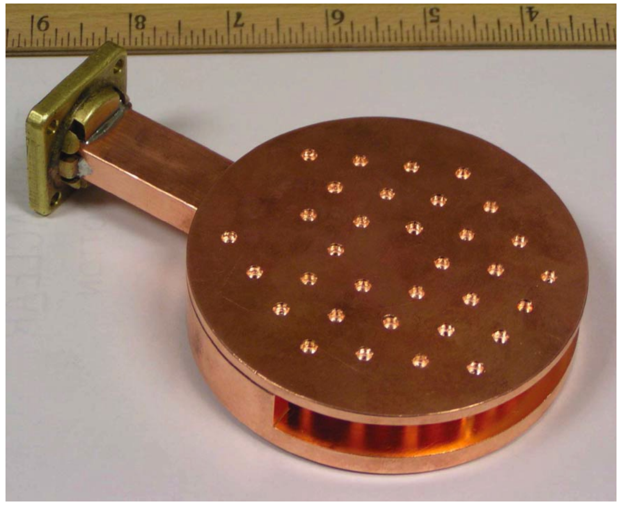

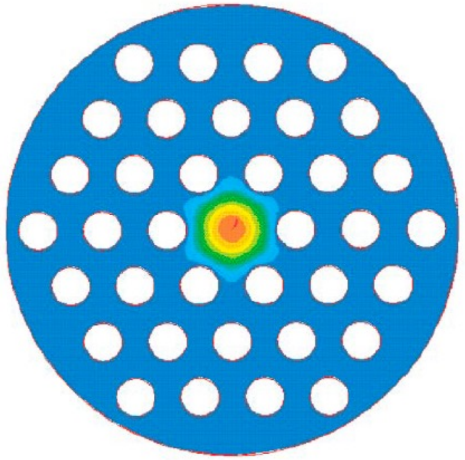

TM_{01}

MIT prototype accelerator cell 17.140 GHz
Phys. Rev. ST Accel. Beams 8, 091302 (2005)

Periodic lattice & unit cell

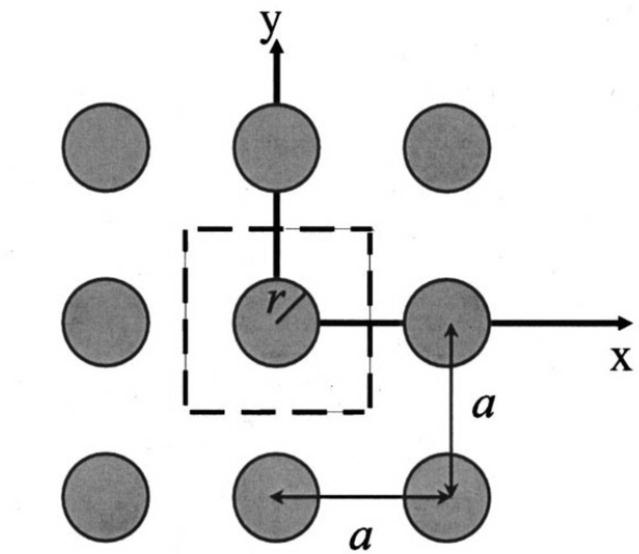

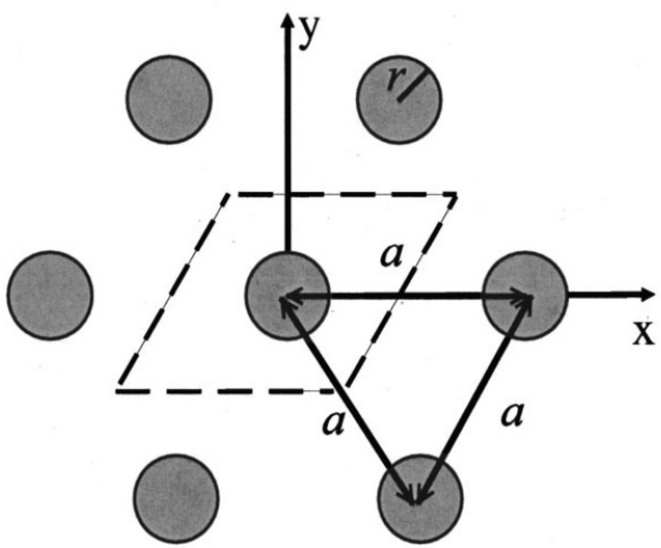

Solve the Helmholtz eqn.

$$\nabla_{\perp}^{2}\psi(\mathbf{x}_{\perp})=\left(k_z^2-\frac{\omega^2}{c^2}\right)\psi(\mathbf{x}_{\perp})$$

with the Bloch condition

$$\psi(\mathbf{x}_{\perp}+\mathbf{T})=\psi(\mathbf{x}_{\perp})e^{i\mathbf{k}_{\perp}\cdot\mathbf{T}}$$

for both TM & TE modes
under their respective b.c.

Reciprocal lattice & irreducible Brillioun zone

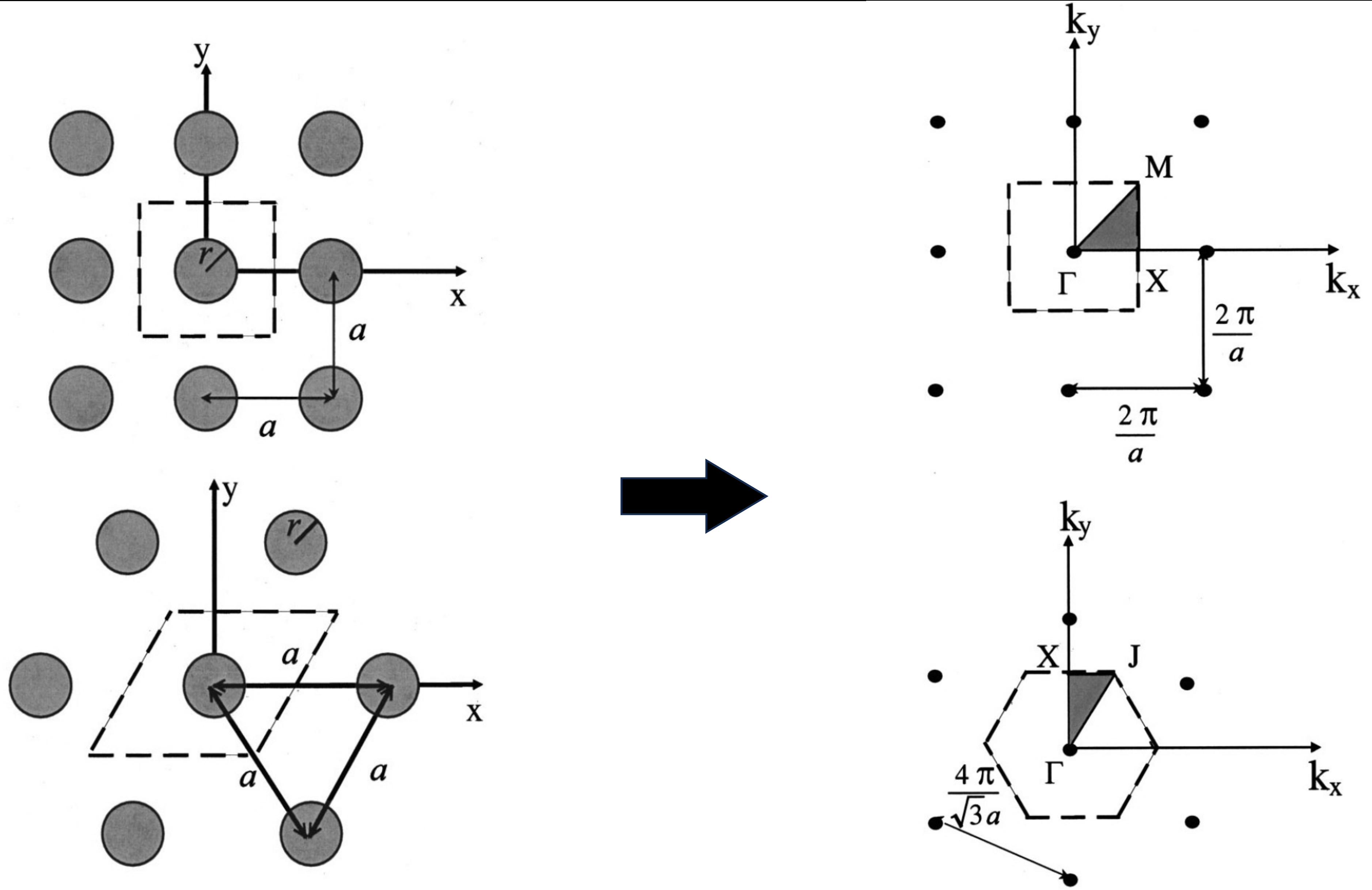

Band structures

E. Smirnova et al., J. Appl. Phys. 91 (2002) 960

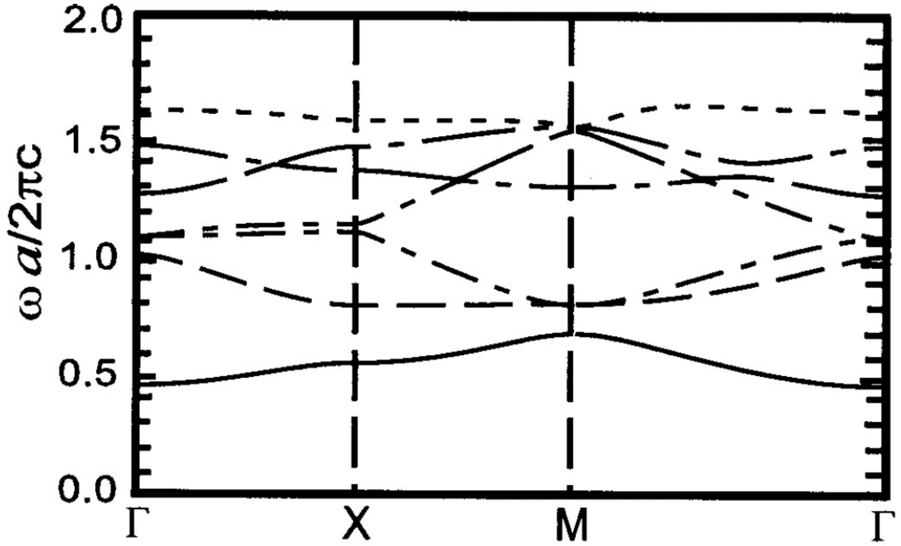

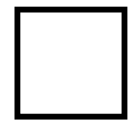

r/a = 0.2

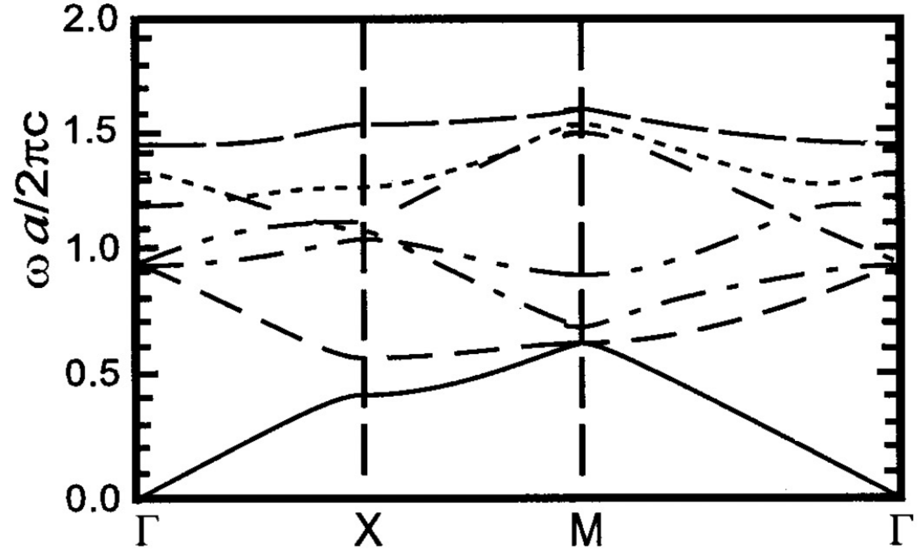

TM

TE

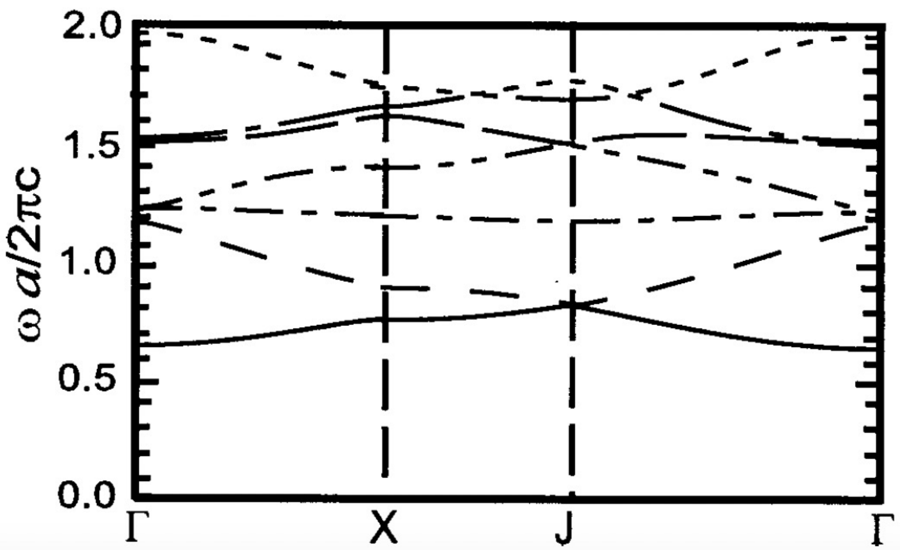

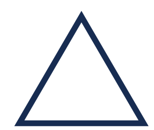

r/a = 0.2

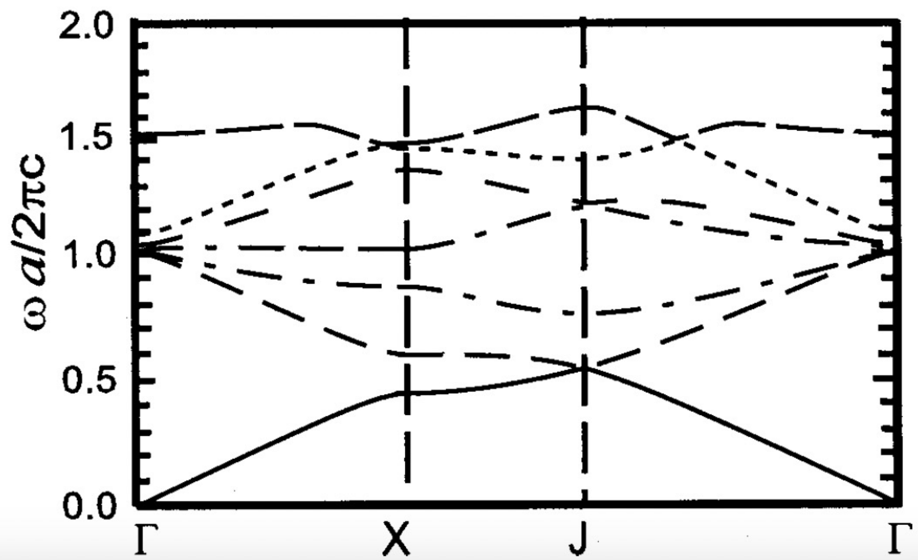

Global band gaps

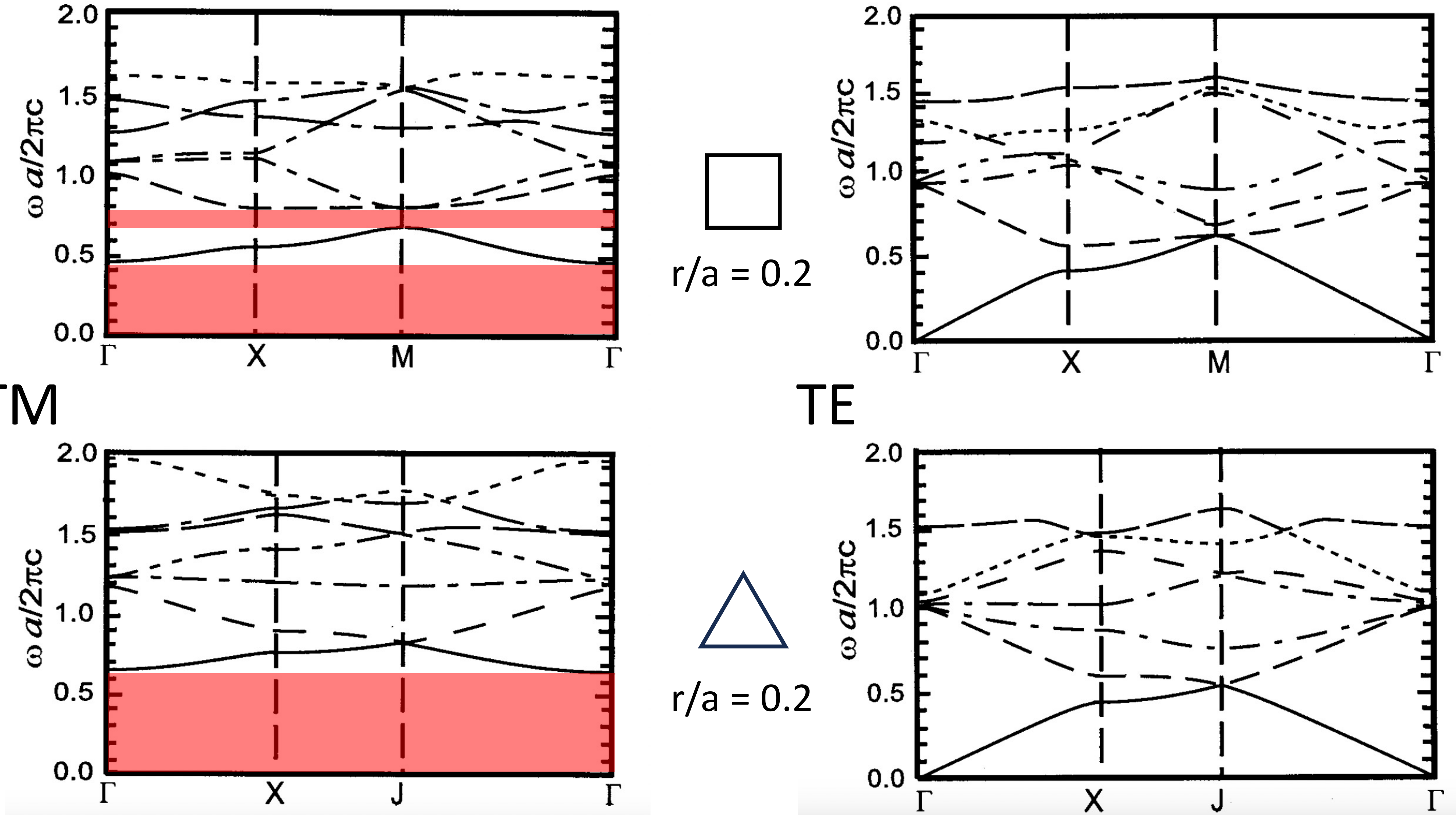

Map out the separatrix between stop bands & pass bands